Physics of the interstellar medium

U.Klein, J. Kerp

Argelander-Institut für Astronomie
Bonn

August 2008
(First edition)

Contents

Chapter 1

Introduction

1.1 Cycle of matter

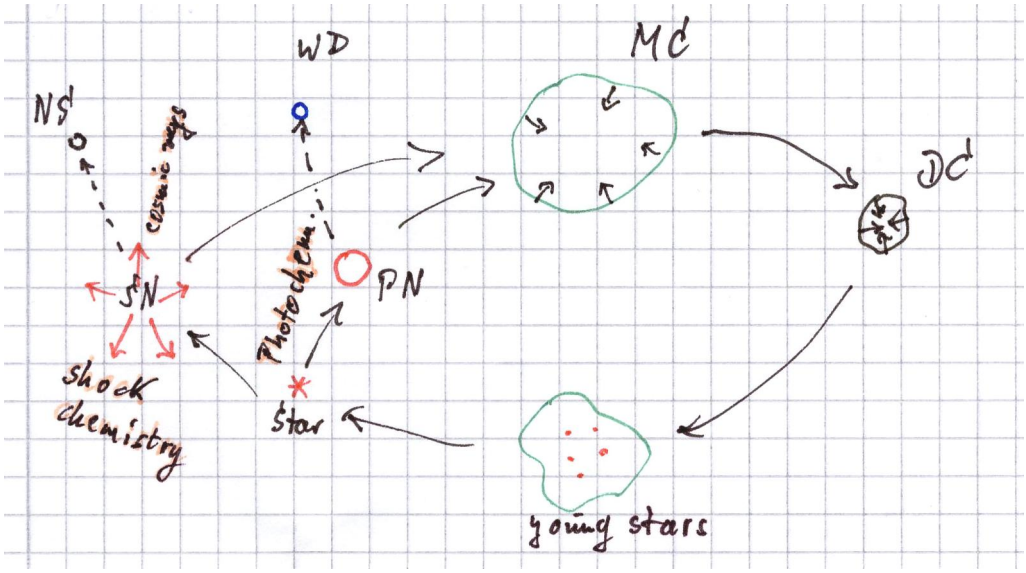

Figure 1.1: Cycle of matter

BBNS[1] 76% H, 24% He, 10^{-4} ^{3}He, 10^{-4} ^{2}H, 10^{-10}-10^{-9} Li, Be

today 66% H, 32% He, 2% "metals" (C, N, O, Mg, Si, S, Fe)

Important *for us* (in this classroom or whereever you are): Chemical evolution

- first step is nucleo-synthesis in stars (up to Fe; higher elements are formed in SNe)
  chemistry in ISM (gas-pahse and on dust grains)
  gas-phase chemistry in photo-dissociation regions and in shocks (allowing also endothermal reactions)
- heating and cooling balance: different gas phases (n,T) have different heating and cooling meachinsms.

1.2 Phases of the ISM

- Chemical composition of the ISM comparable to the elements abundance of the Solar System
- The state of Hydrogen determines the state of the ISM
  - Molecular region H_2
  - Neutral region HI
  - Ionized region HII
- HII regins expand, not held "back by" stars
- molecular clouds maintained by their own gravity

Phase		n [cm^{-3}]	T[K]	$M_{\mathrm{tot}}[\mathrm{M}_\odot]$
atomic (HI)	cold	$\backsim 25$	$\backsim 100$	$1.5 \cdot 10^9$
	warm	$\backsim 0.25$	$\backsim 8000$	$1.5 \cdot 10^9$
molecular (H_2)		$\gtrsim 10^3$	$\lesssim 100$	10^9
ionized	HII	$\backsim 1 \cdots 10^4$	$\backsim 10000$	$5 \cdot 10^7$
	diffuse	$\backsim 0.03$	$\backsim 8000$	10^9
	hot	$\backsim 6 \cdot 10^{-3}$	$\backsim 5 \cdot 10^5$	10^8

Table 1.1: Components of the ISM (phases)

Some of these are in pressure equilibrium

$$P = nk_BT = \frac{B^2}{8\pi} = \frac{1}{3} \cdot u \tag{1.1}$$

Just compute $n \cdot T$ to compare pressures.

1.2.1 Molecular regions

- Diffuse molecular clouds, $T = 40 \cdots 80\,\mathrm{K}$, $n = 100\,\mathrm{cm}^{-3}$
- Dark clouds, $T = 10 \cdots 50\,\mathrm{K}$, $n = 104 \cdots 106\,\mathrm{cm}^{-3}$

1.2.2 Neutral regions

- Dusty cirrus clouds, $T = 80\,\mathrm{K}$, $n = 1\,\mathrm{cm}^{-3}$
- Warm neutral gas, $T = 6000\,\mathrm{K}$, $n = 0.05 \cdots 0.2\,\mathrm{cm}^{-3}$

1.2.3 Ionized regions

- HII regions are envelopes of early-type stars, $T = 10^4\,\mathrm{K}$, $n = 0.1 \cdots 10^4\,\mathrm{cm}^{-3}$
- Coronal Gas $T = 10^6\,\mathrm{K}$, $n = 0.005\,\mathrm{cm}^{-3}$

1.2.4 Dust

- Product of star formation, consists of silicates and graphites
- Insignificant by mass, $M_{\rm gas}/M_{\rm dust} \approx 150$
- Plays important role for chemistry $\rightarrow$ H_2 formation
  dust serves as catalyst

1.2.5 Relativistic plasma

- Galaxies are pervaded by magnetic fields
  $\frac{B^2}{8\pi} \approx nk_BT \Rightarrow B \approx 3 \cdots 10\ \mu$G
- Supernovae produce and accelerate particles, primarily p and e^- $\Rightarrow$ become relativistic
  $\Rightarrow$ synchrotron radiation
  primarily e^-, since $m_{\rm p}/m_{\rm e} \approx 2000$
- n.b.: most of the energy of relativistic particles resides in p, owing to their much larger mass, while radiation is produced by the e^-, owing to their low mass

1.3 Discovery of the ISM

- W. Herschel compiles the first catalog of "nebulae"
- Until ∼1900 absorption lines have been discovered, but it is unclear whether they are stellar (circum-stellar) or interstellar
- 1919 Barnard compiled the first catalog of "Dark Clouds"
- 1933 Plasket & Pearce found a correlation between the CaII absorption line strength and the stellar distance.
- ∼1937 the first interstellar molecules CH, CH+ and CN were discovered
- 1945 van der Hulst predicted the detect ability of the HI 21 cm line
- 1949 discovery of interstellar magnetic field by polarization measurements
- 1950's maps of the Milky Way in HI (10% of the stellar mass is in HI)
- 1960 discovery of the soft X-ray background
- 1963 the first interstellar maser had be discovered (OH)
- 1968 NH_3, the "thermometer" in the Universe was observed for the first time
- 1970 ^{12}CO$(1 \rightarrow 0)$, the second most abundant molecule in the Universe was discovered
- 1970's infrared astronomy opens the window to the most abundant molecule H_2
- $\sim$ 1990 Submillimeter astronomy opened the window to molecular clouds and star forming regions

- 1990 COBE studied the distribution of the dominant cooling line of the ISM CII
- 1995 allowed detailed spectroscopic studies of the dust, the vibrationally excited H_2 emission line and the infrared dark clouds
- 1998 until 2006 SWAS studied the distribution of H_2O, O_2, CI up to 500 GHz
- 2000 until today FUSE observation of H_2 in absorption against background continuum sources, observation of the vertical structure of highly ionized gas like OIV and NV
- 2000 until today Spitzer studies the ISM with high angular resolution

1.3.1 Properties of the 21 cm line

- Natural line width is $10^{-16}\,\mathrm{km\,s^{-1}}$, accordingly the line is ideally suited to trace turbulence and Doppler motions.
- The thermal line width is $\sigma \approx 0.09\sqrt{T}$, which corresponds to $2\,\mathrm{km\,s^{-1}}$ at $T = 100\,\mathrm{K}$

1.3.2 Neutral hydrogen in the Milky Way

- Assuming that the gas encircles the center of the Milky Way on concentric orbits, it is feasible to determine its distance (tangentialpoint method).
- The method is restricted to the inner galaxy. However, it probes a large fraction of the baryonic mass.
- The tangent point method is only applicable for $R < R_\odot$.
- For the outer galaxy we can use stars as tracer for the potential and HI 21 cm line measurements, which reaches about a factor of three further out than stars.

Chapter 2

Continuum radiation processes

2.1 Radiation of an accelerated electron

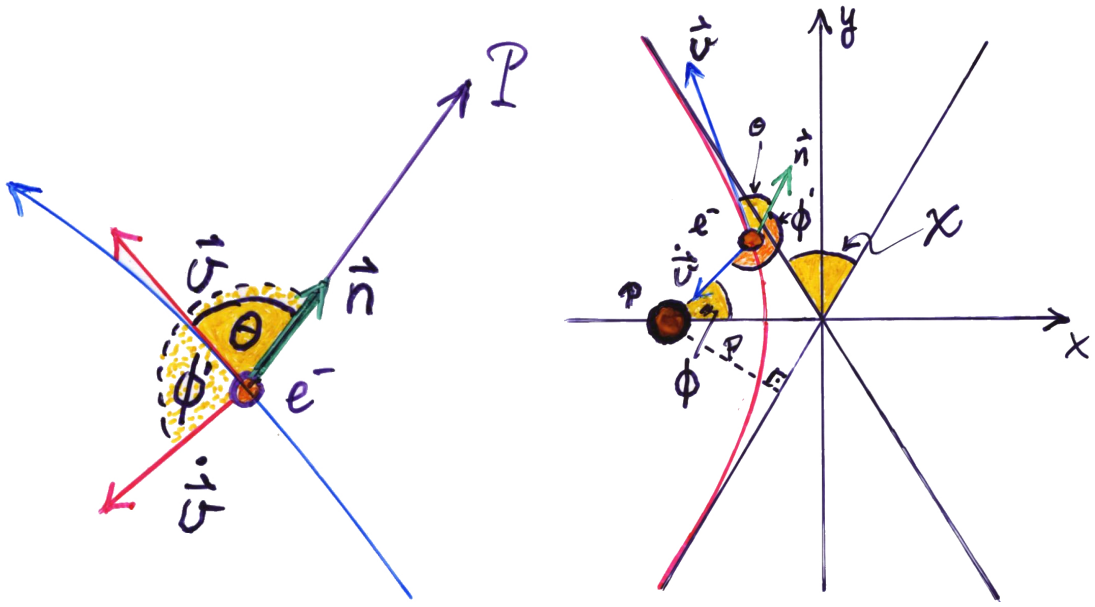

Figure 2.1: Sketches of an accelerated electron

Electric field of an accelerated electron at point P[1]:

$$\vec{E} = \frac{e}{c} \cdot \frac{\vec{n} \times [(\vec{n} - \vec{\beta}) \times \dot{\vec{\beta}}]}{R \cdot (1 - \cos\theta \cdot \beta)^3} \tag{2.1}$$

$$\vec{\beta} = \frac{\vec{v}}{c} \tag{2.2}$$

$$\dot{\vec{\beta}} = \frac{\dot{\vec{v}}}{c} \tag{2.3}$$

[1]See Jackson, Chapt. 14

Poynting vector:

$$\vec{S} = \frac{c}{4\pi} \cdot \vec{E} \times \vec{B} = \frac{c}{4\pi} \cdot |\vec{E}|^2 \cdot \vec{n} \tag{2.4}$$

Radiated power:

$$\frac{dP(t)}{d\Omega} = |\vec{S}| \cdot (1 - \beta \cdot \cos\theta) \cdot R^2 \tag{2.5}$$

$$= \frac{e^2}{4\pi c} \cdot \frac{|\vec{n} \times [(\vec{n} - \vec{\beta}) \times \dot{\vec{\beta}}]|^2}{(1 - \beta \cdot \cos\theta)^5} \tag{2.6}$$

This equation will be used for the case of thermal radiation, where $\beta \ll 1$ and the case of nonthermal radiation, where $\beta \simeq 1$

$\theta = \measuredangle(\vec{v}, \vec{n})$, i.e. $\cos\theta = \vec{n} \cdot \vec{\beta}$

2.2 Free-free radiation

2.2.1 Situation

We first need to compute the emitted power of a single accelerated electron. Situation: Plasma (HII region) with $T \approx 10^4\text{K} \cong 1\text{eV}$, mostly protons and electrons (some He ions); $n_e \approx n_p$ ranges from $0.03\,\text{cm}^{-3}$ to $10^6\,\text{cm}^{-3}$ (e.g. centre of Ori A); electrons move on hyperbolic orbits between protons; acceleration, *mainly* $\dot{\vec{v}} \perp \vec{v}$

Coulomb law:

$$\dot{\vec{v}}(t) = -\frac{Z \cdot e^2}{m_e} \cdot \frac{\vec{r}}{r^3} \tag{2.7}$$

main acceleration acts in the x-direction:

$$\ddot{x} = \frac{Z \cdot e^2}{m_e \cdot r^2} \cdot \cos\phi \tag{2.8}$$

$$\ddot{y} = \frac{Z \cdot e^2}{m_e \cdot r^2} \cdot \sin\phi \tag{2.9}$$

2.2.2 Radiation in the non-relativistic case

$$\frac{dP(t)}{d\Omega} = \frac{e^2}{4\pi c} \cdot \frac{|\vec{n} \times [(\vec{n} - \vec{\beta}) \times \dot{\vec{\beta}}]|^2}{(1 - \beta \cdot \cos\theta)^5}$$

$$= \frac{e^2}{4\pi c^3} \cdot \dot{v}^2(t) \cdot \sin^2\phi' \quad \text{for} \quad \beta \approx 0 \quad \text{i.e.} \quad (1 - \beta\cos\theta) = 1$$

$$\boxed{P(t) = \iint_{4\pi} \frac{dP}{d\Omega} \cdot \Omega = \frac{2e^2}{3c^3} \cdot \dot{v}^2(t)} \tag{2.10}$$

We now have $P(t)$, but need $P(\nu)$ or $P(\omega)$ in order to derive the frequency spectrum of a single particle; usual procedure: Fourier analysis, or Fourier transform.

$$\ddot{x}(t) = \int_0^\infty C(\omega) \cdot \cos \omega t \cdot d\omega \tag{2.11}$$

$$C(\omega) = \frac{1}{\pi} \int_{-\infty}^{+\infty} \ddot{x}(t) \cdot \cos \omega t \cdot dt \tag{2.12}$$

$\ddot{x}(t)$ looks like a "spike" as we have seen. If it were a pulse (δ-function), then the frequency spectrum would be finite. Its finite width gives rise to a finite frequency spectrum.

$$\text{Coulomb's law: } \ddot{x} = \frac{Z \cdot e^2}{m_e \cdot r^2} \cdot \cos \phi \tag{2.13}$$

particles move a distance $v \cdot dt$ during dt:

$$v \cdot dt = d(p \cdot \tan \phi) = p \cdot \frac{d\phi}{\cos^2 \phi} \tag{2.14}$$

(since p doesn't change significantly while $\ddot{x}$ is large)

$$\Rightarrow dt = \frac{p}{v} \cdot \frac{d\phi}{\cos^2 \phi} \tag{2.15}$$

radiation only significant for $-\frac{p}{v} < t < \frac{p}{v}$ for which $\omega t \ll 1 \Rightarrow \cos \omega t \approx 1$. With $p = r \cdot \cos \phi$ we have

$$\begin{aligned} C(\omega) &= \frac{1}{\pi} \cdot \int_{\pi/2}^{\pi/2} \frac{Ze^2}{m_e p^2} \cdot \cos^3 \phi \cdot \frac{p}{v} \cdot \frac{d\phi}{\cos^2 \phi} \\ &= \frac{Ze^2}{\pi m_e p v} \cdot \int_{\pi/2}^{\pi/2} \cos \phi \, d\phi = \frac{2 \cdot ze^2}{\pi m_e p v} \end{aligned} \tag{2.16}$$

Now Parseval's theorem comes[2] into play:

$$\int_{-\infty}^{+\infty} \dot{v}^2(t) dt = \pi \cdot \int_0^\infty C^2(\omega) d\omega \tag{2.17}$$

$$\int_{-\infty}^{+\infty} P(t) dt = \int_0^\infty P(\omega) d\omega \tag{2.18}$$

With

$$P(t) = \frac{2e^2}{3c^3} \cdot \dot{v}^2(t) \tag{2.19}$$

this yields

$$\begin{aligned} P(\omega)d\omega = P(t)dt &= \frac{2e^2}{3c^3} \cdot \pi \cdot C^2(\omega) d\omega \\ &= \frac{16 \cdot e^6 \cdot Z^2}{3 \cdot m_e \cdot p^2 \cdot v^2 \cdot c^3} d\nu \end{aligned} \tag{2.20}$$

[2]Recall that $P(t) \sim \ddot{x}^2$

Recalling that $P(\omega) \approx 0$ for $\nu > \frac{v}{2\pi p}$ we have

$$P(\nu)d\nu = \frac{16 \cdot e^6 \cdot Z^2}{3 \cdot m_e \cdot p^2 \cdot v^2 \cdot c^3} d\nu \qquad \text{for} \quad \nu \leq \frac{v}{2\pi p} \tag{2.21}$$

$$P(\nu)d\nu = 0 \qquad \text{for} \quad \nu \geq \frac{v}{2\pi p} \tag{2.22}$$

estimate of $\nu_{\max}$: e.g. $n_e = n_{\rm i} = 10^3\,{\rm cm}^{-3}$ (centre of Orion), $T_e = 10^4\,{\rm K}$; $n_e \Rightarrow \overline{d} = 0.1\,{\rm cm} \Rightarrow$ $p \leq 0.05\,{\rm cm}$, $v = 700\,{\rm km\,s}^{-1} \Rightarrow \nu = 1/\tau \approx 1.4\,{\rm GHz}$

2.2.3 Total radiation

We now consider the emission of an ensemble of thermal electrons. Let n_e be the number of electrons and $n_{\rm i}$ the number of ions. Electrons have collision parameters between p and $p + dp$; the the number of Coulomb collisions with $(p, p + dp)$ per second of time that an electron with velocity v will experience is equal to the number of ions within a cylindrical ring with length v and, respectivly, inner and outer radii p and $p + dp$; this produces

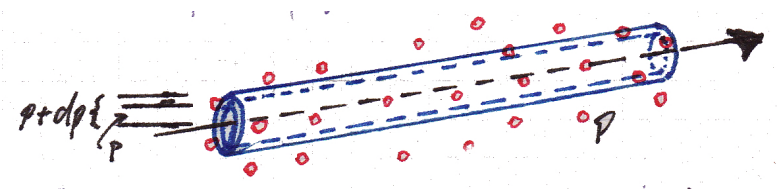

$$n_c = v \cdot 2\pi p \cdot dp \cdot n_{\rm i} \tag{2.23}$$

collisions; the number of collisions per cm^3 involving electrons with velocities between v and $v + dv$ then is

$$dN(v, p) = (v \cdot 2\pi p \cdot dp) \cdot n_{\rm i} \cdot n_e \cdot f(v)dv \quad {\rm cm}^{-3}\,{\rm s}^{-1} \tag{2.24}$$

where $f(v)$ is the Maxwellian velocity distribution:

$$f(v)dv = 4\pi \left(\frac{m_e}{2\pi k_B T_e}\right)^{3/2} e^{-\frac{m_e v^2}{2k_B T_e}} \cdot v^2 \cdot dv \qquad T_e = \text{electron temperature} \tag{2.25}$$

Total energy emitteld per second, per Hz, per cm^3 $= 4\pi \cdot \varepsilon_\nu$

$$\begin{aligned} 4\pi \cdot \varepsilon_\nu &= \int_{p_1}^{p_2} \int_0^\infty P(v, p) \cdot dN(v, p) \\ &= \iint \frac{16 \cdot e^6 \cdot Z^2}{3 \cdot m_e^2 \cdot p^2 \cdot v^2 \cdot c^3} \cdot n_i \cdot n_e \cdot f(v) \cdot 2\pi p \cdot dp \cdot v dv \\ &= \frac{32 \cdot \pi \cdot e^6 \cdot Z^2 \cdot n_i \cdot n_e}{3 \cdot m_e^2 \cdot c^3} \cdot \int_0^\infty \frac{f(v)}{v} dv \cdot \int_{p_1}^{p_2} \frac{dp}{p} \end{aligned}$$

so that

$$\varepsilon_\nu = \frac{8 \cdot e^6 \cdot Z^2 \cdot n_i \cdot n_e}{3 \cdot m_e^2 \cdot c^3} \cdot \int_0^\infty \frac{f(v)}{v} dv \cdot \int_{p_1}^{p_2} \frac{dp}{p} \tag{2.26}$$

here

$$\int_0^\infty \frac{f(v)}{v}dv = \left\langle \frac{1}{v} \right\rangle = \sqrt{\frac{2 \cdot m_e}{\pi \cdot k_B \cdot T_e}} \qquad T_e \approx 10^4\,\mathrm{K} \tag{2.27}$$

$$\int_{p_1}^{p_2} \frac{dp}{p} = \ln \frac{p_2}{p_1} = g_{ff} \qquad \text{“Gaunt factor”} \tag{2.28}$$

$$\boxed{\varepsilon_\nu = \frac{8 \cdot e^6 \cdot Z^2 \cdot n_i \cdot n_e}{3 \cdot m_e^{3/2} \cdot c^3} \cdot \sqrt{\frac{2}{\pi \cdot k_B \cdot T_e}} \cdot g_{ff}} \tag{2.29}$$

Limits p_1, p_2 difficult to estimate;
lower bound

p_1: maximum deflection angle. Consider $\chi_{\max} = 90°$ then, at r_0 we have the closest distance and with $\frac{ze^2}{r_0} \approx \frac{m_e v^2}{2}$

$$p > \frac{2 \cdot Ze^2}{m_e v^2} = \frac{2Ze^2}{3k_B T} \tag{2.30}$$

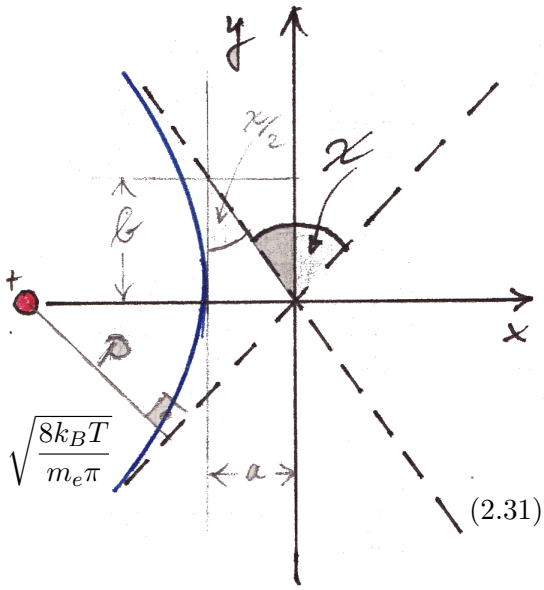

upper bound

p_2: minmum deflection angle. Significant radiation only with frequencies corresponding to the inverse collision time:

$$2\pi\nu = \frac{1}{\tau_{\text{coll}}} = \frac{\langle v \rangle}{p_2} \Rightarrow P < p_2 = \frac{\langle v \rangle}{2\pi\nu} = \frac{1}{2\pi\nu} \cdot \sqrt{\frac{8k_B T}{m_e \pi}} \tag{2.31}$$

Thus, the Gaunt factor becomes

$$g_{ff} = 12.5 + \ln\left[Z^{-1} \cdot \left(\frac{T_e}{10^4\,\mathrm{K}} \right)^{1.5} \cdot \left(\frac{\nu}{\mathrm{GHz}} \right)^{-1} \right] = 10 \cdots 17 \tag{2.32}$$

Now utilize Kirchhoff's law to obtain absorption coefficient:

$$B_\nu(T) = \frac{\varepsilon_\nu}{\varkappa_\nu} = \frac{2h\nu^3}{c^2} \cdot \left(e^{-\frac{h\nu}{k_B T_e}} - 1 \right)^{-1} \tag{2.33}$$

$$\approx \frac{2\nu^2 k_B T_e}{c^2} \quad \text{for} \quad \frac{h\nu}{k_B T_e} \ll 1 \tag{2.34}$$

$$\varkappa_\nu = \sqrt{\frac{2}{\pi}} \cdot \frac{4e^6 Z^2 n_i n_e g_{ff}}{3c(m_e k_B T_e)^{3/2} \nu^2} \tag{2.35}$$

or numerically with the values inserted in c.g.s. units

$$\boxed{\varkappa_\nu = 9.77 \cdot 10^{-3} \cdot n_i \cdot n_e \cdot \nu^{-2} \cdot T^{-3/2} \cdot g_{ff}} \tag{2.36}$$

optical depth:

$$\tau_\nu = \int_0^{s_0} \varkappa_\nu ds \tag{2.37}$$

$$= 8.77 \cdot 10^{-3} \cdot \nu^{-2} \cdot T_e^{-3/2} \cdot g_{ff} \cdot \int_0^{s_0} n_i \cdot n_e ds \tag{2.38}$$

in general the plasma is neutral (zero net charge over the whole volume), i.e. $n_i = n_e$; we define

$$EM = \int_0^{s_0} n_e^2 ds \tag{2.39}$$

as the *emission measure* which has units of $\mathrm{pc\,cm^{-6}}$

$$\boxed{\tau_\nu = 3.01 \cdot 10^{-3} \cdot \left(\frac{EM}{10^6\,\mathrm{pc\,cm^{-6}}}\right) \cdot \left(\frac{\nu}{\mathrm{GHz}}\right)^{-2} \cdot \left(\frac{T_e}{10^4\,\mathrm{K}}\right)^{-1.5} \cdot g_{ff}} \tag{2.40}$$

e.g. Orion nebula: $EM \approx 10^6\,\mathrm{pc\,cm^{-6}} \Rightarrow \tau \simeq 1$ at $\nu = 0.6\,\mathrm{GHz}$

Radiative transfer:

$$I_\nu = B_\nu(T_e) \cdot \left(1 - e^{\,\tau_\nu}\right) \tag{2.41}$$

Consider optically thick and thin case:

$$\tau_\nu \gg 1 : I_\nu = B_\nu(T_e) \rightarrow \text{Planck's law ("featureless")} \tag{2.42}$$

$$\tau_\nu \ll 1 : I_\nu = \tau_\nu \cdot B_\nu(T_e) \approx \frac{2\nu^2 k_B T_e}{c^2} \cdot \tau_\nu \tag{2.43}$$

$$= 8.29 \cdot 10^{-23} \cdot \left(\frac{EM}{10^6\,\mathrm{pc\,cm^{-6}}}\right) \left(\frac{T_e}{10^4\,\mathrm{K}}\right)^{-0.5} g_{ff} \quad \mathrm{erg\,s^{-1}\,cm^{-2}\,Hz^{-1}\,sr^{-1}} \tag{2.44}$$

In radio astronomy, the term "brightness temperature" is commonly used; defined via Rayleigh-Jeans approximation.

$$I_\nu := \frac{2k_B\nu^2}{c^2} \cdot T_\nu \qquad \text{often: } T_b \tag{2.45}$$

$$\boxed{T_\nu = \frac{c^2}{2k_B\nu^2} \cdot I_\nu} \tag{2.46}$$

$$\tau_\nu \gg 1 : I_\nu = B_\nu \Rightarrow T_\nu = T_e \tag{2.47}$$

$$\tau_\nu \ll 1 : I_\nu = \tau_\nu \cdot B_\nu \Rightarrow T_\nu = \tau_\nu \cdot T_e \tag{2.48}$$

$$\left.\begin{array}{rcl} I_\nu & \propto & \nu^2 \\ T_\nu & = & T_e \end{array}\right\} \nu \gg 1 \tag{2.49}$$

$$\left.\begin{array}{rcl} I_\nu & \propto & \nu^{-0.1} \\ T_\nu & \propto & \nu^{-2.1} \end{array}\right\} \nu \ll 1 \tag{2.50}$$

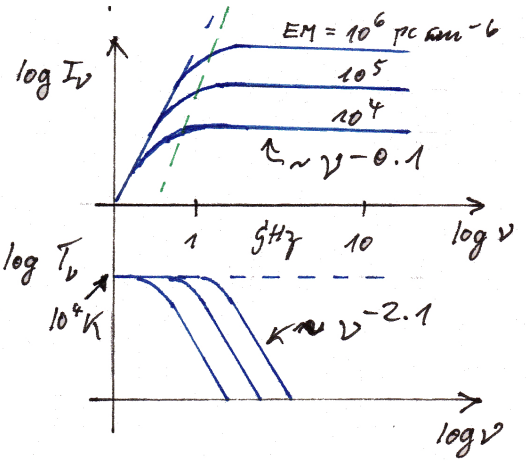

Figure 2.2: Intensity and brightness temperature for different emission measures

measuring T_ν or I_ν over a sufficient freqency range allows to determine the emission measure, which is the dominant factor in the optical depth $\Rightarrow$ $\langle n_e^2 \rangle^{1/2}$.

Apart from the characteristic continuum spectrum described above, thermal free-free radiation is *unpolarized*, since the trajectories of the electrons are randomly oriented.

2.3 Synchrotron radiation

2.3.1 Radiation from a single electron

$$\frac{dP(t)}{d\Omega} = \frac{e^2}{4\pi c} \cdot \frac{|\vec{n} \times [(\vec{n} - \vec{\beta}) \times \dot{\vec{\beta}}]|^2}{(1 - \vec{n} \cdot \vec{\beta})^5} \tag{2.51}$$

The non-relativistic case was treated in the previous chapter. In the relativistic cas we distinguish the

- linear accelerator, $\dot{\vec{\beta}} \parallel \vec{\beta}$ ($\vec{E}$-field)
- cyclotron, $\dot{\vec{\beta}} \perp \vec{\beta}$ ($\vec{B}$-field)

We briefly consider the *linear accelerator* (acceleration in electric field)

$$\theta = \measuredangle(\vec{n}, \vec{\beta}) \quad \text{or} \quad (\vec{n}, \dot{\vec{\beta}}) \tag{2.52}$$

$$(\vec{n} - \vec{\beta}) \times \dot{\vec{\beta}} = \vec{n} \times \dot{\vec{\beta}} \quad \text{since} \quad \vec{\beta} \times \dot{\vec{\beta}} = \vec{0} \tag{2.53}$$

$$= \dot{\beta} \cdot \cos\theta \cdot \vec{n} - \dot{\vec{\beta}} \tag{2.54}$$

$$|\vec{n} \cdot \dot{\vec{\beta}} \cdot \cos\theta - \dot{\vec{\beta}}|^2 = \dot{\vec{\beta}}^2 \cdot \cos^2\theta + \dot{\vec{\beta}}^2 - 2\vec{n} \cdot \dot{\vec{\beta}} \cdot \cos\theta \tag{2.55}$$

$$= \dot{\vec{\beta}}^2 \cdot (1 - \cos^2\theta) = \dot{\vec{\beta}} \cdot \sin^2\theta \tag{2.56}$$

$$\boxed{\frac{dP(t)}{d\Omega} = \frac{e^2 \cdot \dot{v}^2}{4\pi c^3} \cdot \frac{\sin^2\theta}{(1 - \beta \cdot \cos\theta)^5}} \tag{2.57}$$

$$P(t) = \frac{2}{3} \cdot \frac{e^2 \cdot \dot{v}^2}{4\pi c^3} \cdot \gamma^6 \qquad \gamma = \frac{1}{\sqrt{1 - \beta^2}} \tag{2.58}$$

maximum radiation at

$$\theta_{\max} = \frac{1}{2\gamma} \tag{2.59}$$

$$\cos\theta_{\max} = \frac{1}{3\beta} \cdot \left(\sqrt{1 + 15\beta} - 1\right) \tag{2.60}$$

$$\frac{dP(t)}{d\Omega}(\theta_{\max}) \propto \gamma^8 \tag{2.61}$$

e.g.: $E = 1$ GeV, $\gamma = \frac{E}{m_0 c^2}$, $m_0 c^2 = 511$ keV $\Rightarrow \gamma = 2000 \Rightarrow \theta_{\max} \approx 1'$

transverse accelerator is the more important process in astrophysics:

$$\theta = \measuredangle(\vec{n}, \vec{\beta}), \quad \phi' = \measuredangle(\vec{n}, \dot{\vec{\beta}}) \tag{2.62}$$

$$\phi = \text{angle measured along a circle } \perp \vec{v} \tag{2.63}$$

$$\theta = \text{angle measured in the } (\vec{v}, \dot{\vec{v}})\text{-plane} \tag{2.64}$$

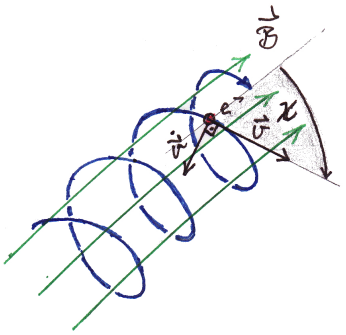

assume that particles move in the interstellar magnetic field → Lorentz force. With $\vec{\beta} \perp \dot{\vec{\beta}}$:

$$\frac{dP(t)}{d\Omega} = \frac{e^2 \cdot \dot{v}^2}{4\pi c^3} \cdot \frac{\left[1 - \frac{\sin^2\theta\cos^2\phi}{\gamma^2(1-\beta\cdot\cos\theta)^2}\right]}{(1-\beta\cdot\cos\theta)^3} \tag{2.65}$$

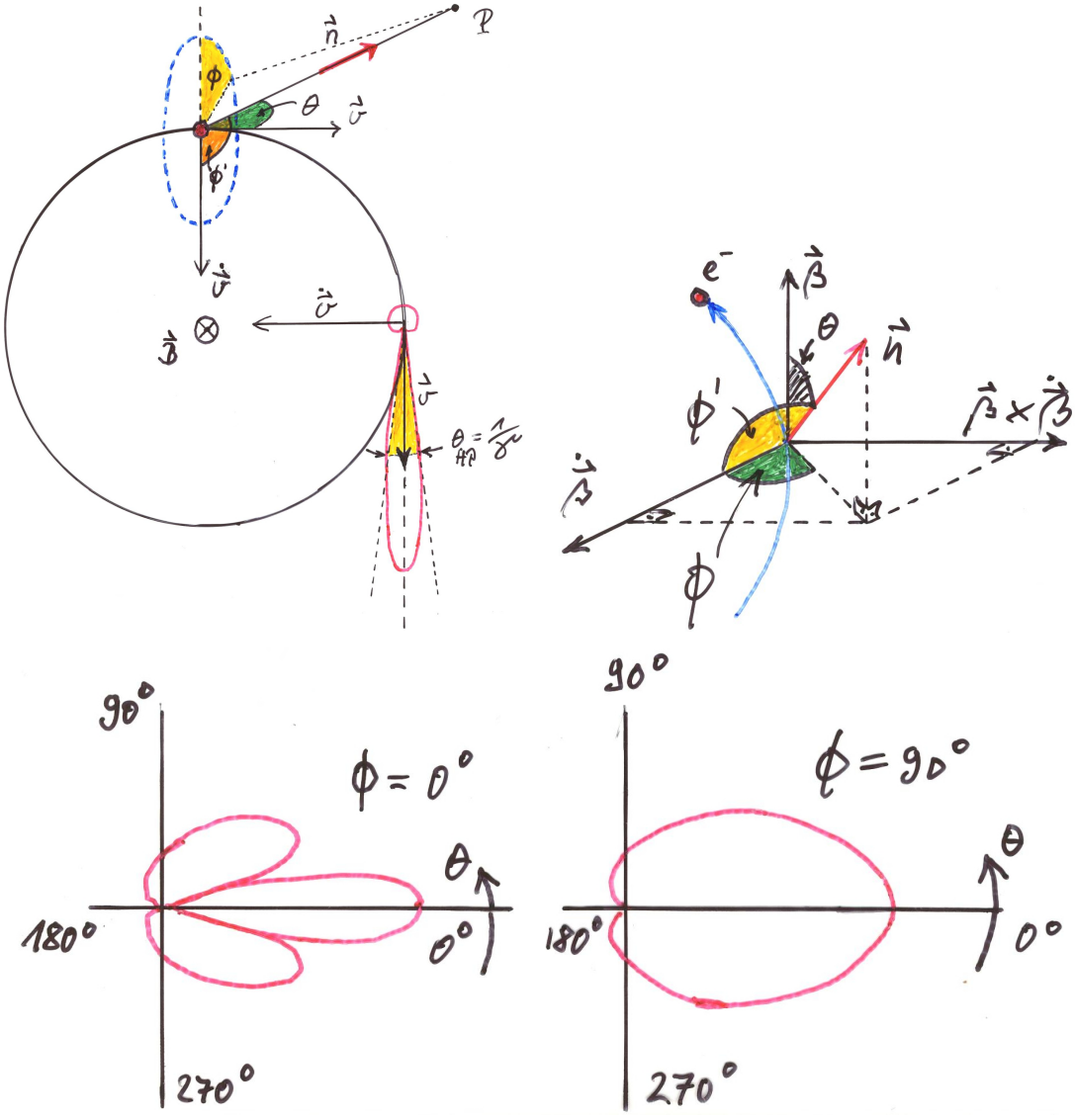

Figure 2.3: Sketches of an accelerated electron

Relativistic motion → relativistic abberation (strong distortion of radiation pattern): *relativistic beaming*; width of radiation pattern: main lobe has width of $1/\gamma$ at half maximum!

Proof: easy for zero-points, since

$$\frac{dP(t)}{d\Omega} = 0 \qquad \text{implies} \qquad 1 - \frac{\sin^2\theta_0 \cos^2\phi}{\gamma^2 \cdot (1 - \beta \cdot \cos\theta_0)^2} = 0 \tag{2.66}$$

go into $\phi' = 0°$-plane

$$\Rightarrow \gamma^2 \cdot (1 - \beta \cdot \cos\theta_0)^2 = \sin^2\theta_0 \tag{2.67}$$

need to consider small angles only, i.e.

$$\left.\begin{array}{rcl} \sin\theta_0 & \approx & \theta_0 \\ \cos\theta_0 & \approx & 1 - \frac{\theta_0^2}{2} \end{array}\right\} \gamma \approx \frac{\theta_0}{1 - \beta \cdot \left(1 - \frac{\theta_0^2}{2}\right)} \tag{2.68}$$

$$= \frac{2}{\theta_0} \qquad (\beta \approx 1) \tag{2.69}$$

half-power width: $\theta_{\mathrm{HP}} = \frac{1}{2}\theta_0$

$$\boxed{\theta_{\mathrm{HP}} \approx \frac{1}{\gamma} = \frac{m_0 c^2}{E^2}} \tag{2.70}$$

E.g.: $E = 1$ GeV $\Rightarrow \gamma = 2000 \Rightarrow \theta_{\mathrm{HP}} = 1'.7$

Apart from relativistic aberration, the time evolution as seen in the observer's frame of reference will come into play. Before we look at that, we work out the so-called Larmor circle; equation of motion:

$$m\dot{\vec{v}} = m \cdot (\vec{v} \times \vec{\omega}_L) = -\frac{e}{c} \cdot (\vec{v} \times \vec{B}) \qquad \text{Lorentz force} \tag{2.71}$$

$$\omega_L = \text{Larmor frequency} \tag{2.72}$$

$$\chi = 90° \Rightarrow m \cdot \omega_L^2 \cdot r_L = m \cdot \frac{v^2}{r_L} = \frac{e}{c} \cdot v \cdot B \tag{2.73}$$

$$\Rightarrow m\frac{v}{r_L} = \frac{e \cdot B}{c} \tag{2.74}$$

$$\text{or } \boxed{\omega_L = \frac{e \cdot B}{m \cdot c}} \qquad \text{Larmor frequency} \tag{2.75}$$

Note: $m = m_0 \cdot \gamma$, since $\gamma = \frac{E}{m_0 \cdot c^2}$, i.e. $E = mc^2 = \gamma \cdot m_0 \cdot c^2$

$$\boxed{\omega_L = \frac{e \cdot B}{\gamma \cdot m_0 \cdot c}} \tag{2.76}$$

in the relativistic case, the Larmor frequency is decreased by a factor γ! The Larmor radius is easily obtained via

$$r_L = \frac{v}{\omega_L} = \frac{m_0 \cdot v \cdot c}{e \cdot B} \cdot \gamma \approx \frac{m_0 \cdot c^2}{c \cdot B}\gamma = \frac{E}{e \cdot B} \tag{2.77}$$

or in general ($\chi \neq 90°$)

$$\boxed{r_L = \frac{E \cdot \sin\chi}{e \cdot B}} \qquad \text{Larmor radius} \tag{2.78}$$

Table 2.1: Some examples for $B = 10\ \mu$G:

E [eV]	r_L	ν_L [Hz]	γ
10^9	$3.3 \cdot 10^6$ km	$1.4 \cdot 10^{-2}$	2000
$4.5 \cdot 10^{10}$	$1.5 \cdot 10^8$ km	$3.1 \cdot 10^{-4}$	$9 \cdot 10^4$
10^{20}	10 kpc !	$1.4 \cdot 10^{-13}$	$2 \cdot 10^{14}$

Note: $\nu_L = 28\,\text{Hz}$ for $\gamma = 1$, $B = 10\,\mu$G

How, then, can we detect synchrotron radiation in the radio regime? $\Rightarrow$ need to calculate the time dependence of the radiation as seen by the observer. Duration of pulse:

$$\Delta t = \frac{r_L \cdot \theta_{\text{HP}}}{v} \approx \frac{r_L \cdot \theta_{\text{HP}}}{c} \qquad (\beta \approx 1) \tag{2.79}$$

$$r_L \approx \frac{E}{e \cdot B} \qquad (\chi = 90°,\ \beta \approx 1) \tag{2.80}$$

$$\Rightarrow \Delta t = \frac{E \cdot \theta_{\text{HP}}}{e \cdot B \cdot c} = \frac{m_0 \cdot c^2 \cdot E}{E \cdot e \cdot B \cdot c} \tag{2.81}$$

so this yields

$$\boxed{\Delta t = \frac{m_0 \cdot c}{e \cdot B}} \tag{2.82}$$

which is about 6 ms in a 10 μG field. This corresponds to a frequency of $\nu = 180$ Hz.

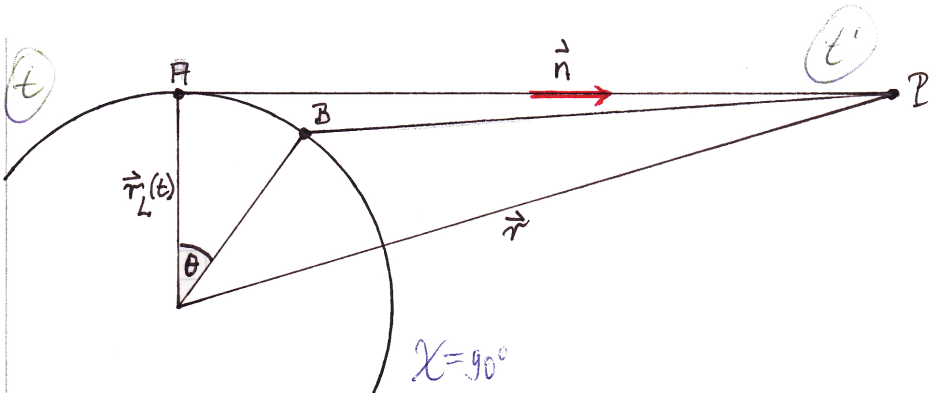

$t' = t +$ time from A $\rightarrow$ B, i.e.

$$t' = t + \frac{|\vec{r} - \vec{r}_L(t)|}{c} \tag{2.83}$$

$$\frac{dt'}{dt} = 1 - \frac{1}{c} \cdot \frac{\vec{r} - \vec{r}_L(t)}{|\vec{r} - \vec{r}_L(t)|} \cdot \frac{d\vec{r}_L}{dt} = 1 - \frac{\vec{n} \cdot \vec{v}}{c} = 1 - \beta \cdot \cos\theta_{\mathrm{HP}} \tag{2.84}$$

$$\approx 1 - \beta \cdot \sqrt{1 - \theta_{\mathrm{HP}}^2} = 1 - \beta \cdot \sqrt{1 - \frac{1}{\gamma^2}} = 1 - \beta^2 = \frac{1}{\gamma^2} \tag{2.85}$$

$$\boxed{\Delta t' = \frac{\Delta t}{\gamma^2}} \tag{2.86}$$

This means that the frequency spectrum is shifted towards a γ^2-times higher range; e.g. $E = 1$ GeV $\Rightarrow \gamma = 2000 \Rightarrow \nu \approx 700$ MHz for a 10 μG magnetic field!

A more precise determination of the radiation sprectrum (of a single electron) requires a Fourier analysis (such as in the non-relativistic case).

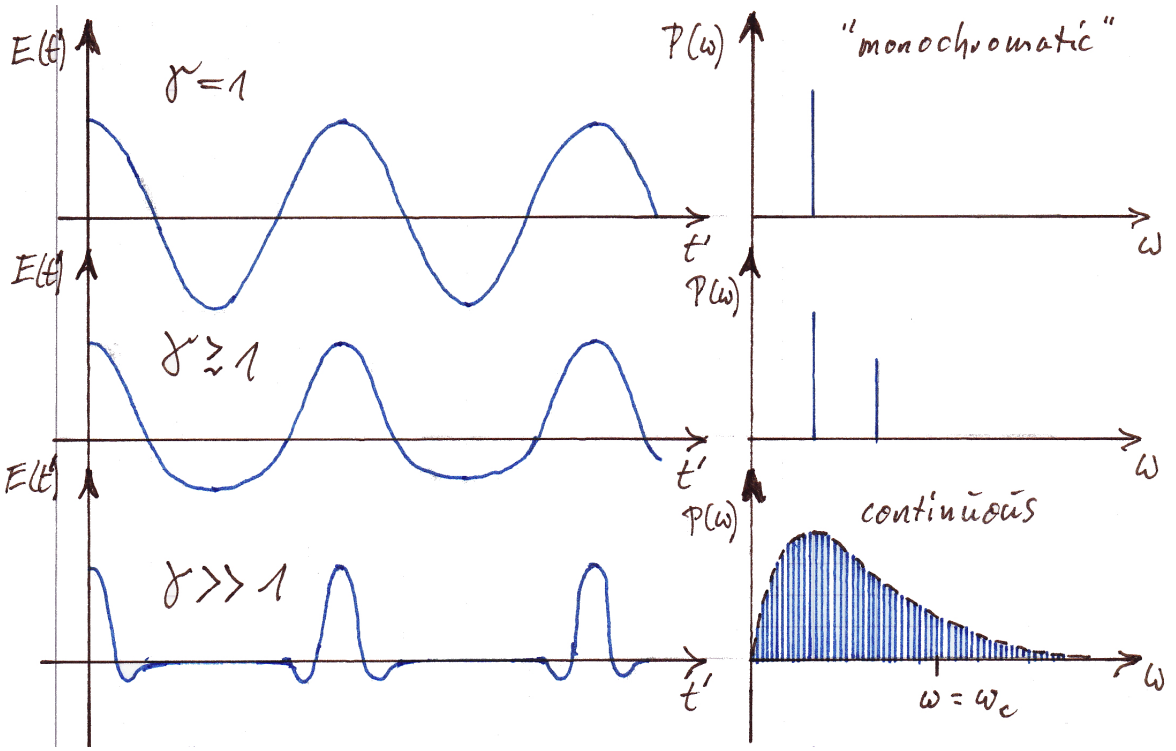

We define a critical frequency such that the particles produce significant power up to that frequency ω_c. Various definitions are found in the literature:

$$\omega_c = 2\pi\nu_c \overset{\text{Schwinger}}{=} \frac{3}{2 \cdot \Delta t'} \tag{2.87}$$

$$\omega_c = 2\pi\nu_c \overset{\text{Ginzburg}}{=} \frac{1}{\Delta t'} \tag{2.88}$$

$$\omega_c = 2\pi\nu_c \overset{\text{Jackson}}{=} \frac{3}{\Delta t'} \tag{2.89}$$

In what follows, we'll use Schwingers[3] definition.

$$\Rightarrow \boxed{\nu_c = \frac{3}{4\pi} \cdot \frac{eB_\perp}{m_0 c} \cdot \gamma^2} \tag{2.90}$$

$$B_\perp = B \cdot \sin\chi \tag{2.91}$$

E [GeV]	γ	ν_L
1	2000	170 MHz
45	$9 \cdot 10^4$	340 GHz
10^{11}	$2 \cdot 10^{14}$	$1.7 \cdot 10^{30}$

Table 2.2: Some examples for $B = 10\ \mu$G:

What about protons? The cyclotron radiation energy spectrum observed near earth exhibits $\simeq 100$ times more protons than electrons *at the same energy.* Nevertheless, they do not contribute significantly to the emission, since

$$\nu_c = \frac{3}{4\pi} \cdot \frac{eB_\perp}{m_0 \cdot c} \cdot \gamma^2 = \frac{3}{4\pi} \cdot \frac{eB_\perp \cdot E^2}{m_0^3 \cdot c^5} \quad . \tag{2.92}$$

Thus, ν_c depends on the mass of the radiating partikle like m^{-3}

$$\left(\frac{m_p}{m_e}\right)^{-3} = 1.6 \cdot 10^{-10} \qquad \Rightarrow \qquad \frac{\nu_{c,p}}{\nu_{c,e}} = 1.6 \cdot 10^{-10} \tag{2.93}$$

Put differently, we can calculate how much more kinetic energy a proton must have in order to radiate at the same frequency as the electron:

$$E_p = \left(\frac{m_p}{m_e}\right)^{3/2} \cdot E_e = 8 \cdot 10^4 \tag{2.94}$$

Hence, even the ratio of the number densities $n_p/n_e \approx 100$ does not help. Fourier analysis together with equation 2.65 (for small θ and large γ) yields:

$$\frac{dP}{d\Omega} = \frac{2}{\pi} \cdot \frac{e^2 \cdot \dot{v}^2}{c^3} \gamma^6 \cdot \frac{1}{(1+\gamma^2\theta^2)^3} \cdot \left[1 - \frac{4\gamma^2\theta^2 \cos^2\phi}{(1+\gamma^2\theta^2)^2}\right] \tag{2.95}$$

$$\int_0^\pi \int_0^{2\pi} \frac{dP}{d\Omega} d\Omega = \frac{2}{3} \cdot \frac{e^2 \cdot \dot{v}^2}{c^3} \gamma^4 \tag{2.96}$$

$$P(\nu) = \frac{\sqrt{3} c^3}{m_0 c^2} \cdot B_\perp \cdot F\left(\frac{\nu}{\nu_c}\right) \tag{2.97}$$

where

$$F\left(\frac{\nu}{\nu_c}\right) = \frac{\nu}{\nu_c} \cdot \int_{\nu/\nu_c}^\infty K_{5/3}(x) dx \tag{2.98}$$

[3] J. Schwinger: 1949, Phys.Rev.75, 1912-1925

$F\left(\frac{\nu}{\nu_c}\right)$ is the so-called Airy integral of the modified Bessel function $K_{5/3}(x)$. It is well approximated by Wallis' approximation[4]:

$$F\left(\frac{\nu}{\nu_c}\right) = 1.78 \cdot \left(\frac{\nu}{\nu_c}\right)^{0.3} \cdot e^{-\frac{\nu}{\nu_c}} \tag{2.99}$$

2.3.2 Synchrotron radiation from relativistic electrons with an energy spectrum

Need to know energy spectrum, which has been measured in the vicinity of the earth. A power-law of the following form is found:

$$N(E)dE = A \cdot E^{-g} dE \tag{2.100}$$

where A is a constant[5] and $g = 2.4$. As usual, we compute the intensity via the emissivity as follows:

$$4\pi \cdot \varepsilon_\nu = \int_{E_1}^{E_2} P(\nu) \cdot N(E) dE \tag{2.101}$$

$$I_\nu = S_\nu(T) \cdot (1 - e^{-\tau_\nu}) \qquad \text{no background radiation} \tag{2.102}$$

$$\approx S_\nu(T) \cdot \tau_\nu \qquad \tau_\nu \ll 1 \,;\, S_\nu = \text{source function} \overset{\text{LTE}}{=} B_\nu(T) \tag{2.103}$$

Kirchhoff's law:

$$S_\nu(T) = \frac{\varepsilon_\nu}{\varkappa_\nu} \qquad \Rightarrow \qquad I_\nu = \int_0^{s_0} \varepsilon_\nu ds \tag{2.104}$$

Hence

$$I_\nu = \frac{1}{4\pi} \cdot \int_0^{s_0} \int_0^{\infty} P(\nu) \cdot N(E) \cdot dE \cdot ds \qquad \text{W m}^{-2} \text{ Hz}^{-1} \text{ sr}^{-1} \tag{2.105}$$

For the sake of simplicity, we assume that neither $P(\nu)$ or $N(E)$ are depending on s, i.e. $dP/ds = dN/ds = 0$. Then

$$I_\nu = \frac{s_0}{4\pi} \cdot \frac{\sqrt{3} \cdot e^3}{m_0 \cdot c^2} \cdot B_\perp \cdot A \cdot \int_0^{\infty} F\left(\frac{\nu}{\nu_c}\right) \cdot E^{-g} dE \tag{2.106}$$

Wallis approximation delivers

$$I_\nu = \frac{s_0}{4\pi} \cdot \frac{\sqrt{3} e^3}{m_0 c^2} \cdot B_\perp \cdot A \cdot 1.78 \cdot \int_0^{\infty} \left(\frac{\nu}{\nu_0}\right)^{0.3} \cdot e^{-\frac{\nu}{\nu_c}} \cdot E^{-g} dE \tag{2.107}$$

Define

$$C := 1.78 \cdot \frac{\sqrt{3} e^3}{4\pi m_0 c^2} = 3.32 \cdot 10^{-23} \text{ esu}^3 \text{ erg}^{-1} \tag{2.108}$$

$$\nu_c = \frac{3}{4\pi} \cdot \frac{eB_\perp}{m_0^3 c^5} \cdot E^2 := \eta \cdot B_\perp \cdot E^2 \quad \text{where} \quad \eta = 6.26 \cdot 10^{18} \text{ s}^4 \text{ g}^{-5/2} \text{ cm}^{-1/2} \tag{2.109}$$

[4] G. Wallis; 1959 in "Paris Symp. on Radio Astronomy", ed. R. N. Bracewell, p. 595-597

[5] A refers to the local conditions. It contains the local number density of relativistic particles per energy interval.

substitution:

$$x = \left(\frac{\eta \cdot B}{\nu}\right)^{1/2} \cdot E \quad \Rightarrow \quad dE = \left(\frac{\nu}{\eta \cdot B}\right)^{1/2} \cdot dx \tag{2.110}$$

$$I_\nu = s_0 \cdot C \cdot A \cdot \eta^{\frac{g-1}{2}} \cdot B_\perp^{\frac{g+1}{2}} \cdot \nu^{-\frac{g-1}{2}} \cdot \int_0^\infty x^{-(g+0.6)} \cdot e^{-\frac{1}{x^2}}\, dx \tag{2.111}$$

It conveniently turns out that $g \approx 2.4$[6] so that the integral has a trivial soulution. With

$$\frac{1}{x^2} = u \quad \text{i.e.} \quad -\frac{2}{x^3} dx = du \tag{2.112}$$

it follows that

$$\int_0^\infty x^{-3} \cdot e^{-\frac{1}{x^2}}\, dx = \frac{1}{2} \int_0^\infty e^{-u}\, du = \frac{1}{2} \tag{2.113}$$

With $g \approx 2.4$ we arrive at

$$I_\nu = 2.4 \cdot 10^{-10} \cdot \left(\frac{s_0}{\text{cm}}\right) \left(\frac{A}{\text{erg}^{1.4}\ \text{cm}^{-3}}\right) \left(\frac{B_\perp}{\text{G}}\right)^{1.7} \left(\frac{\nu}{\text{Hz}}\right)^{-0.7} \quad \text{erg s}^{-1}\ \text{cm}^{-2}\ \text{Hz}^{-1}\ \text{sr}^{-1} \tag{2.114}$$

Close to the earth $A = 8.2 \cdot 10^{-17}$ erg$^{1.4}$ cm^{-3}. If this constant would hold over a line of sight of 10 kpc, then with $B = 10\ \mu$G we would expect

$$I_\nu = 10^{-18}\ \text{erg s}^{-1}\ \text{cm}^{-2}\ \text{Hz}^{-1}\ \text{sr}^{-1} \quad \text{at} \quad \nu = 10\text{GHz} \tag{2.115}$$

In general, with

$$N(E)dE \propto E^{-g} dE \tag{2.116}$$

for the synchrotron intensity we arrive at

$$\boxed{I_\nu \propto B_\perp^{1+\alpha} \cdot \nu^{-\alpha}} \tag{2.117}$$

where

$$\alpha = \frac{g-1}{2} \approx 0.7 \quad \text{(typically)} \tag{2.118}$$

Note: The factor of 1/2 arises from $E \propto \nu^{1/2}$. What's happening in computing I_ν is that for each e$^-$ the radiation spectrum $P(\nu)$ (of the single particle) is multiplied successively by the particle density for each energy. The integration over the whole energy range yields the frequency spectrum. In the log-log plot this means that we have to add (logarithmically) the "weighting functions", given by N(E). If the energy spectrum has a cut-off at some energy $E_{\max}$, the spectrum will fall off exponentially beyond the corresponding frequency

$$\nu_c = \frac{3}{4\pi} \cdot \frac{e \cdot B_\perp}{m_0 \cdot c} \cdot \gamma_{\max}^2 \tag{2.119}$$

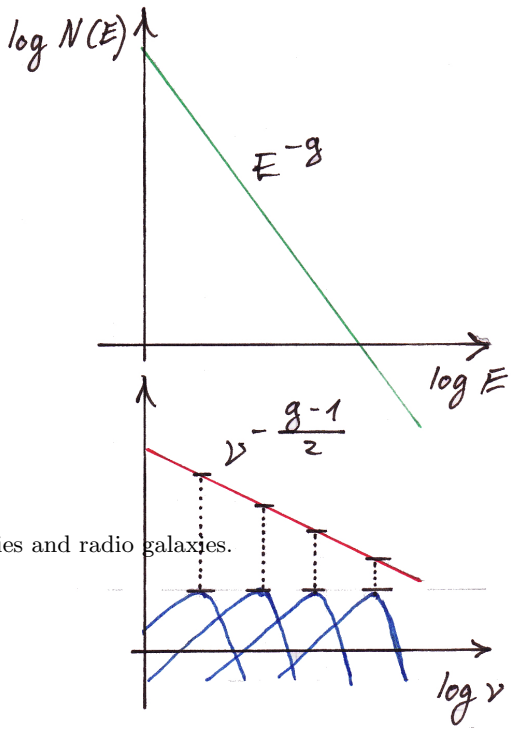

Figure 2.4: Synchrotron radiation power

[6] This value is valid for the Milky Way, external galaxies and radio galaxies.

2.3.3 Polarization properties

Relativistic particles radiate within a narrow beam width of $\theta_{\rm HP} = \gamma^{-1}$. Considering theier helical motion around the magnetic field, the radiation is emitted into a *velocity cone*, which is the cone described by the velocity vector $\vec{v}$; hence the opening angle of the cone is twice the pitch angle χ. The cone axis is parallel to the $\vec{B}$-field and $\vec{v}$ precesses at relativistic gyrofrequency about this direction.

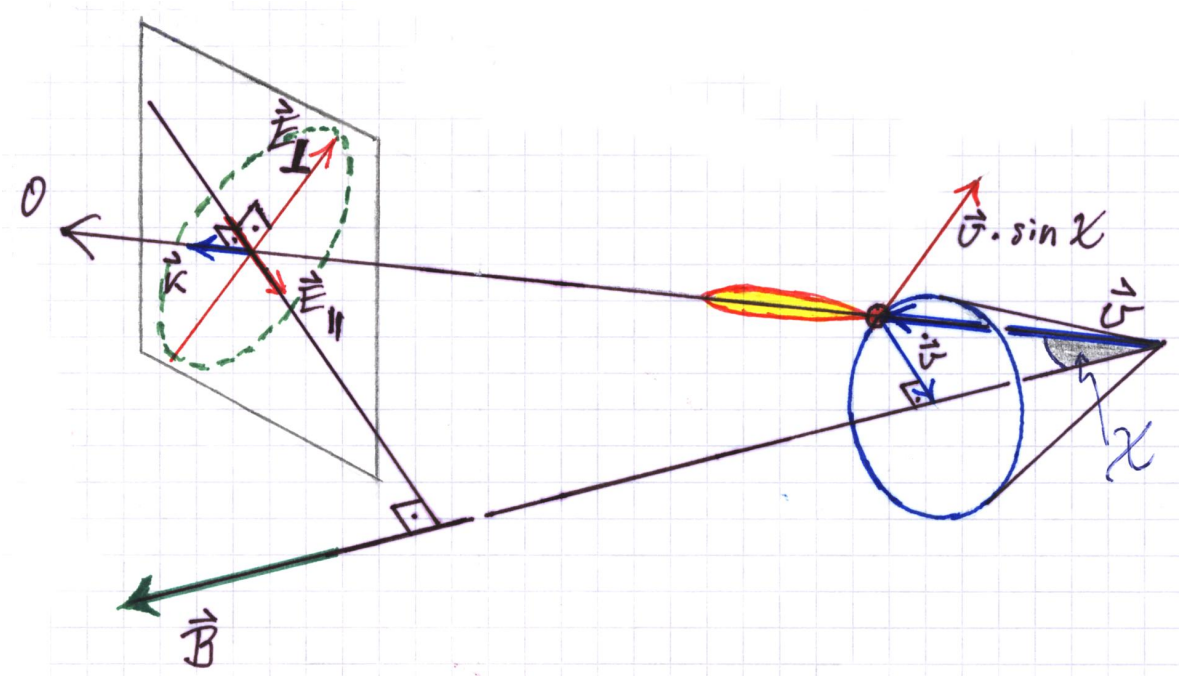

Figure 2.5: Polarization of synchrotron radiation

In the non-relativistic case, looking along the magnetic field lines we would measure circular polarization, or, if viewing at some angle with respect to $\vec{B}$, elliptical polarization. The fundamental difference in case of relativistic particles is that significant radiation is only measured if the trajectory of the electrons lies within the very narrow angle $1/\gamma$ of the line of sight.

The details are rather complicated. The full algebra can be found in Longair (1994)[7]. The best way to understand how a single particle produces elliptical polarization and how an ensemble of particles with a pitch-angle distribution produces net linear polarization is by looking at 3-D velocity cones (paper models). In the case of non- or mildly relativistic particles the radiation pattern would be broad and we would observe the (rotating)$\vec{E}$-vector over the full gyro-circle around the $\vec{B}$-field. If the particles are highly relativistic, then we

[7]M. S. Longair: High Energy Astrophysics, Vol. 2, Chapt. 18, Cambridge University Press, 1994

see the light pulse of width $1/\gamma$ only for a *very* short time, and we see a light pulse only from particles with *one specific pitch angle*. We record the pulse only over a very small fraction of the velocity cone. This automatically implies that the polarization is essentially linear. However, during the finite time that we recive the pulse, it undergoes a slight rotation, giving rise to small amount of elliptical polarization. How can we then understand that the particle ensemble with a random pitch-angle distribution produces net linear polarization?

In order to "see" many particles with different pitch-angles at the same time, we to introduce irregularities of the magnetic field. Otherwise, for a given line of sight we would see one and only one particular velocity cone.

Since the $\vec{E}$-vector traces a circle if the $\vec{B}$-vector is exactly along the line of sight, we would expect circular polarization in the first place. This is actually observed in cyclotron radiation (non- or mildly relativistic electrons, e.g. radiation from the active sun), because in that case the radiation pattern is broad enough that the electron is seen over the full cycle. This changes, however, fundamentally if the particles are highly relativistic. In that case, as we have seen above, we observe a short pulse only if the narrow $(1/\gamma)$ beam sweeps across the line of sight. The result is that we record the $\vec{E}$-vector turning over a small segment of the circle or, in case of the $\vec{B}$-field inclined with respect to the line of sight, of an ellipse. We hence would measure elliptical polarization from particles with a given pitch angle, the dominant polarization being, however, linear, with the $\vec{E}$-vector perpendicular to the $\vec{B}$-field.

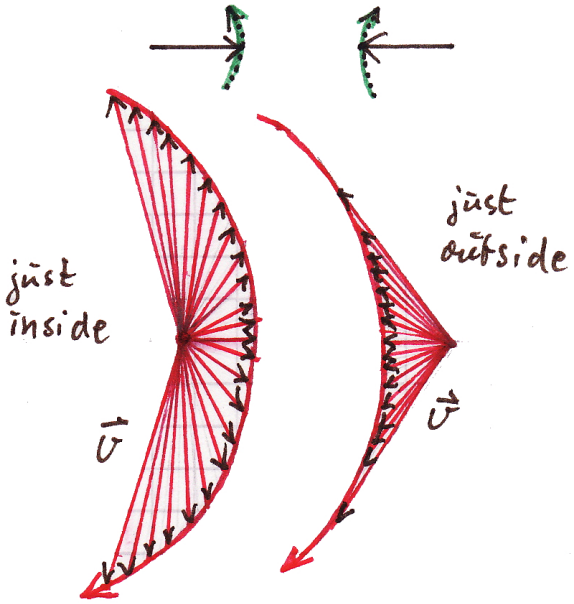

Figure 2.6: Velocity vector

Illustration 2.6 shows that, as seen from the observer, the velocity vector turns right if the velocity cone is viewed such that the line of sight lies just inside the maximum radiation pattern, while it turns left if viewed from just outside. Hence, the corresponding elliptical polarization produced during the short moment that the radiation pattern sweeps across our line of sight is correspondingly right- and left-handed. Since in the presence of a tangled magnetic field and a distribution of pitch-angles we will see an equal number of particles with opposite elliptical polarization. It will cancel nearly perfectly and we will be left with pure linear polarization of the $\vec{E}$-vector measured to be perpendicular to the $\vec{B}$-field.

Precise calculation of degree of polarization from Fourier analysis of $P_\perp(t)$ and $P_\parallel(t)$ yielding

$$P_\perp(\nu) = \frac{\sqrt{3} \cdot e^3 \cdot B_\perp}{m_0 \cdot c^2} \cdot [F(x) + G(x)] \tag{2.120}$$

$$P_\parallel(\nu) = \frac{\sqrt{3} \cdot e^3 \cdot B_\perp}{m_0 \cdot c^2} \cdot [F(x) - G(x)] \tag{2.121}$$

where

$$F(x) = x \cdot \int_x^\infty K_{5/3}(z)dz \qquad \text{(as before)} \tag{2.122}$$

$$G(x) = x \cdot K_{5/3} \tag{2.123}$$

and $x = \nu/\nu_c$. The degree ofpolarization for a single energy is

$$\Pi(\nu) = \frac{P_\perp(\nu) - P_\parallel(\nu)}{P_\perp(\nu) + P_\parallel(\nu)} \tag{2.124}$$

Integrating over a power-law energy spectrum, i.e. $N(E)dE \propto E^{-g}dE$, yields

$$\boxed{\Pi = \frac{g+1}{g+7/3}} = \frac{2\alpha+2}{2\alpha+10/3} = \frac{\alpha+1}{\alpha+5/3} \tag{2.125}$$

With $g = 2.4$, i.e. $\alpha = 0.7$, we expect a maximum degree of linear polarization of a synchrotron source of $\Pi = 72\%$. This assumes that the magnetic field is absoulutely uniform and that there are no depolarizing effects such as beam or Faraday depolarization.

2.3.4 Losses and particle lifetimes

$$P = \frac{2}{3} \cdot \frac{e^2 \cdot \dot{v}^2}{c^3} \cdot \left(\frac{E}{m_0 \cdot c^2}\right)^4 \qquad \text{for synchrotron radiation} \tag{2.126}$$

$$\dot{v} = \frac{v^2}{r_L} = \omega_L \cdot v \tag{2.127}$$

$$\omega_L = \frac{e \cdot B}{m_0 \cdot c} \cdot \frac{1}{\gamma} \tag{2.128}$$

$$\dot{v} = \frac{v \cdot e \cdot B}{m_0 \cdot c} \cdot \frac{m_0 \cdot c^2}{E} \tag{2.129}$$

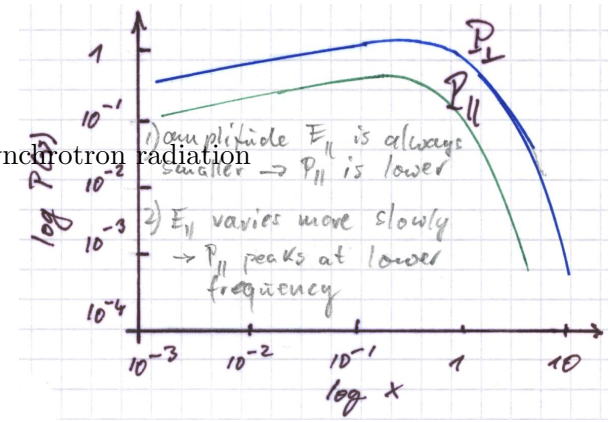

Figure 2.7: Power of polarized radiation

and thus ($v \approx c$)

$$P = \frac{2}{3} \cdot \frac{e^4}{m_0^4 \cdot c^7} \cdot \left(\frac{B}{\mathrm{G}}\right)^2 \left(\frac{E}{\mathrm{erg}}\right)^2 \tag{2.130}$$

Since

$$P \stackrel{!}{=} -\frac{dE}{dt} \tag{2.131}$$

it follows that

$$\frac{dE}{dt} = -2.37 \cdot 10^{-3} \cdot \left(\frac{B}{\mathrm{G}}\right)^2 \left(\frac{E}{\mathrm{erg}}\right)^2 \quad \mathrm{erg\ s^{-1}} \tag{2.132}$$

$$= -1.48 \cdot 10^{-3} \cdot \left(\frac{B}{\mu\mathrm{G}}\right)^2 \left(\frac{E}{\mathrm{eV}}\right)^2 \quad \mathrm{eV\ s^{-1}} \tag{2.133}$$

$$\frac{dE}{E^2} = -a \cdot B^2 \cdot dt \qquad a = 2.37 \cdot 10^{-3}, \quad [E] = \mathrm{erg} \tag{2.134}$$

$$\frac{1}{E_0} - \frac{1}{E} = a \cdot B^2 \cdot (t - t_0) \tag{2.135}$$

Assume that the e^- had energy E_0 at $t_0 = 0$. The half-lifetime $t_{1/2}$ is defined as the time after which the particle hast lost half its energy, i.e. $E(t_{1/2}) = E_0/2$. With

$$E(t) = \frac{1}{\frac{1}{E_0} + a \cdot B^2 \cdot t} = \frac{E_0}{1 + a \cdot B^2 \cdot E_0 \cdot t} \tag{2.136}$$

$$\frac{E_0}{2} = \frac{E_0}{1 + a \cdot B^2 \cdot E_0 \cdot t_{1/2}} \tag{2.137}$$

or

$$t_{1/2} = \frac{1}{a} \cdot B^{-2} \cdot E_0^{-1} \tag{2.138}$$

Inserting a and expressing B in μG and E in GeV, we arrive at

$$\boxed{t_{1/2} = 8.24 \cdot 10^9 \cdot \left(\frac{B}{\mu\mathrm{G}}\right)^{-2} \left(\frac{E}{\mathrm{GeV}}\right)^{-1} \quad \text{years}} \tag{2.139}$$

Assume $B = 10$ μG (e.g. in galaxies)

E [GeV]	$t_{1/2}$ [years]
1	$8 \cdot 10^7$
10	$8 \cdot 10^6$
100	$8 \cdot 10^5$

Evolution of a radio source: Once the energy supply has been switched off, the energy spectrum will have a cutoff that gradually migrates towards lower energies. As a result, the synchrotron radiation sprechtrum exhibits a corresponding exponential decline beyond the cut-off frequency ν_c, which we obtain from

$$\nu_c = \frac{3}{4\pi} \cdot \frac{e \cdot B \cdot E_c^2}{m_0^3 \cdot c^5} \tag{2.140}$$

This cutoff frequency ν_c beyond which the source is rendered undetectable tells us something about the age of the source. Stricly speaking, this is rather the duration of the remnant phase, but it is frequently used as the *source age* synonymously.

$$\boxed{t_{\mathrm{source}} = 5.83 \cdot 10^8 \cdot \left(\frac{B}{\mu\mathrm{G}}\right)^{-3/2} \left(\frac{\nu_c}{\mathrm{GHz}}\right)^{-1/2} \quad \text{years}} \tag{2.141}$$

2.4 Inverse-Compton radiation

Compton scattering: photon transfers energy and momentum to an electron (bound to an atom). If free electrons have sufficiently high kinetic energy, $mc^2 \ll h\nu$, the reverse may happen, i.e. net energy will be transferred from the electron to the photon.

Relativistic electrons in photon field (e.g. FIR radiation from galaxies or CMB) my thus "boost" such photons to X-ray (or even γ-ray) regime. Derivation of radiated power is very

similar to that of synchroton radiation. We only quote the result here (with σ_T being the Thomson cross-section):

$$\int \frac{dP_{\rm IC}}{d\Omega} d\Omega = P_{\rm IC} = \frac{4}{3} \cdot \sigma_T \cdot c \cdot \gamma^2 \cdot \beta^2 \cdot u_{\rm rad} \tag{2.142}$$

where

$$u_{\rm rad} = \frac{4\sigma}{c} \cdot T^4 \qquad \sigma \text{ being the Stefan-Boltzmann constant} \tag{2.143}$$

is the energy densitiy of the radiation field. We can express the radiated synchrotron power in an analogous form.

$$P_{\rm syn} = \frac{2 \cdot e^2}{3 \cdot c^3} \cdot \dot{v}_\perp^2 \cdot \gamma^4 \tag{2.144}$$

where

$$\dot{v}_\perp = \frac{e \cdot v_\perp \cdot B}{\gamma \cdot m_0 \cdot c} \tag{2.145}$$

Hence

$$P_{\rm syn} = \frac{2 \cdot e^4}{3 \cdot m_0^2 \cdot c^3} \cdot \beta_\perp^2 \cdot \gamma^2 \cdot B^2 \tag{2.146}$$

Need to average over all $\beta_\perp^2$; with $\beta_\perp = \beta \cdot \sin\chi$

$$\langle \beta_\perp^2 \rangle = \frac{\beta^2}{4\pi} \cdot \int_0^{2\pi} \int_0^{\pi} \sin\chi d\Omega = \frac{\beta^2}{4\pi} \cdot \int_0^{2\pi} \int_0^{\pi} \sin^3\chi d\chi d\psi \tag{2.147}$$

$$= \frac{2}{3}\beta^2 \tag{2.148}$$

$$P_{\rm syn} = \frac{4 \cdot e^4}{9 \cdot m_0^2 \cdot c^3} \cdot \beta^2 \cdot \gamma^2 \cdot B^2 = \frac{32 \cdot \pi \cdot e^4}{9 \cdot m_0^2 \cdot c^3} \cdot \beta^2 \cdot \gamma^2 \cdot \frac{B^2}{8\pi} \tag{2.149}$$

$$= \frac{4}{3}\sigma_T \cdot c \cdot \beta^2 \cdot \gamma^2 \cdot u_{\rm mag} \tag{2.150}$$

where

$$\sigma_T = \frac{8\pi}{3} r_e^2 = 6.65 \cdot 10^{-25} \text{ cm}^2 \qquad \text{Thomson cross section} \tag{2.151}$$

$$r_e = \frac{e^2}{m_0 \cdot c^2} \qquad \text{classical electron radius} \tag{2.152}$$

Interesting: Assume synchrotron source (e.g. radio galaxy) embedded in CMB, $T_0 = 2.728$ K. Now calculate ratio

$$\frac{P_{\rm syn}}{P_{\rm IC}} \stackrel{!}{=} \frac{u_{\rm mag}}{u_{\rm rad}} = \frac{\text{magnetic energy density}}{\text{radiation energy density}} \tag{2.153}$$

$$= \frac{B^2}{8\pi} \cdot \frac{c}{4\sigma} \cdot T^{-4} \tag{2.154}$$

where

$$T = T_0 \cdot (1+z) \tag{2.155}$$

We can calculate from this an "equivalent magnetic field of the CMB". i.e.

$$\frac{B_{\rm eq}^2}{8\pi} = \frac{4\sigma}{c} \cdot T_0^4 \cdot (1+z)^4 \tag{2.156}$$

$$B_{\rm eq} = \sqrt{\frac{32 \cdot \pi \cdot \sigma}{c}} \cdot T_0^2 \cdot (1+z)^2 = 3.51 \cdot (1+z)^2 \quad \mu{\rm G} \tag{2.157}$$

Example: 3C294 (Erlund et al. 2006); exhibits extended Inverse-Compton emission. $z = 1.779 \Rightarrow B_{\rm eq} \approx 27$ μG! Synchrotron-cooled relativisitc electrons still produce IC at X-rays $\Rightarrow$ allows to calculate total energy of relativistic plasma deposited by central AGN.

$$\boxed{t_{1/2} = 6.62 \cdot 10^{10} \cdot \left(\frac{T}{\rm K}\right)^{-4} \left(\frac{E_0}{\rm GeV}\right)^{-1} \quad \text{years}} \tag{2.158}$$

2.5 Examples

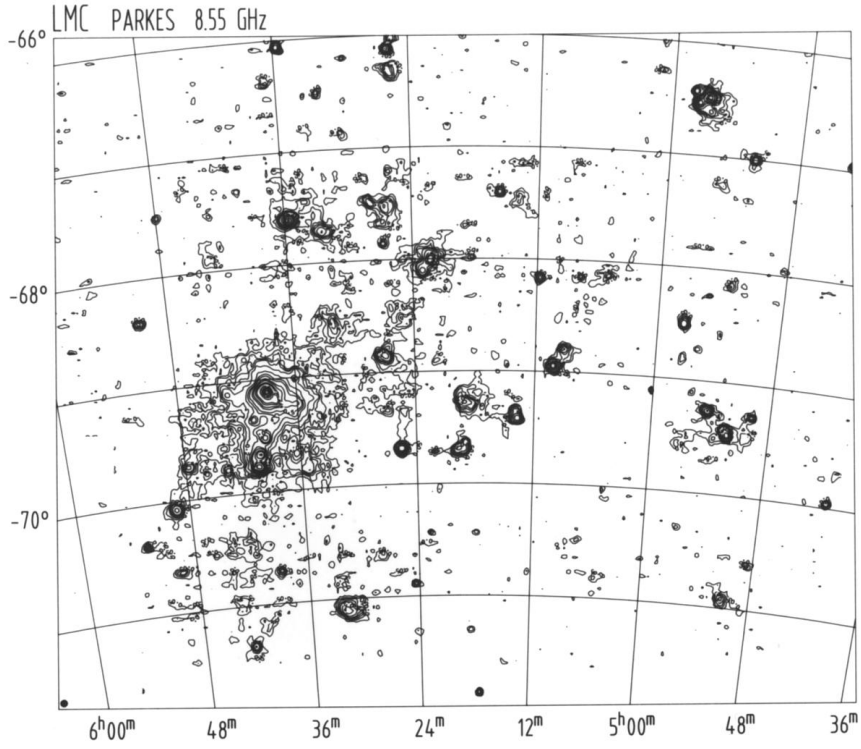

(a) $\lambda = 3\,\mathrm{cm}$

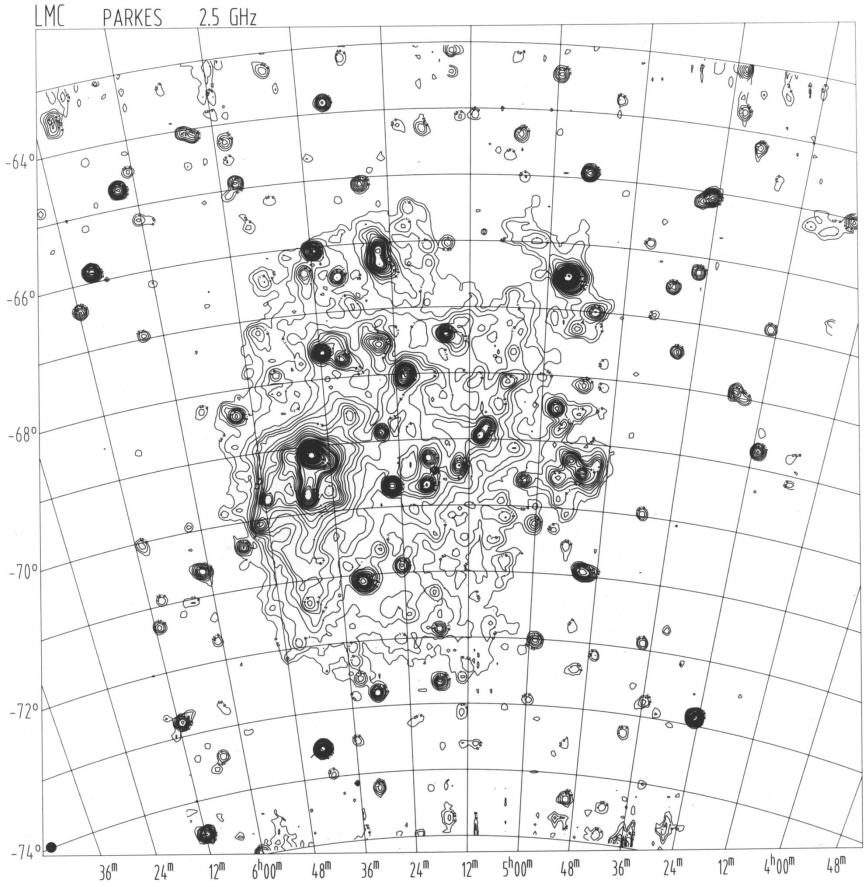

(b) $\lambda = 13\,\mathrm{cm}$

Figure 2.8: The Large Magellanic Cloud at two different wavelenghts

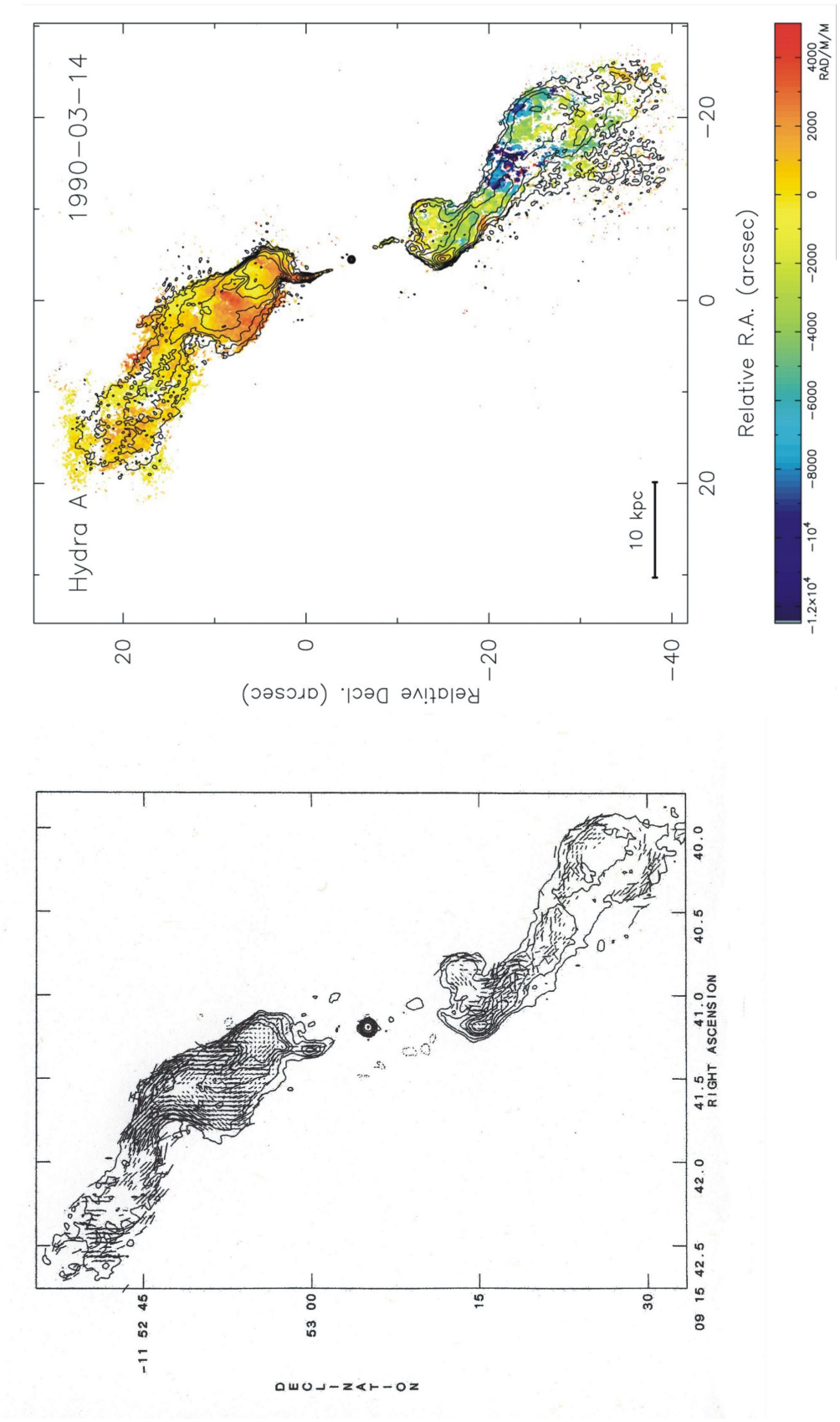

Figure 2.9: The galaxy cluster Hydra A in the radio regime

Chapter 3

Neutral Gas

3.1 Absorption lines

Absorption coefficient

$$\varkappa_\nu = \frac{c^2 \cdot n_l \cdot g_u}{8\pi \cdot \nu^2 \cdot g_l} \cdot A_{ul} \cdot \left[1 - \exp\left(-\frac{h\nu_0}{k_B \cdot T_{\rm ex}}\right)\right] \cdot \phi_{ul}(\nu) \tag{3.1}$$

n_l	=	number density of particles in lower state
g_u	=	statistical weight of upper state
g_l	=	statistical weight of lower state
A_{ul}	=	probability for spontaneous emission
ν_0	=	emission frequency
$T_{\rm ex}$	=	excitation temperature
$\phi_{ul}(\nu)$	=	normalized spectral distribution ("profile shape")

Interstellar absorption lines much narrower than stellar ones.

Visible, UV, NIR: atoms (Na, K, Ca), ions (Ca^+, Ti^+), molecules (CN, CH, CH^+, C_2, OH)

FUV: Lyman series of H; molecules, in particular H_2 (HST, FUSE)

Radio: HI, OH against strong (mostly synchrotron) continuum sources

In what follows we work out how one can determine column densities from absorption lines. Equivalent width of a line defined by

$$W = \int_0^\infty \frac{I_C - I_\lambda}{I_C} d\lambda \tag{3.2}$$

where I_C is the intensity of the stellar continuum on either side of the line; given in units of wavelength. With only absorption radiative transfer reads

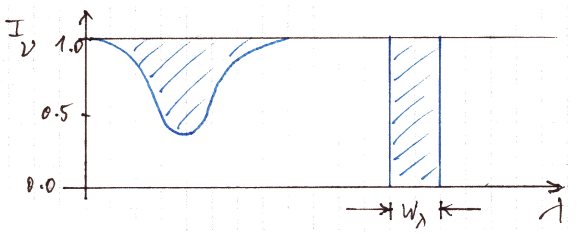

Figure 3.1: Definition of the equivalent width

$$I_\lambda = I_{0,\lambda} \cdot e^{-\tau_\lambda} \tag{3.3}$$

where

$$\tau_\nu = \int_0^{s_0} \varkappa_\nu ds \tag{3.4}$$

is the optical depth. Hence

$$W_\lambda = \int (1 - e^{-\tau_\nu}) d\lambda = \int (1 - e^{-\tau_\nu}) \frac{d\nu}{c} \cdot \lambda \tag{3.5}$$

For small optical depth

$$W_\lambda = \int \tau_\nu d\lambda = \int \tau_\nu \lambda^2 \frac{d\nu}{c} \tag{3.6}$$

Let us assume that $h\nu \ll k_B T_{\rm ex}$ (always valid in FIR and higher frequency regimes):

$$\varkappa_\nu = \frac{c^2 \cdot n_l \cdot g_u}{8\pi \cdot \nu^2 \cdot g_l} \cdot A_{ul} \cdot \phi_{ul}(\nu) \tag{3.7}$$

Integration over the line-of-sight will convert number density n_l into column density N_l

$$\varkappa_\nu = \frac{c^2 \cdot N_l \cdot g_u}{8\pi \cdot \nu^2 \cdot g_l} \cdot A_{ul} \cdot \phi_{ul}(\nu) \tag{3.8}$$

One often uses the oscillator strength

$$f = \frac{m_e \cdot c^3}{8\pi^2 \cdot e^2 \cdot \nu^2} \cdot A_{ul} \cdot \frac{g_u}{g_l} \quad \Rightarrow \quad \tau_\nu = \frac{\pi \cdot e^2 \cdot N_l}{m_e \cdot c} \cdot \phi_{ul}(\nu) \cdot f \tag{3.9}$$

so that

$$W_\lambda = \int_0^\infty \left[1 - \exp\left(-\frac{\pi e^2}{m_e c} \cdot N_l \cdot f \cdot \phi_{ul}(\nu)\right)\right] \lambda^2 \frac{d\nu}{c} \tag{3.10}$$

In all of the above it was assumed that various quantities do not vary along the line-of-sight.

3.1.1 Shape of line profile

Shape of line profile $\phi_{ul}(\nu)$ depends on intrinsic (natural) line profile and broadening effects (Doppler and pressure broadening). Natural line profile is given by the Lorentz curve

$$L(\nu) = \frac{1}{\pi} \cdot \frac{\gamma/2}{[2\pi(\nu - \nu_0)^2] + (\gamma/2)^2} \tag{3.11}$$

The lifetime τ of the transition is the reciprocal of the damping constant γ. The function is normalized such that

$$\int_0^\infty L(\nu) d\nu = 1 \tag{3.12}$$

Individual atoms move about according to the temperature of the gas. This gives rise to the so called Doppler profile ($\Delta\nu$ = Doppler shift, $\Delta\nu_D$ = Doppler width)

$$D(\nu) = \frac{1}{\sqrt{\pi}\Delta\nu_D} \cdot e^{-\left(\frac{\Delta\nu}{\Delta\nu_D}\right)^2} \tag{3.13}$$

which results form translating Maxwell-Boltzmann velocity distribution to frequency. Real line profile is the convolution of $L(\nu)$ and $D(\nu)$:

$$\phi(\nu) = \int_{-\infty}^{+\infty} L(\nu - \nu') \cdot D(\nu') d\nu' \tag{3.14}$$

the so called Voight profile. It requires to calculate the integral

$$\phi(\nu) = \frac{\alpha}{2 \cdot \pi^{5/2} \cdot \Delta\nu_D} \cdot \int_{-\infty}^{+\infty} \frac{e^{-y^2}}{(z-y)^2 + \alpha^2} dy \tag{3.15}$$

where

$$\alpha = \frac{\gamma/2}{2\pi \cdot \Delta\nu_D}, \qquad z = \frac{\nu - \nu_0}{\Delta\nu_D}, \qquad y = \frac{\Delta\nu}{\Delta\nu_D} \tag{3.16}$$

Common practice: Use of dimensionless equivalent width, i.e. (referred to centre frequency, wavelenght or velocity)

$$W = \frac{W_\lambda}{\lambda_0} = \frac{W_\nu}{\nu_0} = \frac{W_v}{c} \tag{3.17}$$

Now consider three cases concerning opacity:

1. optically thin case, $\tau \ll 1$, damping effects neglible

   $$\boxed{W = \frac{\pi e^2}{m_e c^2} \cdot N_l \cdot \lambda \cdot f} \tag{3.18}$$

   Measured equivalent width directly proportional to column density.

2. intermediate optical depth No analytic solution of integral for W_λ exists. Approximation yields

   $$W \propto \log(N_l \cdot \lambda \cdot f) \tag{3.19}$$

3. large optical depth, $\tau \gg 1$ In this case (Unsöld, 1955)

   $$W \propto \sqrt{N_l \cdot \lambda \cdot f} \tag{3.20}$$

   For still stronger lines absorption in the line wings becomes possible, hence the damping part of the line profile now dominates the "Doppler core".

$$\alpha \to 0 \Rightarrow \qquad H(\alpha, z) \to e^{-z^2} \qquad \text{doppler dominated} \tag{3.21}$$

$$\alpha \to \infty \Rightarrow \qquad H(\alpha, z) \to \frac{\alpha}{\sqrt{\pi}(z^2 + \alpha^2)} \qquad \text{broad damping wings} \tag{3.22}$$

$$\phi(\nu) = \frac{1}{\Delta\nu_D \cdot \sqrt{\pi}} \cdot H(\alpha, z) \tag{3.23}$$

$$H(\alpha, z) = \frac{\alpha}{\pi} \cdot \int_{-\infty}^{+\infty} \frac{e^{-y^2}}{(z-y)^2 + \alpha^2} dy \tag{3.24}$$

3.1.2 Curve of growth

At low optical depth, damping effects are small compared to Doppler broadening; shape of line profile is approximatly that of Doppler function. Equivalent width is proportional to column density; for intermediate column densities the equivalent width depends only litte on column density ⇒ "Doppler plateau"; for very large column densities, the equivalent width is governed by the damping-part of the line profile.

Example: curve of growth for different absorption lines (elements) observed towards the same cloud; if their Doppler boradening is the same, the growth curve is a single line up to the end of the Doppler plateau; they split in the damping regime, owing to different trasition probabilities, hence damping constants.

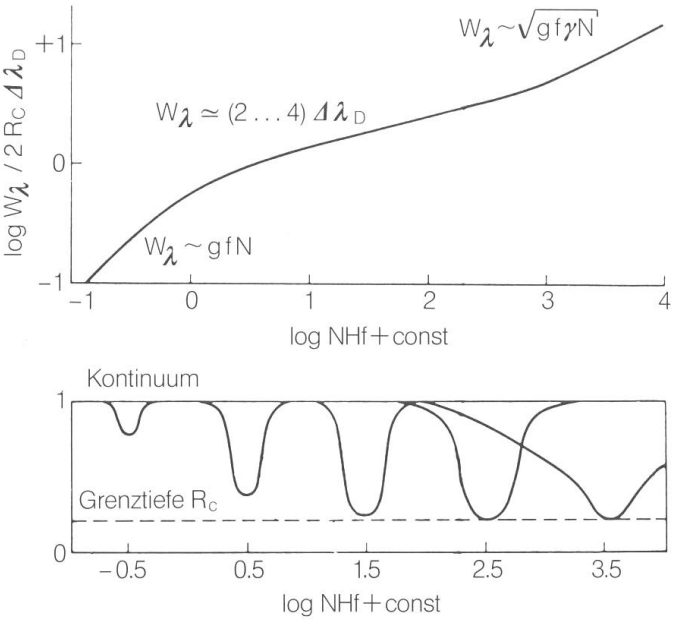

Figure 3.2: Curve of growth

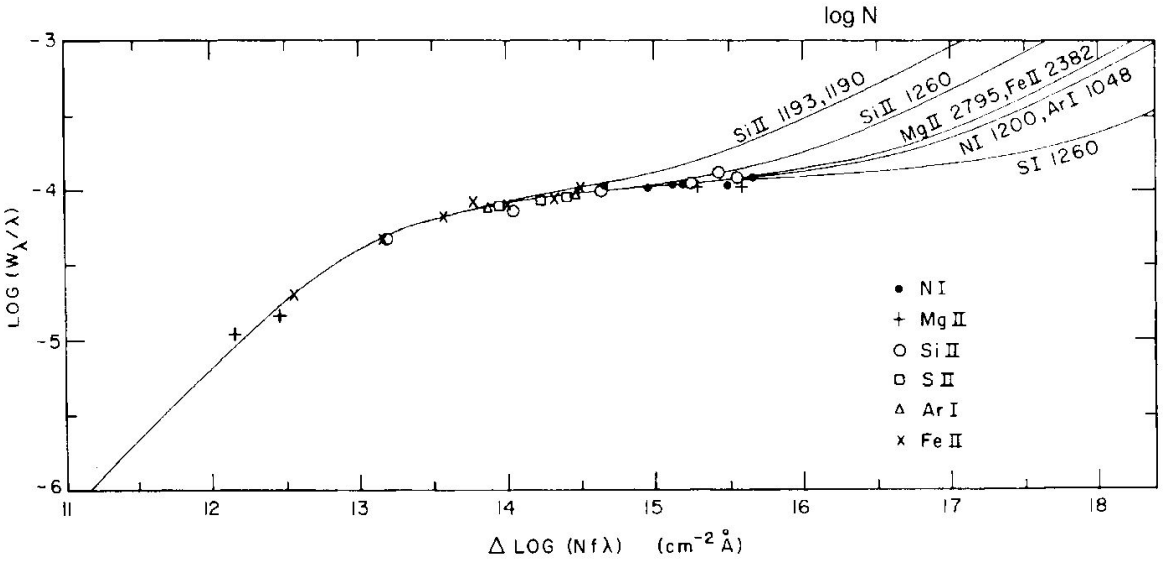

Figure 3.3: Observed curve of growth

In the general ISM it is the Doppler broadening that mostly dominates emission and ab-

sorption lines. Dampings wings are seen in stellar absorption spectra (collisional broadening). Outside of stars broad wings are seen in the absorption lines of "Damped Lyman α sysyems" (DLA).

ISM: most absorption lines lie in UV range

optical

- D_1 and D_2 doublet of neutral Na (5889 - 5895 Å) but always saturated → better use UV lines of Na at 3302.4 Åand 3303.0 Å
- H and K doublet of Ca^+ at 3933 Åand 3968 Å
- neutral Ca at 4226 Å

UV a host of lines, mostly saturated → column densities difficult to derive

Main goal: determination of abundances; referred to strong Ly α at 1215.67 Å; almost always damping in part of cog → column density can be derived.

Difficulty with other elemtents: column density can only be derived if all possible ionization states are measured; O and N and noble gases are not ionized in "neutral medium"

- one problem in determination of abundances: heavy elements may be depleted, owing to condensation onto dust grains.
- another method of abundance determination is to use emission lines from HII regions; these are close to solar, except for Fe, which is underabundant (most likely due to depletion onto dust grains)
- cosmological significance: dtermination of primeordial He abundance; we expect $Y = 0.25$ (by mass and 0.08 by number) abundance of N and O measured in low-metallicity galaxies (dwarf galaxies); measure Y as a function of N and/or O and extrapolate to zero N and/or O; the ordinate should then indicate primordial He abundance.
- results: $Y_{\rm gas} = 0.245 \pm 0.006$, $Y_{\rm stars} = 0.232 \pm 0.009$, $\langle Y \rangle_{\rm Prim.} = 0.239$, very close to prediction!

We shall encounter another cosmological application of absorption lines, viz. of molecules, in a cosmological context.

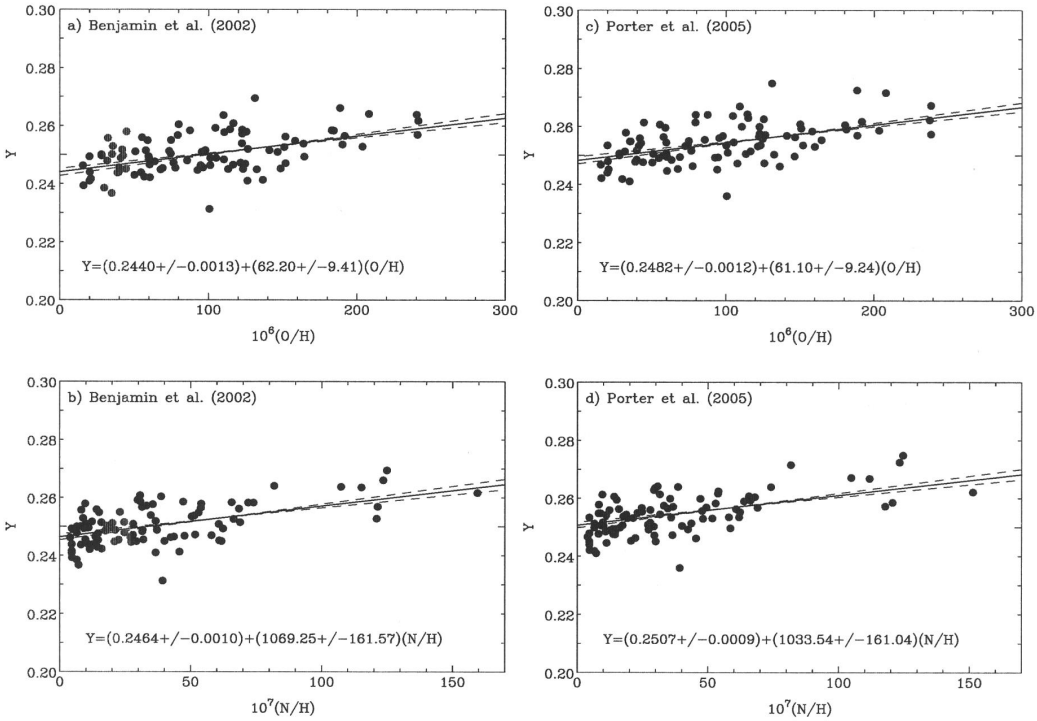

Figure 3.4: Determination of primordial abundance of H

3.2 Neutral atomic hydrogen

3.2.1 Transition

In the cold ISM, atomic hydrogen is neutral and in its ground state $1^2S_{1/2}$. Hyperfine splitting produces two energy levels of trhis ground state, owing to the interaction of the proton and electron spins. Description $n^{2S+1}L_J$

S = total spin quantum number
L = total orbital angular momentum quantum number
J = total angular momentum (for the electrons) quatum number $= L + S$
I = nuclear spin quantum number
F = total angular momentum (for the atom) quantum number $= I + J$
n = electronic quantum number

here: $n = 1, \quad S = 1/2, \quad L = 0, \quad I = 1/2, \quad J = 1/2 \Rightarrow F = 0, 1$

The probability for a spontaneous transition from the higher state $F = 1$ to the lower state $F = 0$ is extremely low:

$$A_{10} = 2.86888 \cdot 10^{-15} \quad \mathrm{s}^{-1} \qquad \text{magnetic dipole radiation} \tag{3.25}$$

i.e. this would occur once everey 11.1 million years on average for a given H atom. However, in the ISM any given hydrogen atom experiences a collision with another one every 400 years,

which can be calculated as follows

$$\tau_{\text{coll.}} \approx 4 \cdot 10^{11} \cdot \left(\frac{T}{\text{K}}\right)^{-1/2} \cdot \left(\frac{n_{\text{HI}}}{\text{cm}^{-3}}\right)^{-1} \quad \text{s} \tag{3.26}$$

During this collision, hydrogen atoms exchange their electrons, this being the chief mode of the hyperfine transition. If the spin orientation of the exchanged e^- changes, there will be a corresponding change in energy. Hence, collisions can result in no change, excitation, or in de-excitation. Comparing the above numbers it is clear that the relative population of the HFS levels will be governed by collisions. This eventually leads to an equilibrium stat with a ratio of aligned-to-opposed spins of 3:1, as

$$\frac{n_1}{n_0} = \frac{g_1}{g_0} \cdot e^{-\frac{h\nu_{10}}{k_B T_{\text{sp}}}} \qquad \text{and} \quad g = 2F + 1 \tag{3.27}$$

($h\nu_{10} \ll k_B T_{\text{sp}}$) T_{sp} is called "spin temperature". The energy difference corresponds to a frequency of

$$\nu_{10} = 1.420405751786(30) \text{ GHz} \tag{3.28}$$

The radiation is commonly referred to as the "21 cm emission of neutral hydrogen" or the "HI line". The fact that there is such a vast number of HI atoms along the line-of-sight means that the Hi line emission can be easily measured. The prediction that the line could be detected was made by van de Hulst in 1944 and was detected in 1951 by three groups: Euwen & Purcell, Muller & Oort and Christiansen et al..

Example: flux density of HI line within the beam of the 100 m telescope from region with $n_{\text{HI}} = 1$ cm^{-3} with size $L = 100$ pc which yields a column density of $N_{\text{HI}} = 3 \cdot 10^{20}$ cm^{-2}. Monochromatic power:

$$P_\nu = \frac{\dot{N} \cdot h\nu}{\nu} \cdot \Omega_{\text{mb}} \cdot D^2 \qquad D = \text{ distance} \tag{3.29}$$

$$\Omega_{\text{mb}} = 1.133 \cdot \text{HPBW}^2 = 7.8 \cdot 106{-}6 \text{ sr} \qquad \text{HPBW} = 70^\circ \cdot \frac{\lambda}{D} = 9' \tag{3.30}$$

flux density

$$S_\nu = \frac{P_\nu}{4\pi \cdot D^2} = \dot{N} \cdot h \cdot \frac{\Omega_{\text{mb}}}{4\pi} = n_{\text{HI}} \cdot L \cdot \frac{h}{4\pi} \cdot \frac{\Omega_{\text{mb}}}{\tau_{\text{coll}}} \tag{3.31}$$

photon flux

$$\dot{N} = n_{\text{HI}} \cdot \tau_{\text{coll}}^{-1} \cdot L \tag{3.32}$$

$$\Rightarrow \dot{N} = 2.4 \cdot 10^{10} \quad \text{photons cm}^{-2} \text{ s}^{-1} \tag{3.33}$$

and

$$S_\nu \approx 10^{-22} \quad \text{erg s}^{-1} \text{ cm}^{-2} \text{ Hz}^{-1} = 10 \text{ Jy} \tag{3.34}$$

...easily detectable!

3.2.2 Determination of $N_{\rm H}$ and $T_{\rm sp}$

Because of large number of hydrogen atoms along the line-of-sight we do not know a priori whether the HI line radiation is optically thin or not. Hence, we have to go through the standard radiative transfer calculation. From Chapter ?? we have

$$\frac{dI_\nu}{ds} = \frac{1}{4\pi} \cdot n_1 \cdot A_{10} \cdot h\nu_{10} \cdot f(\nu) + \frac{I_\nu}{c} \cdot h\nu_{10} \cdot f(\nu) \cdot (B_{10} \cdot n_1 - B_{01} \cdot n_0) \tag{3.35}$$

where we identify the absorption coefficient with

$$\varkappa_\nu = -\frac{h\nu_{10}}{c} \cdot (B_{10} \cdot n_1 - B_{01} \cdot n_0) \cdot f(\nu) \tag{3.36}$$

The optical depth is

$$\tau_\nu(s) = \int_0^s \varkappa_\nu(s')ds' \tag{3.37}$$

Relate intensity I_ν to brightness temperature $T_b(\nu)$ via Rayleigh-Jeans approximation:

$$I_\nu = \frac{2k_B \cdot \nu^2}{c^2} \cdot T_\nu \tag{3.38}$$

The spin temperature is defined via the Boltzmann statistics of the population of the HFS levels:

$$\frac{n_1}{n_0} = \frac{g_1}{g_0} \cdot e^{-\frac{h\nu_{10}}{k_B T_{\rm sp}}} \approx \frac{g_1}{g_0} \cdot \left(1 - \frac{h\nu_{10}}{k_B T_{\rm sp}}\right) =: \frac{g_1}{g_0} \cdot \left(1 - \frac{T_{10}}{T_{\rm sp}}\right) \tag{3.39}$$

$$T_{10} = \frac{h\nu_{10}}{k_B} = 0.068 \text{ K} \ll T_{\rm sp} \tag{3.40}$$

We furthermore use the relations between the Einstein coefficients

$$g_0 \cdot B_{01} = g_1 \cdot B_{10} \qquad \text{and} \qquad A_{10} = \frac{8\pi \cdot h \cdot \nu_{10}^3}{c^3} \cdot B_{10} \tag{3.41}$$

With the above we derive

$$\varkappa_\nu = \frac{h\nu_{10}}{c} \cdot B_{01} \cdot n_0 \cdot \left(1 - \frac{B_{10}}{B_{01}} \cdot \frac{n_1}{n_0}\right) \cdot f(\nu) \tag{3.42}$$

$$= \frac{h\nu_{10}}{c} \cdot \frac{g_1}{g_0} \cdot B_{01} \cdot n_0 \cdot \left(1 - \frac{g_0}{g_1} \cdot \frac{n_1}{n_0}\right) \cdot f(\nu) \tag{3.43}$$

$$= \frac{3c^2 \cdot A_{10} \cdot n_0}{8\pi \cdot \nu_{10}^2} \cdot \left(1 - e^{-\frac{h\nu_{10}}{k_B T_{\rm sp}}}\right) \cdot f(\nu) \tag{3.44}$$

$$\approx \frac{3c^2 \cdot A_{10} \cdot n_0}{8\pi \cdot \nu_{10}^2} \cdot \frac{h\nu_{10}}{k_B T_{\rm sp}} \cdot f(\nu) \tag{3.45}$$

Since

$$n_{\rm HI} = n_0 + n_1 = n_0 + 3n_0 = 4n_0 \tag{3.46}$$

we finally obtain

$$\boxed{\varkappa_\nu = \frac{3 \cdot h \cdot c^2}{32\pi} \cdot \frac{A_{10}}{\nu_{10}} \cdot \frac{n_{\rm HI}}{k_B T_{\rm sp}} \cdot f(\nu)} \tag{3.47}$$

translate $f(\nu)$ to $f(v)$:

$$f(\nu)d\nu = f(v)dv \tag{3.48}$$

$$f(\nu) = f(v) \cdot \frac{dv}{d\nu} \tag{3.49}$$

$$\frac{v}{c} = \frac{\nu_{10} - \nu}{\nu_{10}} \Rightarrow \frac{dv}{d\nu} = -\left(\frac{v_{10}}{c}\right)^{-1} \tag{3.50}$$

and with

$$d\tau_\nu = d\varkappa_\nu ds \tag{3.51}$$

we have

$$d\tau(v) = 5.4728 \cdot 10^{-19} \cdot \left(\frac{n_{\rm HI}}{\rm cm^{-3}}\right) \cdot \left(\frac{T_{\rm sp}}{\rm K}\right)^{-1} \cdot \left(\frac{f(v)}{\rm km^{-1}\ s}\right) \cdot \left(\frac{ds}{\rm cm}\right) \tag{3.52}$$

Integrating over all velocities (= frequencies) on the left side and over the whole line-of-sight on the right, can proceed to arrive at the total HI column density:

$$\int_{-\infty}^{+\infty} \tau(v) \left(\frac{dv}{\rm km\ s^{-1}}\right) = 5.47 \cdot 10^{-19} \cdot \left(\frac{T_{\rm sp}}{\rm K}\right)^{-1} \cdot \int_0^{s_0} \left(\frac{n_H(s)}{\rm cm^{-3}}\right) \left(\frac{ds}{\rm cm}\right) \tag{3.53}$$

or, defining the column density as

$$N_H = \int_0^{s_0} n_H(s)ds \quad \text{, or here} \quad N_H(v) \int_0^{s_0} n_H(s,v)ds \tag{3.54}$$

we derive this column densitiy by integrating the optical depth over velocity

$$\left(\frac{N_{\rm HI}}{\rm cm^{-2}}\right) = 1.823 \cdot 10^{18} \cdot \left(\frac{T_{\rm sp}}{\rm K}\right) \cdot \int_{-\infty}^{+\infty} \tau(v) \left(\frac{dv}{\rm km\ s^{-1}}\right) \tag{3.55}$$

The frequency or velocity dependence of optical depth is

$$d\tau(v) = c \cdot n_{\rm HI} \cdot T_{\rm sp}^{-1} \cdot f(v)ds \tag{3.56}$$

with $c = 5.47 \cdot 10^{-19}$ cm^2 K km s^{-1}; from radiative transfer we have

$$T_b(v) = T_{\rm sp} \cdot \left[1 - e^{-\tau(v)}\right] + T_c \cdot e^{-\tau(v)} \tag{3.57}$$

where T_c is the brightness temperature of a background source. For $\tau(v) \ll 1$ we simplify this to

$$T_b(v) = \tau(v) \cdot T_{\rm sp} \tag{3.58}$$

Then $T_b(v)$ is the brightness temperature measured in each velocity interval dv. Inserting numbers for c we find

$$\boxed{N_{\rm HI} = 1.823 \cdot 10^{18} \cdot \int_0^\infty \left(\frac{T_b(v)}{\rm K}\right) \cdot \left(\frac{dv}{\rm km\ s^{-1}}\right) \quad \text{atoms cm}^{-2}} \tag{3.59}$$

In the most general case, the radiative transfer calculation would result in a an observed brightness temperature of

$$T_b(v) = T_{\rm bg}(v) \cdot e^{-\tau(v)} + T_{\rm sp} \cdot \left[1 - e^{-\tau(v)}\right] \tag{3.60}$$

where $T_{\rm bg}(v)$ is the brightness temperature incident of the far side of an HI cloud. As we are only interested in the HI emission (and wish to get rid of the background continuum), we usually measure the difference between the two components

$$\Delta T_b(v) = T_b(v) - T_{\rm bg} = (T_{\rm sp} - T_{\rm bg}) \cdot \left[1 - e^{-\tau(v)}\right] \tag{3.61}$$

This is accomplished either by on-off measurements, also called position switching, or by frequency-switching. In order to gain some physical feeling for the above equation, let us consider the two extreme cases of $\tau \ll 1$ and $\tau \gg 1$ for a single cloud and without any background radiation.

- $\tau(v) \ll 1$
  In this case, with $T_{\rm bg} = 0$, we have

  $$T_b(v) = T_{\rm sp} \cdot \tau(v) = c \cdot N_{\rm HI}(v) \tag{3.62}$$

  i.e. the measured brightness temperature is proportional to the column density of HI per unit velocity. This means that essentially all of the spontaneously emitted 21 cm photons escape the cloud without being absorbed. The emission is pracically independent of $T_{\rm sp}$, since $T_0 = h\nu_{10}/k_B$ is much smaller than any reasonable $T_{\rm sp}$. Thus the number of photons leaving the cloud tells us directly what the HI column density is.

- $\tau(v) \gg 1$
  In this case, we have (with $T_{\rm bg} = 0$)

  $$T_b = T_{\rm sp} \tag{3.63}$$

  i.e. we directly measure the spin temperature. Any 21 cm photons emitted some where within the cloud are intantly absorbed by foreground HI atoms. Only photons with $\tau \lesssim 1$ emitted from the front surface (facing us) leave the cloud. Hence, the observed brightness temperature is independent of the column density and depends only on the cloud temperature (analogy to black body radiation in case of thermal continuum).

Measuring $\Delta T_b(v)$ implies that we see emission or absorption, depending on whether $T_{\rm sp} > T_{\rm bg}$ or $T_{\rm sp} < T_{\rm bg}$.

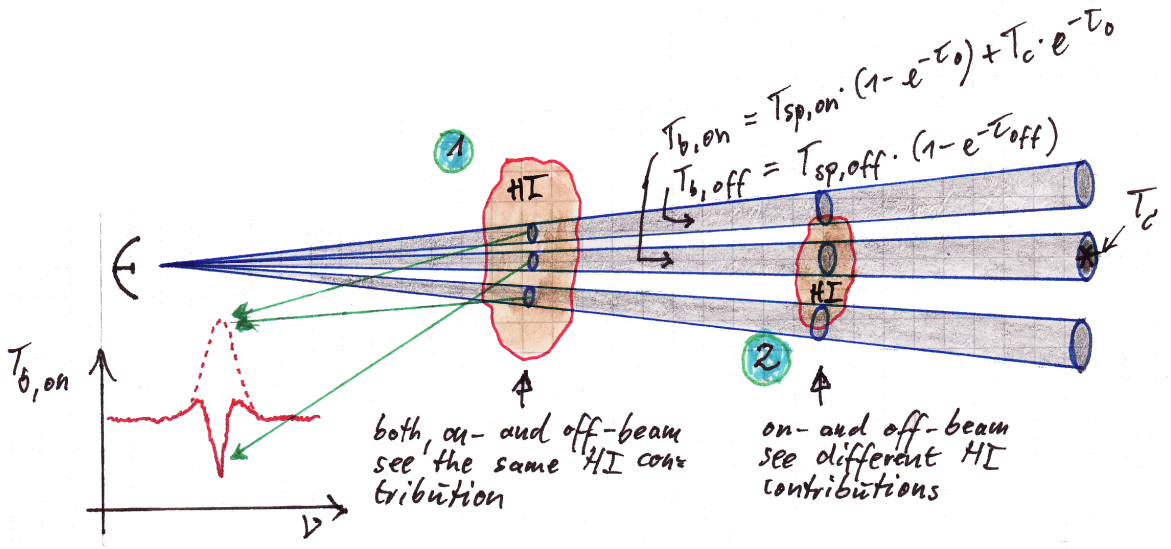

Figure 3.5: Scematic of position switching

If the 3 K CMB were the only excitation mechanism for the 21 cm line, the we would be faced with the special case $T_{\rm sp} = T_{3\ {\rm K}} = 2.728$ K. The neutral hydrogen would then remain ivisible except in the direction of strong radio continuum sources, where $T_{\rm bg}$ would exceed the 3 K background. Fortunatly, there are two other excitation mechanisms at work: collisions and Ly-α radiation.

$$T_{b,{\rm on}} = T_{\rm bg} \cdot e^{-\tau_{\rm on}} + T_{\rm sp,on} \cdot \left(1 - e^{-\tau_{\rm on}}\right) \tag{3.64}$$

With frequency switching, we measure the above and, sufficiently far off the line, we measure the pure continuum of the background source. Substracting them, we obtain

$$\Delta T_b = T_{b,{\rm on}} - T_{\rm bg} = (T_{\rm sp,on} - T_{\rm bg}) \cdot \left(1 - e^{-\tau_{\rm on}}\right) \tag{3.65}$$

The pure line emission can be estimated using several off-spectra that still see HI emission from the cloud:

$$T_{b.{\rm HI}} \approx \langle T_{b,{\rm off}} \rangle = \langle T_{\rm sp,off} \rangle \cdot \left(1 - e^{-\langle \tau_{\rm off} \rangle}\right) \tag{3.66}$$

Generally, we have $\langle \tau_{\rm off} \rangle \neq \tau_{\rm on}$ and $\langle T_{\rm sp,off} \rangle \neq T_{\rm sp,on}$. If, however, the two conditions are nearly fulfilled, then we can derive $T_{\rm sp}$ and/or $\tau_{\rm on}$.

- $\langle T_{\rm sp,off} \rangle = T_{b,{\rm HI}}$
  This is nearly fulfilled if the antenna beam is small compared to the angular dimension of the HI cloud (denoted 1 in the figure). Then, from equation 3.65 it follows that

$$\frac{\langle T_{\rm sp,off} \rangle - \Delta T_b}{T_{\rm bg}} = \frac{T_{b,{\rm HI}} - \Delta T_b}{T_{\rm bg}} \tag{3.67}$$

$$= \frac{T_{\rm sp,off} \cdot \left(1 - e^{-\tau_{\rm on}}\right) - (T_{\rm sp,on} - T_{\rm bg}) \cdot \left(1 - e^{-\tau_{\rm on}}\right)}{T_{\rm bg}} \tag{3.68}$$

$$= 1 - e^{-\tau_{\rm on}} \tag{3.69}$$

If $\tau_{\rm on} \ll 1$

$$\tau_{\rm on} = \frac{\langle T_{\rm sp,off}\rangle - \Delta T_b}{T_{\rm bg}} \tag{3.70}$$

otherwise

$$\boxed{\tau_{\rm on} = -\ln\left(1 - \frac{T_{b,\rm HI} - \Delta T_b}{T_{\rm bg}}\right)} \tag{3.71}$$

- $\langle T_{\rm sp,off}\rangle = T_{\rm sp,on}$, $\langle \tau_{\rm off}\rangle = \tau_{\rm on}$

We have seen that

$$\varkappa_\nu \propto T_{\rm sp}^{-1} \quad \text{,i.e. } \tau_\nu \propto T_{\rm sp}^{-1} \tag{3.72}$$

and

$$\Delta T_b(v) = (T_{\rm sp} - T_{\rm bg}) \cdot \left[1 - e^{-\tau(v)}\right] \tag{3.73}$$

That means, if $T_{\rm sp}$ is large we have emission and if $T_{\rm sp}$ is small we have absorption, i.e. cold gas clouds are seen in absorption and warm (hot) gas is seen in emission.

Observations indicate that $T_{\rm sp}$ is in between 10 K and 5000 K, and the number density $n_{\rm HI}$ is between 0.2 cm^{-3} and 10 cm^{-3}. With pressure balance holding, i.e.

$$P_1 = n_1 \cdot k_B \cdot T_1 = P_2 = n_2 \cdot k_B \cdot T_2 \tag{3.74}$$

e.g. $n_1 = 10$ cm^{-3}, $n_2 = 0.2$ cm^{-3}, $T_1 = 50$ K, $T_2 = 2500$ K

Frames of reference for v:

heliocentric corrects for earth rotation and motion about the sun $\rightarrow \quad v_{\rm rel}$

local standard of rest corrects in addition for peculiar motion of the sun with respect to surrounding nearby stars, as measured from their proper motions; the sun moves at 20 km s^{-1} towards $\alpha_{1900} = 18^{\rm h}$, $\delta_{1900} = 30^\circ \Rightarrow v_{\rm LSR}$

3.3 Constituents of the diffuse ISM

Gas, dust, relativistic plasma; for the gas we know 5 components (see Wolfire et al., 1996, Ap. J. 443, 152)

	MM	CNM	WNM	WIM	HIM
n [cm^{-3}]	$10^2 \cdots 10^5$	$4 \cdots 80$	$0.1 \cdots 0.6$	$\simeq 0.2$	$10^{-3} \cdots 10^{-2}$
T [K]	$10 \cdots 50$	$50 \cdots 200$	$5500 \cdots 8500$	$\simeq 8000$	$10^5 \cdots 10^7$
h [pc]	$\simeq 70$	$\simeq 140$	$\simeq 400$	$\simeq 900$	$\geqq 1000$
$f_{\rm vol}$	$< 1\%$	$\simeq 2 \cdots 4\%$	$\simeq 30\%$	$\simeq 20\%$	$\simeq 50\%$
$f_{\rm mass}$	$\simeq 20\%$	$\simeq 40\%$	$\simeq 30\%$	$\simeq 10\%$	$\simeq 1\%$

MM molecular medium

CNM cold neutral medium

WNM warm neutral medium

WIM warm ionized medium

HiM hot ionized medium

CNM resident in relatively dense clouds, occupying a significant fraction of the interstellar volume. High density implies high cooling rates ⇒ a lot of energy is needed to keep the temperature: $L \approx 10^{42}$ erg s^{-1}. Produces narrow ($\langle\sigma_v\rangle \approx 1.7$ km s^{-1}) features in emission spectrum, which can be readily identified as narrow ones in absorption[1]; termed "HI clouds"; they turn out, however, to be filamentary and sheet-like, rather than spherical; don't show up on every line-of-sight, in contrast to WNM

WNM roughly 30% of total HI; low volume density, but non-negligible filling factor; low density ⇒ low cooling rates, so total power required to heat is comperatively small; distribution derived from HI emission; Mebold (1972) decomposed $\simeq 1200$ spectra into narrow ($\sigma_v \lesssim 5$ km s^{-1}) and broad (5 km s^{-1} $< \sigma_v <$ 17 km s^{-1}) gaussian components, showing ominpresence of broad components.

Neutral hydrogen distributed in a flaring disk, according to the gravitational potential. The scale heights for the CNM and WNM are $h_{\rm CNM} \approx 140$ pc and $h_{\rm WNM} \approx 400$ pc. Radial distribution frequently exhibits a central depression, reaches maximum at about $8 \cdots 10$ kpc, beyond which it declines below the (current) detection threshold, i.e. $N_{\rm HI} \lesssim 10^{19}$ cm^{-2}.

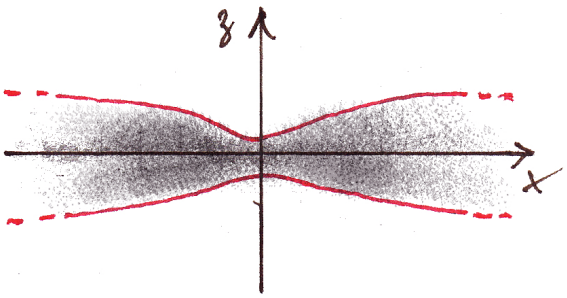

N.B.: at column densities $\lesssim 10^{21}$ cm^{-2} star formation is strongly suppressed (shielding against UV radiation that dissociates molecules; Jeans instabilities).

Kinematically, one distinguishes between:

- low-velocity gas, LVCs = low-velocity clouds
- intermediate-velocity gas, IVCs = intermediate-velocity clouds
- high-velocity gas, HVCs = high velocity clouds

LVCs follow normal galactic rotation and are located within the gaseous disk

[1] Since $\tau \propto T_{\rm sp}^{-1}$

IVCs have velocities between LVCs and HVCs (see below), with metallicities close, $|z| \lesssim 1$ kpc.

HVCs have $|\Delta v| = |v_{\rm HVC} - v_{\rm rot}| > 50$ km s^{-1}; more distant than IVCs, but few reliable distance determinations only; e.g.
"complex A": $D = 2.5 \cdots 7$ kpc $\rightarrow$ $M_{\rm HI} = 10^5 \cdots 2 \cdot 10^6$ M$_\odot$
"Magellanic Stream": $M_{\rm HI} \approx 10^8$ M$_\odot$(for $D = 50$ kpc)

Origin: LVCs disk clouds; IVCs galactic fountains "raining back" onto disk; LVCs ?? former fountains ? but low metals or: tidal debris from infalling [ler. gals.], gas from outer disk

Data cubes. Mapping HI line with a radio telescope results in so-called data cube, with brightness temperature $T_b = T_b(\xi, \eta, v)$. The arrangement is usually such that a map of T_b is computed for each velocity channel. From this, the so-called moment maps are calculated:

$$N_{\rm HI}(\xi,\eta) = C \cdot \int T_b(\xi,\eta)\, dv \qquad \text{moment 0 or column density} \tag{3.75}$$

$$\langle v(\xi,\eta)\rangle = \frac{\int T_b(\xi,\eta)\, v(\xi,\eta)\, dv}{\int T_b(\xi,\eta)\, dv} \qquad \text{moment 1 or velocity field} \tag{3.76}$$

$$\langle \sigma(\xi,\eta)\rangle = \frac{\int T_b(\xi,\eta)\, v^2(\xi,\eta)\, dv}{\int T_b(\xi,\eta)\, dv} \qquad \text{moment 2 or velocity dispersion} \tag{3.77}$$

HI in galaxies. ellipticals generally lack neutral gas; dwarf irregular and spiral galaxies invariably possess disks of neutral gas; relative amount of HI

$$\frac{M_{\rm HI}}{M_{\rm rot}} = \underbrace{3\%}_{\text{massive spirals}} \cdots \underbrace{20\%}_{\text{gas-rich dwarfs}} \qquad \text{but mostly dark matter!} \tag{3.78}$$

3.4 Examples

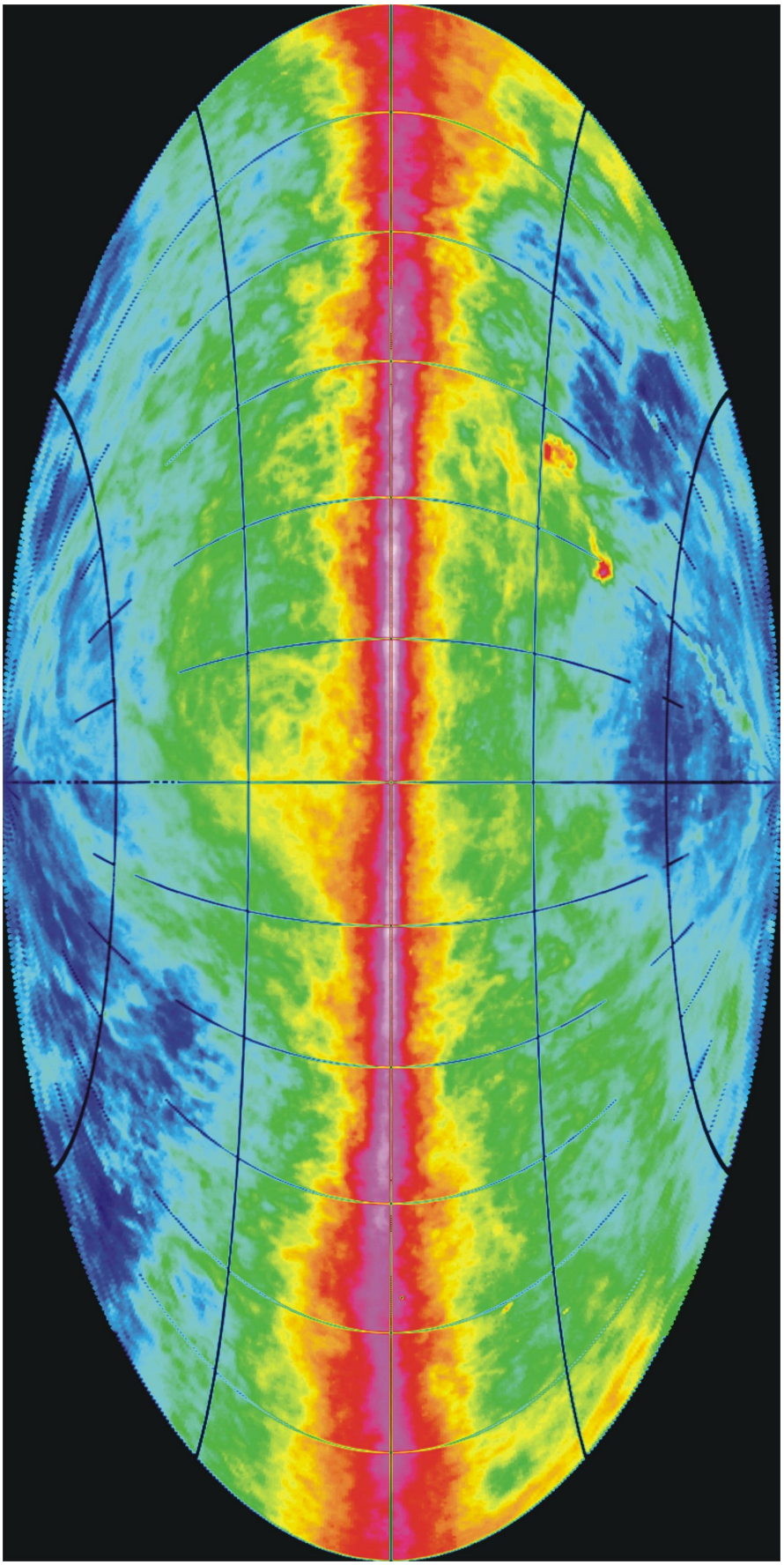

Figure 3.6: The Milky Way in neutral hydrogen

Figure 3.7: NGC6946 in the optical and neutral hydrogen

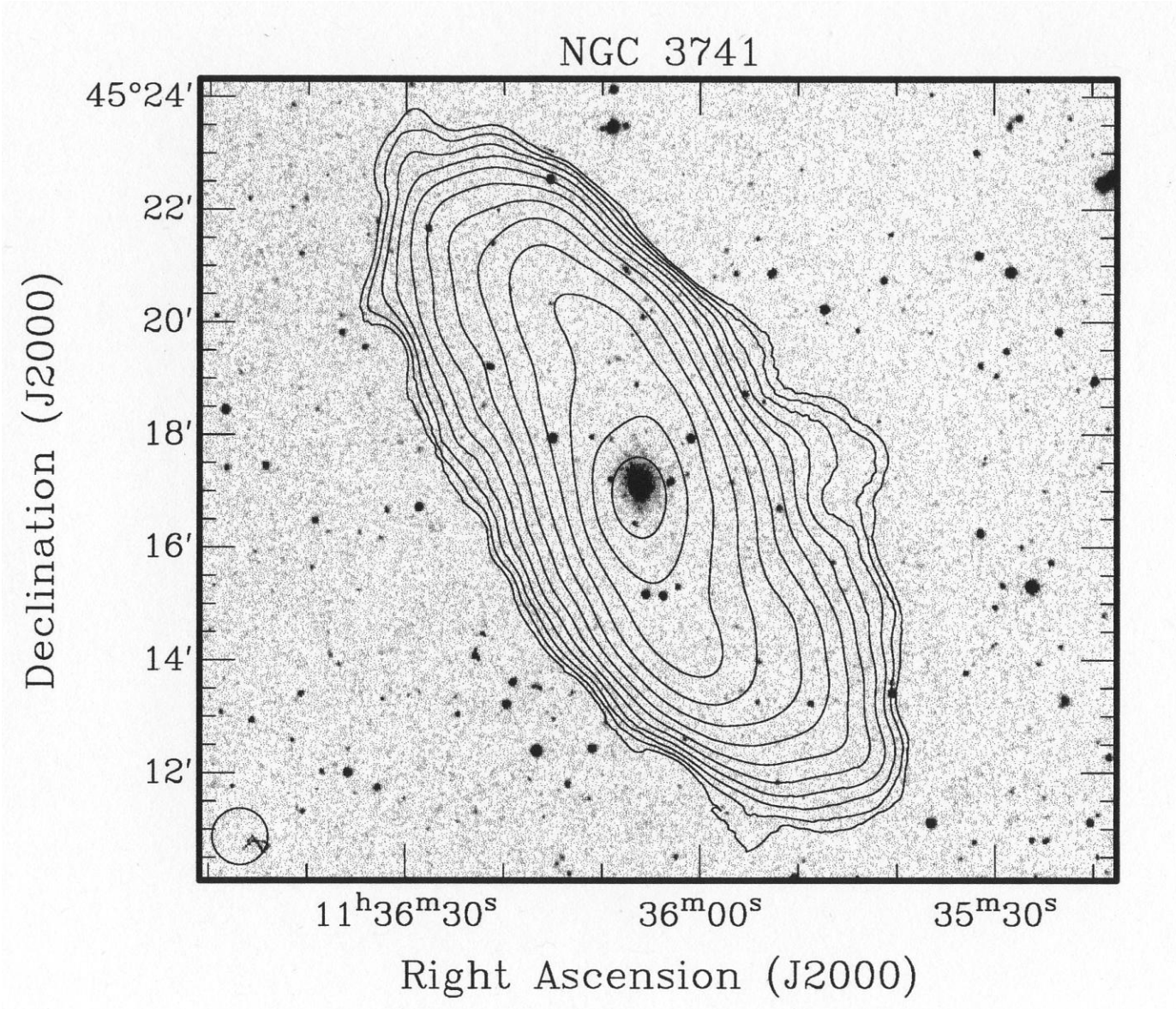

Figure 3.8: NGC3741 in the optical with a neutral hydrogen map superimposed

Chapter 4

Molecular Gas

Molecules known to exist prior to invention of radio astronomy: electronic transitions of CH, CH^+, CN in optical regime, against bright stars (1937). However, there is a wealth of molecular lines in the radio regime, in particular in the mm/submm domain.

1963	OH, absorption, Weinreb et al.
1968	NH_3, emission and absorption, 23.6 GHz, Cheang et al.
1969	H_2O, maiser emission, 22 GHz
1969	H_2CO, absorption against 3 K background, Palmer et al.; emission Snyder et al.
1970	CO, 115 GHz
after 1970	discovery of a multitude of molecules, owing to development of mm astrononmy

significance of molecular gas

- chemical evolution, isotopes; after decoupling of solar system from ISM → more nucleosynthesis → isotope ratios in solar system compared to ISM yield information about chemical evolution of ISM thereafter ($5 \cdot 10^9$ years back)
- molecules are of cardinal importance for chemical evolution (in particular ions)
- molecules act as efficient coolants → star formation (HI is a slow coolant)

... countably ifinite number of transitions

4.1 Model for diatomic molecules

symmetries of atoms get lost upon formation of molecules; however, ther quantum mechanical properties may be simplified such as to treat the motions of their electrons and nuclei separatly. Consider a diatomic molecule AB with charges $Z_A \cdot e$ and $Z_B \cdot e$ at $\vec{r}_A$, $\vec{r}_B$ respectively, and $N = Z_A + Z_B$ electrons located at $\vec{r}_i$, $(i = 1 \cdots N)$. Since mean separations are large compared to the particle sizes we a dealing with a system of point masses.

$$\vec{r} = \vec{r}_A - \vec{r}_B = \vec{r}_{AB} \tag{4.1}$$

system forms stable configuration at some minimum energy, given by radius $\vec{r} = \vec{r}_e$. The energies E and relative particle densitiy $\Psi\Psi^*$, under the motion of nuclei and e^- under the

influence of coulomb forces are given by the Schrödinger equation

$$H\Psi(\vec{r}_A, \vec{r}_B, \vec{r}_i) = E\Psi(\vec{r}_A, \vec{r}_B, \vec{r}_i) \tag{4.2}$$

with

$$H = H_{\text{kin}} + H_{\text{pot}} \tag{4.3}$$

where

$$H_{\text{kin}} = \frac{\vec{p}_A^{\,2}}{2m_A} + \frac{\vec{p}_B^{\,2}}{2m_B} + \sum_i \frac{\vec{p}_i^{\,2}}{2m_e} \tag{4.4}$$

$$H_{\text{pot}} = \frac{Z_A Z_B e^2}{\vec{r}_{AB}} + \sum_{i>j}^{N} \sum_{j=1}^{N} \frac{e^2}{r_{ij}} - \sum_{i=1}^{N} e^2 \cdot \left(\frac{Z_A}{r_{Ai}} + \frac{Z_B}{r_{Bi}} \right) \tag{4.5}$$

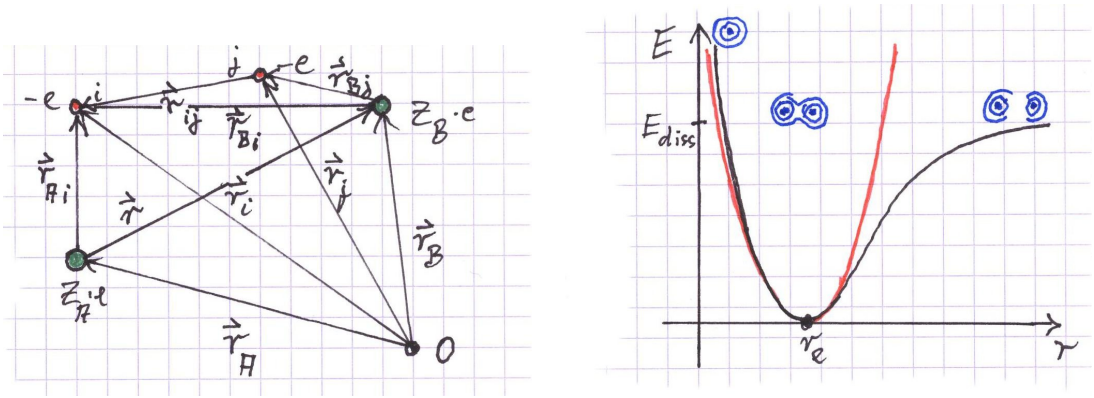

(a) Model (b) Potential

Figure 4.1: Model and Potential of a diatomic molecule

Exact solution of above Schrödinger equation is not possible, hence one resorts to so called Born-Oppenheimer approximation: Since $m_{A,B} \ll m_e$, the motion of the nuclei can be neglected, so for the time being one assumes them to be fixed (they have zero kinetic energy); the the Schrödinger equation reads

$$\left(\sum_i \frac{\vec{p}_i^{\,2}}{2m_e} + H_{\text{coul.}} \right) \Psi^{\text{el}}(\vec{r}, \vec{r}_i) = E^{\text{el}} \Psi^{\text{el}}(\vec{r}, \vec{r}_i) \tag{4.6}$$

where the superscript "el" stands for electrons; this equation now describes the motion of the electrons in the electric field of two arbitrarily fixed nuclei. Eigenvalue E^{el} is the electron energy, and the transitions of a molecule are now subdevided into

- electronic transitions; typical energies of a few eV (optical, UV)
- vibrational transtions; typical energies $0.01 \cdots 0.1$ eV (infrared)
- rotational transitions; typical energies 10^{-3} eV (radio)

dissociation energy

$$E_{\text{diss.}} = E(\infty) - E(r_e) \tag{4.7}$$

diatomic molecules: "Morse potential"

$$E(r) = E_{\text{diss.}} \cdot \{1 - \exp[-a(r - r_e)]\}^2 \tag{4.8}$$

Harmonic approximation:

$$E(r) = a^2 \cdot E_{\text{diss.}} \cdot (r - r_e)^2 \tag{4.9}$$

(identical for small $r - r_e$)

4.1.1 Rotational spectra of diatomic molecules

effective radius of molecule $\sim 10^5$ times that of an atom $\Rightarrow$ moment of inertia $\sim 10^{10}$ times that of an atom with the same mass; hence need to consider rotational energy of the form

$$H = H^{\text{rot}} = \frac{1}{2}\Theta_e \cdot \vec{\omega}^2 = \frac{1}{2\Theta_e}\vec{\mathrm{J}}^2 \tag{4.10}$$

with ω the angular frequency, Θ_e the moment of inertia and $\vec{\mathrm{J}}$ the spin or angular momentum. Schrödinger equation

$$H^{\text{rot}}\Psi^{\text{rot}}(\vartheta, \varphi) = E^{\text{rot}}\Psi^{\text{rot}}(\vartheta, \varphi) = \frac{1}{2\Theta_e}\vec{\mathrm{J}}^2 \cdot \Psi^{\text{rot}}(\vartheta, \varphi) \tag{4.11}$$

with eigenvalues (rotational energy)

$$E^{\text{rot}} = E(J) = \frac{\hbar^2}{2\Theta_e} \cdot J(J+1) \tag{4.12}$$

where J is now the quatum number of angular momentum with integer values $J = 0, 1, \ldots$.

$$\Theta_e = m_A \cdot r_A^2 + m_B \cdot r_B^2 = m \cdot r_e^2 \tag{4.13}$$

$$m = \frac{m_A \cdot m_B}{m_A + m_B} \quad \text{reduced mass} \tag{4.14}$$

It is common practice to convert energies to wave numbers

$$\frac{E(J)}{hc} = \frac{h\nu}{hc} = \frac{\nu}{c} = \tilde{\nu} \tag{4.15}$$

which, according to 4.12 is

$$F(J) = B_e \cdot J(J+1) \tag{4.16}$$

where

$$B_e = \frac{\hbar}{4\pi c \cdot \Theta_e} = \frac{h}{8\pi^2 \cdot m \cdot r_e^2} \tag{4.17}$$

is the rotational constant. This is correct only for absolutely rigid molecule; for slightly elastic molecule,r_e will increase whith rotational energy because of centrifugal stretching. Since Θ_e is in the denominator, increasing r implies decreasing E^{rot}; we can account for the by regarding equation 4.12 as the linear term of a Taylor expansion, the 2nd term of wich must be negative, i.e.

$$E(J) = \frac{\hbar^2}{2\Theta_e} \cdot J(J+1) - d_e \cdot [J(J+1)]^2 \pm \cdots \tag{4.18}$$

The stretching constant may then be written as $D_e = d_e/hc$ so that now

$$F(J) = B_e \cdot J(J+1) - D_e \cdot [J(J+1)]^2 \tag{4.19}$$

Typically, $D_e/B_e \approx 10^{-4} \cdots 10^{-3}$! The deviations from the rotational energies become rapidly larger with increasing J, such that the obeserving frequency are lower than those calculated for a rigid rotator.

4.1.2 Vibrational states of diatomic molecules

consinder non-rotating ascillator; bringing molecule out of equlibrium configuration → oscillations around equilibrium; mathematically: motion of point mass with reduced mass m around point $r - r_e = 0$ within central potential V; Schrödinger equation then

$$\left[\frac{p^2}{2m} + V(r)\right] \Psi^{\text{vib}}(x) = E^{\text{vib}} \cdot \Psi^{\text{vib}}(x) \tag{4.20}$$

where

$$x = r - r_e$$
$$m = \text{reduced mass}$$
$$p = -i\hbar \frac{d}{dx}$$

For $x \ll r_e$ we can resort to harmonic approximation

$$V(r) = \frac{1}{2}\kappa x^2 = \frac{1}{2} m\omega^2 x^2 \tag{4.21}$$

where

$$\omega = 2\pi\nu = \sqrt{\frac{\kappa}{m}}$$
$$\kappa = \text{elastic constant}$$

resulting eigenvalues are

$$E^{\text{vib}} = E(v) = \hbar\omega \left(v + \frac{1}{2}\right) \tag{4.22}$$

with $v = 0, 1, 2, \ldots$ being the vibrational quantum number. Again, one can write these in terms of wave numbers:

$$\frac{E(v)}{hc} = \frac{\nu}{c} \cdot \left(v + \frac{1}{2}\right) = \tilde{\nu}\left(v + \frac{1}{2}\right) = G(v) = \omega_e \cdot \left(v + \frac{1}{2}\right) \tag{4.23}$$

N.B.: $\omega_e \gg B_e$ for all molecules, $[\omega_e] = \text{cm}^{-1}$

4.1.3 Rotation-vibrational transitions

thermal equilibrium: whenever a vibrational level is excited, there will be exited rotational levels, too; correct model then: vibrating rotator or rotating oscillator; because $\omega_e \gg B_e$, the vibrational frequency is always much larger than the rotational frequency, which means that the molecule has vatying r, hence Θ_e during rotation; furthermore, centrifugal force changes with r which means that both B_e and D_e depend on v:

$$B_e = \frac{\hbar}{4\pi c \cdot \langle \Theta_e \rangle} = B_e - \alpha \left(v + \frac{1}{2} \right) + \cdots \tag{4.24}$$

$$D_e = D_e + \beta \left(v + \frac{1}{2} \right) + \cdots \tag{4.25}$$

the smaller the restoring force of the "spring", the larger the expansion, owing to larger centrifugal force.

electronic transitions yield band spectra; for there exists for each electronic transition a large number of vibrational transitions, and for each vibrational transition there are many rotational ones; this leads to bands in optical spectra

Allowed dipole radiation for rotational transitions only if molecule possesses a permanent electric dipole moment; homonuclear diatomic molecules such as H_2, O_2, N_2 do not possess such a permanent dipole moment, hence they will not produce such lines, neither in emission nor in absorption; for diatomic molecules with different atomic species the dipole radiation is emitted in the plane of rotation (classical picture); quantum theory tells us that this radiation is restricted to discrete frequencies, corresponding to $\Delta J = \pm 1$.

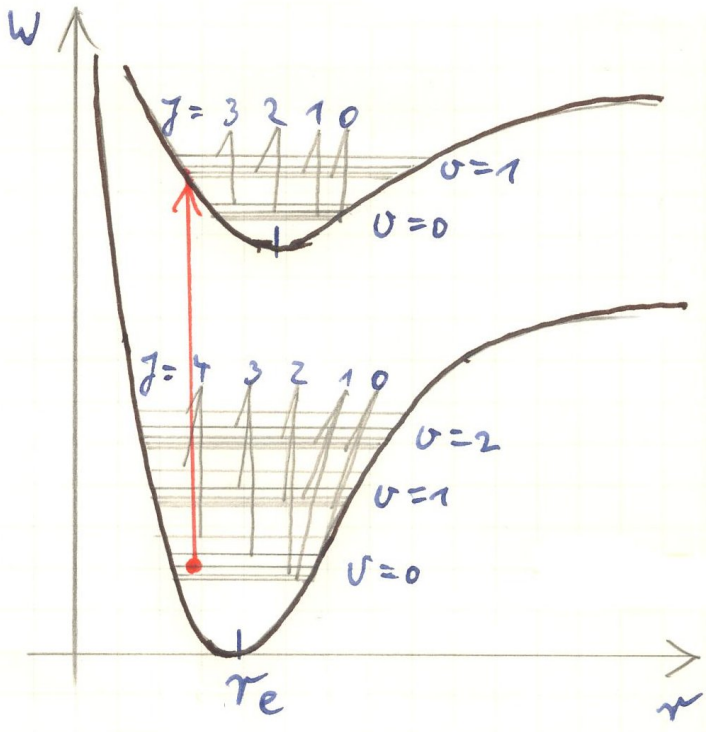

Figure 4.2: Energy levels of rotation vibrational transitions

rotational quantum numbers	$J = 0, 1, 2, \ldots$; $\Delta J = \pm 1$
vibrational quantum numbers	$v = 0, 1, 2, \ldots$; $\Delta v = 0, 1, 2, \ldots$
projection of angular momentum	$K = 0, 1, 2, \ldots$; $\Delta K = 0$
electronic transitions	$\Lambda = 0, 1, 2, \ldots$; $\Delta \Lambda = 0$
electronic spin transitions	$\Sigma = -S, -S+1, \ldots, +S$; $\Delta \Sigma = 0$

4.1.4 Symmetric and asymmetric top molecules

Rotation of rigid molecule with arbitrary shape can be considered as superposition of three free rotations about three principle axes of an inertial ellipsoid;

all 3 axes different	asymmetric top	H_2CO
2 axes equal	symmetric top	NH_3
all 3 axes equal	spherical top	CH_4

Proper Hamilton operator must be solved in Schrödinger equation and eigenvalues be determined to compute the angular parts of the wave function; Hamilton operator for description of rotational energy then reads

$$H = E = \frac{1}{2}\left(\Theta_1\omega_1^2 + \Theta_2\omega_2^2 + \Theta_3\omega_3^2\right) = \frac{J_1^2}{2\Theta_1} + \frac{J_2^2}{2\Theta_2} + \frac{J_3^2}{2\Theta_3} \tag{4.26}$$

In the case of the *symmetric top* the inertial ellipsoid is a rotational ellipsoid with

$$\Theta_1 = \Theta_2 = \Theta_\perp$$
$$\Theta_3 = \Theta_\parallel$$
$$\Theta_\perp > \Theta_\parallel$$

classical motion of such is illustrated in figure 4.3; vector diagramme; assume the body has been set in motion such that $\vec{J}$ is oblique to figure axis 3, this means that the figure axis nutates about the fixed direction of $\vec{J}$; at the same time, the molecule rotates about the figure axis with constant J_3; then $\vec{J}^2$ and J_3 are quantized, i.e. they commutate

$$\left[\vec{J}^2, J_3\right] = 0 \tag{4.27}$$

The Hamilton operator takes the form

$$H = \frac{1}{2\Theta_\perp}\left(J_1^2 + J_2^2\right) + \frac{1}{2\Theta_\parallel}J_3^2 \tag{4.28}$$

with eigenvalues

$$E(J,K) = \frac{\hbar^2}{2\Theta_\parallel}\cdot J(J+1) + \frac{\hbar^2}{2}\left(\frac{1}{\Theta_\parallel} - \frac{1}{\Theta_\perp}\right)\cdot K^2 \tag{4.29}$$

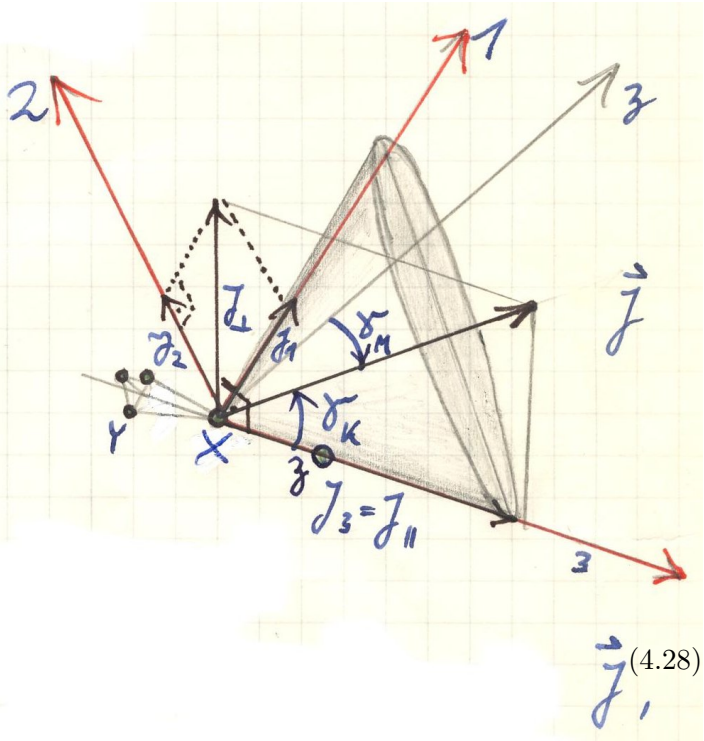

Figure 4.3: Vector diagram of a symmetric top molecule

thus defining the two quantum numbers

$$J = 0, 1, 2, \ldots$$
$$K = 0, 1, 2, \ldots$$

quantum number K defines $\gamma_K = \sphericalangle\left(\vec{J}, J_3\right)$, i.e.

$$\cos\gamma_K = \frac{\langle J_3\rangle}{\langle|\vec{J}|\rangle} = \frac{K}{\sqrt{J(J+1)}} \tag{4.30}$$

which is half the opening angle of the nutation cone. Eigenvalues $E(J, K)$ depend on $|K|$, which means there is degeneracy $(\pm K)$. In case there is a preferred axis (z-axis), e.g. in case of external magnetic field, $\vec{J}$ precesses about z-axis and the angle $\gamma_M = \sphericalangle\left(\vec{J}, J_3\right)$ can only take discrete values $(2J + 1)$:

$$\cos\gamma_M = \frac{\langle J_3\rangle}{\langle|\vec{J}|\rangle} = \frac{M}{\sqrt{J(J+1)}} \tag{4.31}$$

where $M = 0, \pm1, \pm2, \ldots, \pm J$. Without an external magnetic field there is a $2 \cdot (2J + 1)$-fold degeneracy ($2J + 1$-fold for $K = 0$).

- linear molecule: $\Theta_\parallel \to 0$, i.e. $1/2\Theta_\parallel \to \infty$, which means that K_A must vanish. In this case, finite energies only feasible if generally $K = 0$.

  $$E(J) = \frac{\hbar^2}{2\Theta_\perp} \cdot J(J+1) \tag{4.32}$$

  (see rigid rotator); each eigenvalue is $(2J + 1)$-fold degnerate

- spherical top: $\Theta_\parallel = \Theta_\perp$, also yields

  $$E(J) = \frac{\hbar^2}{2\Theta_\perp} \cdot J(J+1) \tag{4.33}$$

  but now with $(2J + 1)^2$-fold degeneracy ($(2J + 1)$-fold each for K and M).

- asymmetric top: there is no more figure axis with constant spin, i.e. only $\vec{J}$ is quantized which means that only J and M are quantum numbers; eigenvalues difficult to obtain, which is why we assume small asymmetry $\Theta_2 = \Theta_1 + \Delta\Theta$, and then start out from $E(J, K)$ as given above and consider $\Delta\Theta$ as small deformation for which we can use perturbation theory; in this case, K is not a good quantum number anymore and $\pm K$ degeneracy disappears; then the energy values fall close to each other in pairs, the levels are split into pairs K_3, K_1 (also denoted K_a, K_c).

4.1.5 H_2, molecular hydrogen

by far the most abundant molecule in interstellar space; discovered in FUV (rocket, Carruthers 1970); owing to its perfect symmetry, it lacks an electric dipole moment; quadrupolar radiation with $\Delta J = 2$ ($J = 2 \rightarrow 0$) is possible but of course very weak, and its energy corresponds to 509 K, which is not representative for the bulk of the ISM. $D_e \approx 11.5 - 12$ eV; dissociation: no direct excitation out of electronic ground state; must be excited to Lyman or Werner bands from which it can fall back into ground state (flourescence) or dissociate. Intensity of transitions

$$I_{ul} = \frac{h\nu}{4\pi} \cdot x(u) \cdot N_{\mathrm{H_2}} \cdot A_{ul} \tag{4.34}$$

where A_{ul} is the Einstein coefficient for spontaneous emission and $x(u)$ is the fraction of molecules in the upper level, $N_{\mathrm{H_2}}$ column density. At LTE, $x(u)$ is given by

$$x(J) = \frac{(2J+1) \cdot g_J \cdot e^{-\frac{h\nu}{k_B T_K}}}{Q(T_K)} \tag{4.35}$$

where $Q(T_K)$ is the partition function

$$Q(T_K) = \sum_J (2J+1) \cdot g_J \cdot \exp\left(-\frac{h\nu_J}{k_B T_K}\right) \tag{4.36}$$

statistical weight $g_J = 1$ for para (even J) nad. spins $\uparrow\downarrow$ or $g_J = 3$ for ortho (odd J) nad. spins $\uparrow\uparrow$, e.g. S(0) line: $v = 0 \rightarrow 0, J = 2 \rightarrow 0, \lambda = 28.2$ μm, ($A_{20} = 2.95 \cdot 10^{-11}$) has been observed with ISO in war regions of the ISM

We shall see later now one may use the CO line to infer the H_2 column density from its (the CO) intensity, using empirical relations. Another possibility is the so-called LVG approximation (Large Velocity Gradient), which will be also tuched upon later.

4.1.6 CO (carbon monoxide)

second most abundant molecule in the ISM. Important: owing to its high abundance, it experiences frequent collisions with H_2 and can therefor be used as an indirect tracer of total molecular gas. CO important: owing to its high abundance, it experiences frequent collisions with H_2 and can be used as indirect tracer of total molecular gas.

Molecule	Transition	A_{ul}	ν_{ul} / GHz
^{12}CO	$1 \rightarrow 0$	$7.4 \cdot 10^{-8}$	111.271203
^{12}CO	$2 \rightarrow 1$	$7.1 \cdot 10^{-7}$	230.538001
^{13}CO	$1 \rightarrow 0$	$6.5 \cdot 10^{-8}$	110.201370
^{13}CO	$2 \rightarrow 1$	$6.2 \cdot 10^{-7}$	220.398714
C^{18}O	$1 \rightarrow 0$	$6.5 \cdot 10^{-8}$	109.782182
C^{18}O	$2 \rightarrow 1$	$6.2 \cdot 10^{-7}$	219.560319

$\nu(J+1 \rightarrow J) = 2B_e \cdot c \cdot (J+1) = 2 \cdot B \cdot (J+1)$, $B = B_e \cdot c$, no K quantization (it is linear)

$B(^{12}\mathrm{CO}) = 57.6356$ GHz

$B(^{13}\mathrm{CO}) = 55.1007$ GHz because of slightly larger Θ_E

$X(\mathrm{CO}) \approx 10^{-4}$ relative to H_2; $^{13}\mathrm{CO}/^{12}\mathrm{CO} \approx 1/60$; CO is very stable; $D_e = 11.09$ eV, dissociation only at 912 Å $< \lambda <$ 1118 Å, discovered 1970 by Wilson et al.

4.1.7 NH_3 (ammonia)

ammonia is the "interstellar thermometer"; has J and K quantization (symmetric rotator) different spins of H atoms, ortho and para
ortho: all spins parallel, $K = 3n$
para: not all spins parallel, $K = 3n + 1$ (n integer)

inversion: all levels except $K = 0$ are split; selection rules for electric dipole transitions are $\Delta K = 0, \Delta J = 0, \pm 1$

- transitions between different K-numbers are forbidden
- lowest levels of each K (i.e. those with $J = K$) are metastable
- metastable states are entirely defined by collisions, population hence function of temperature

$n_{\mathrm{crit.}} \approx 10^7$ cm^{-3}, for inversion transitions $n_{\mathrm{crit.}} \approx 10^3 \cdots 10^4$ cm^{-3}; NH_3 probes a large range of densities

hyperfine transition: inversion transitions are further split $F = J + I, J + I - 1, \ldots, J - I$

$\nu(J, K)$ inversion

$\nu(1, 1) = 23.694$ GHz
$\nu(2, 2) = 23.722$ GHz
$\nu(3, 3) = 23.870$ GHz
$\nu(4, 4) = 24.139$ GHz

discovered in 1968 by Cheung et al.

4.1.8 H_2CO (formaldehyde)

prolate symmetric top, with dipole moment along a-axis (#3); quantum numbers are here J, K_3, K_1; para: even K_3; ortho: odd K_3

energy-level diagramme: J_{K_a,K_c} (manifests complex physics)

radio regime: transitions with

$$\begin{array}{rl} \Delta J = 0 & \nu(1_{11} \to 1_{10}) = 4.830 \text{ GHz} \\ \Delta K_a = 0 & \nu(2_{12} \to 2_{11}) = 14.488 \text{ GHz} \\ \Delta K_c = 1 & \nu(3_{13} \to 2_{12}) = 28.975 \text{ GHz} \end{array}$$

$\Delta J = 1$: mm regime; K_a projection of total spin onto a-axis, K_c projection of total spin onto c-axis; discovery by Snyder et al. in 1969 at $\lambda = 6$ cm ($1_{11} \to 1_{10}$)

4.2 Relation between line intensity and column density

Spontaneous transition between upper (u) and lower (l) level given by Einstein coefficient A_{ul}[1]:

$$A_{ul} = \frac{64\pi^4}{3hc^3} \cdot \nu^3 \cdot |\mu_{ul}|^2 = 1.165 \cdot 10^{-11} \cdot \left(\frac{\nu}{\mathrm{GHz}}\right)^3 \cdot \left|\left(\frac{\mu_{ul}}{\mathrm{Debye}}\right)\right|^2 \ \mathrm{s}^{-1} \tag{4.37}$$

general relation for any transition. $|\mu_{ul}|^2$ contains a term that depends on integral over angular part of wave functions of final and initial states; radial part contained in the value of μ; dipole transitions between two rotational levels of linear molecule can be absorption or emission; with $|\mu_{ul}|^2 = |\mu_J|^2$ the dipole moment reads

$$|\mu_J|^2 = \mu^2 \cdot \frac{J+1}{2J+1} \qquad J \to J+1 \text{ i.e. absorption} \tag{4.38}$$

$$|\mu_J|^2 = \mu^2 \cdot \frac{J+1}{2J+3} \qquad J+1 \to J \text{ i.e. emission} \tag{4.39}$$

μ is the permanent electric dipole moment of the molecule. Inserting $|\mu_J|^2$ for emission into equation for A_{ul} we obtain transition probability for dipole emission between to energy levels of a linear molecule:

$$A_{J+1,J} = 1.165 \cdot 10^{-11} \cdot \left(\frac{\mu}{\mathrm{Debye}}\right)^2 \cdot \left(\frac{\nu}{\mathrm{GHz}}\right)^3 \cdot \frac{J+1}{2J+3} \ \mathrm{s}^{-1} \tag{4.40}$$

LTE: energy levels populated according to Boltzmann distribution at temperature T_{ex}:

$$\varkappa_\nu = \frac{c^2}{8\pi} \cdot \frac{1}{\nu_{ul}^4} \cdot \frac{g_u}{g_l} \cdot n_l \cdot A_{ul} \cdot \left(1 - e^{-\frac{h\nu_{ul}}{k_B T_{\mathrm{ex}}}}\right) \cdot \phi_{ul}(\nu) \tag{4.41}$$

general relation between line optical depth, column density of level l and excitation temperature can be calculated now.

Now, as before in the case of HI integrate over frequency (velocity) and along path (line of sight):

$$\int_0^{s_0} \int_{-\infty}^{+\infty} \varkappa_\nu \, d\nu \, ds = \frac{c^2}{8\pi} \cdot \frac{A_{ul}}{\nu_{ul}^2} \cdot \left(1 - e^{-\frac{h\nu_{ul}}{k_B T_{\mathrm{ex}}}}\right) \cdot \int_0^{s_0} n_l \cdot \int_{-\infty}^{+\infty} \phi_{ul}(\nu) \, d\nu \, ds \tag{4.42}$$

$$\int_{-\infty}^{+\infty} \phi_{ul}(\nu) \, d\nu = 1 \qquad \text{by normalization} \tag{4.43}$$

$$\int_0^{s_0} n_l \, ds = N_l \qquad \text{column density} \tag{4.44}$$

$$\int_0^{s_0} \varkappa_\nu \, ds = \tau_\nu \tag{4.45}$$

$$\frac{d\nu}{dv} = \frac{\nu_0}{c} \qquad \text{because} \quad \frac{\nu - \nu_0}{\nu_0} = \frac{v}{c} \tag{4.46}$$

Hence

$$\int_{-\infty}^{+\infty} \tau_\nu = \frac{c^3}{8\pi \cdot \nu_{ul}^3} \cdot \frac{g_u}{g_l} \cdot N_l \cdot A_{ul} \cdot \left(1 - e^{-\frac{h\nu_{ul}}{k_B T_{\mathrm{ex}}}}\right) \tag{4.47}$$

[1] 1 Debye $= 10^{-19}$ esu $= 10^{-18}$ cm$^{5/2}$ g$^{1/2}$ s^{-1}

so that the column density is

$$N_l = 93.5 \cdot \frac{g_l}{g_u} \cdot \left(\frac{A_{ul}}{\mathrm{s}^{-1}}\right)^{-1} \cdot \left(\frac{\nu_{ul}}{\mathrm{GHz}}\right)^{3} \cdot \frac{1}{1 - \exp\left[-0.048 \cdot \left(\frac{\nu}{\mathrm{GHz}}\right) \cdot \left(\frac{T_{\mathrm{ex}}}{\mathrm{K}}\right)^{-1}\right]} \cdot \int_{-\infty}^{+\infty} \tau \left(\frac{dv}{\mathrm{km\ s}^{-1}}\right)\ \mathrm{cm}^{-2} \tag{4.48}$$

In the low-frequency regime (dm, cm wavelengths) the Rayleigh-Jeans approximation holds:

$$N_l = 1948 \cdot \frac{g_l}{g_u} \cdot \left(\frac{A_{ul}}{\mathrm{s}^{-1}}\right)^{-1} \cdot \left(\frac{\nu_{ul}}{\mathrm{GHz}}\right)^{2} \cdot \left(\frac{T_{\mathrm{ex}}}{\mathrm{K}}\right) \cdot \int_{-\infty}^{+\infty} \tau \left(\frac{dv}{\mathrm{km\ s}^{-1}}\right)\ \mathrm{cm}^{-2} \tag{4.49}$$

if emission is optically thin, i.e.

$$T_b = T_{\mathrm{ex}} \cdot \left(1 - e^{-\tau}\right) \approx \tau \cdot T_{\mathrm{ex}} \tag{4.50}$$

and if the telescope beam is filled with the source, i.e.

$$T_{\mathrm{mb}} \approx T_b \tag{4.51}$$

then the column density does no longer depend of the excitation temperature

$$N_l = 1948 \cdot \frac{g_l}{g_u} \cdot \left(\frac{A_{ul}}{\mathrm{s}^{-1}}\right)^{-1} \cdot \left(\frac{\nu_{ul}}{\mathrm{GHz}}\right)^{2} \cdot \left(\frac{T_b}{\mathrm{K}}\right) \left(\frac{dv}{\mathrm{km\ s}^{-1}}\right)\ \mathrm{cm}^{-2} \tag{4.52}$$

excitation does not play a role in determining column densities for optically thin case.

4.2.1 Column density of CO under LTE conditions

CO of caridnal importance

- H_2 most abundant molecule
- lacks electric dipole moment
- CO 2nd-most abundant molecule
- connected to H_2 via collisions

⇒ diagnostic tool for distribution of general molecular gas

Have to make two measurements, one on the line, one away from it (frequency switching), to get rid of continuum; at mm wavelengths, the strongest continuum is that from the CMB, except for clouds located in front of strong extragalactic sources.

$$I_\nu = I_{\nu,\mathrm{line}} \cdot \left(1 - e^{-\tau_\nu}\right) + I_{\nu,\mathrm{bg}} \cdot e^{-\tau_n u} \qquad \text{line + CMB} \tag{4.53}$$

$$I_\nu = I_{\nu,\mathrm{bg}} \qquad \text{only CMB} \tag{4.54}$$

Difference of the two yields line intensity

$$\Delta I_\nu = I_{\nu,\mathrm{line}} \cdot \left(1 - e^{-\tau_\nu}\right) + I_{\nu,rmbg} \cdot \left(1 - e^{-\tau_\nu}\right) \tag{4.55}$$

$$= \left(I_{\nu,\mathrm{line}} - I_{\nu,\mathrm{bg}}\right) \cdot \left(1 - e^{-\tau_\nu}\right) \tag{4.56}$$

$$= \left[\frac{2h\nu^3/c^2}{\exp\left(-\frac{h\nu}{k_B T_{\mathrm{ex}}}\right) - 1} - \frac{2h\nu^3/c^2}{\exp\left(-\frac{h\nu}{k_B T_{\mathrm{CMB}}}\right) - 1}\right] \cdot \left(1 - e^{-\tau_\nu}\right) \tag{4.57}$$

Expressing ΔI_ν by a Rayleigh-Jeans brightness temperature $T_b(\nu)$ and inserting numerical values ($\nu_{10} = 115.271$ GHz), we arive at a simple expression for the excitation temperature if the line is optically thick (i.e. $1 - e^{-\tau_\nu} \approx 1$)

$$T_{\rm ex} = 5.53 \cdot \left[\ln \left(\frac{1}{T_b/5.53 + 0.151} \right) + 1 \right] \tag{4.58}$$

If the line is optically thin (e.g. rarer isotopomer ^{13}CO), then optical depth can be determined as

$$\tau_{^{13}\rm CO} = -\ln \left[1 - \frac{T_b}{5.29} \cdot \left\{ \left[\exp\left(\frac{5.29}{T_{\rm ex}} \right) - 1 \right]^{-1} - 0.151 \right\}^{-1} \right] \tag{4.59}$$

with $\nu_{10} = 110.201$ GHz in this case. Fraction of population in state J for CO ($2J + 1$ degeneracy):

$$\frac{n(J)}{n_{\rm tot}} = \frac{2J+1}{Q} \cdot \exp\left(-\frac{hB \cdot J(J+1)}{k_B T_{\rm ex}} \right) \tag{4.60}$$

where

$$Q = \sum_{J=0}^{\infty} (2J+1) \cdot \exp\left(-\frac{hB \cdot J(J+1)}{k_B T_{\rm ex}} \right) \tag{4.61}$$

is the partition function. Assuming LTE, one can now calculate total population, hence column density, using one transition and corresponding $N(J)$. If excitation temperature is large compared to separation of energy levels, then the above sum can be approximated by an integral, the value of which is

$$Q \approx \frac{k_B T_{\rm ex}}{hB} = 2 \cdot \frac{k_B T_{\rm ex}}{h\nu_{10}} \tag{4.62}$$

because for CO, $\nu(J+1 \to J) = 2 \cdot B \cdot (J+1)$, i.e. $B = 1/2 \cdot \nu_{10}$. Applying the above to the $J = 0$ level, i.e. $J = 1 \to 0$, we can now obtain the column density of (optically thin) ^{13}CO using equation 4.48 on page 55. $T_{\rm ex}$ can be be obtained by observing optically thick ^{12}CO and using equation 4.58, while $\tau_{^{13}\rm CO}$ is given by equation 4.59, assuming $T_{\rm ex}$ to be the same for both isotopmers. We then obtain

$$N_{\rm tot}(^{13}{\rm CO}) = 2.43 \cdot 10^{14} \cdot \left(\frac{T_{\rm ex}}{\rm K} \right) \frac{\int_{-\infty}^{+\infty} \tau_{^{13}\rm CO} \cdot \left(\frac{dv}{\rm km\ s^{-1}} \right)}{1 - \exp\left[-5.29 \cdot \left(\frac{T_{\rm ex}}{\rm K} \right)^{-1} \right]} \tag{4.63}$$

4.2.2 Determination of H_2 column densities/masses

H_2 most abundant, but radiates in warm/hot regions only (vicinity of stars); not representative for general ISM; therefore, indirect traces are used: extinction, far-infrared emission, X-ray absorption, γ-ray, emission, masses of molecular clouds; 2 examples here:

1. *γ-rays*; cosmic rays collide with interstellar hydrogen, produce π^0, which decay into 2 γ-rays; if distribution of cosmic rays is constant anlog the line-of-sight

$$I_\gamma = q_\gamma \left(N_{\mathrm{HI}} + 2 \cdot N_{\mathrm{H_2}}\right) \qquad q_\gamma = \text{parameter to be determined} \tag{4.64}$$

towards molecular gas or clouds, we measure

$$W_{\mathrm{CO}} = \int_{\mathrm{line}} T_b \, dv \tag{4.65}$$

Relating columnn density of H_2 and this line integral, we define the $N_{\mathrm{H_2}}$ to W_{CO} conversion factor:

$$X_{\mathrm{CO}} = \frac{N_{\mathrm{H_2}}}{W_{\mathrm{CO}}} \tag{4.66}$$

Oberserving regions without molecular gas one can determine q_γ. Then, by observing γ-ray emission towards molecular gas one can solve

$$I_\gamma = q_\gamma \cdot (N_{\mathrm{HI}} + 2 \cdot X_{\mathrm{CO}} \cdot W_{\mathrm{CO}}) \tag{4.67}$$

for X_{CO}. Bloemen et al. (1986) obtained $2.8 \cdot 10^{20}$ cm^{-2} K^{-1} km^{-1} s, consistant with findings from other methods.

2. *cloud viral masses*; The virial theorem

$$E_{\mathrm{kin}} = -\frac{1}{2} \cdot E_{\mathrm{pot}} \tag{4.68}$$

allows to infer total masses of molecular clouds, assuming them to consist of molecular hydrogen in the first place (the correction must be made, too). This results in a mass of

$$M = K_1' \cdot \frac{\sigma_v^2 \cdot R}{\mathrm{G}} = K_1 \cdot \left(\frac{\Delta v}{\mathrm{km\ s^{-1}}}\right)^2 \cdot \left(\frac{R}{\mathrm{pc}}\right) \quad \mathrm{M_\odot} \tag{4.69}$$

Observed line width (assuming gaussian velocity distribution):

$$\Delta v = \sqrt{8 \cdot \ln 2} \cdot \sigma_{\mathrm{obs}} \tag{4.70}$$

$$\sigma_{\mathrm{obs}}^2 = \frac{1}{3} \cdot \sigma_v^2 \tag{4.71}$$

$$\Delta v^2 = \frac{8 \cdot \ln 2}{3} \cdot \sigma_v^2 \tag{4.72}$$

$$K_1 = 126 \cdot K_1' \qquad \text{going from cgs to pc, km s}^{-1} \tag{4.73}$$

$$\tag{4.74}$$

derivation of K_1':

$$E_{\mathrm{pot}} = -G \cdot \int_0^M \frac{M(r)}{r} \, dM \tag{4.75}$$

insert

$$\rho(r) = \rho_0 \cdot \left(\frac{r}{r_0}\right)^{-n} \tag{4.76}$$

good angular and spectral resolution; determine $L_{\rm CO}$, σ_v, R and compute

$$X_{\rm CO} = \frac{M_{\rm vir}}{m_{\rm H} \cdot L_{\rm CO} \cdot 1.4} \tag{4.77}$$

This method is supported by the well-established relation between virial mass and CO luminosity of galactic molecular clouds. Current, most frequently used value $X_{\rm CO} = 1.8 \cdot 10^{20}$ cm^{-2} K^{-1} km^{-1} s.

4.2.3 Critical density

In general, radiative transitions cannot be neglected relative to collisions in populating energy levels; assuming statistical equilibrium of levels populated by radiation and collisions, then number of upward transitions must equal the downward ones:

$$n_l \cdot (R_{lu} + C_{lu}) = n_u \cdot (R_{ul} + C_{ul}) \tag{4.78}$$

where R_{lu} and R_{ul} are probabilities for radiative excitations and de-excitations, respectively; C_{lu} and C_{ul} the equivalent for all collisions, must be proportional to number densities; assuming LTE

$$n_l C_{lu} = n_u C_{ul} \tag{4.79}$$

and

$$\frac{n_u}{n_l} = \frac{g_u}{g_l} \cdot \, e^{-\frac{h\nu}{k_B T_{\rm K}}} \tag{4.80}$$

i.e.

$$C_{lu} = C_{ul} \cdot \frac{g_u}{g_l} \cdot \, e^{-\frac{h\nu}{k_B T_{\rm K}}} \tag{4.81}$$

this expression contains only atomic properties,remains valid in general case, provided LTE holds; we now recall that the Einstein coefficient for absorption B_{lu} is related to that of spontaneous emission A_{ul} via

$$A_{ul} = \frac{2h\nu^3}{c^2} \cdot B_{ul} \tag{4.82}$$

and that of stimulated emission B_{ul} to B_{lu} via

$$g_l B_{lu} = g_u B_{ul} \tag{4.83}$$

Probability for upward transition in radiation field with monochromatic energy density u_ν is

$$R_{lu} = B_{lu} \cdot \frac{c u_\nu}{4\pi} \tag{4.84}$$

Isotropic radiation (ISM!) implies

$$\frac{c u_\nu}{4\pi} = I_\nu \tag{4.85}$$

this means

$$R_{lu} = B_{lu} \cdot I_\nu \quad \text{upward probability} \tag{4.86}$$
$$R_{ul} = A_{ul} + B_{ul} \cdot I_\nu \quad \text{downward probability} \tag{4.87}$$

Hence from equation 4.78 on page 58, we obtain

$$\frac{n_u}{n_l} = \frac{g_u}{g_l} \cdot \frac{A_{ul} \cdot I_\nu \cdot \frac{c^2}{2h\nu^3} + C_{ul} \cdot \exp\left(-\frac{h\nu}{k_B T_\mathrm{K}}\right)}{A_{ul}\left(1 + I_\nu \cdot \frac{c^2}{2h\nu^3}\right) + C_{ul}} \tag{4.88}$$

Using Rayleigh-Jeans approximation, i.e. $I_\nu \approx \frac{2\nu^2 k_B T_b}{c^2}$ and $\exp\left(-\frac{h\nu}{k_B T}\right) \approx 1 - \frac{h\nu}{k_B T}$ and $\frac{C_{lu}}{C_{ul}} = \frac{g_u}{g_l} \cdot \exp\left(-\frac{h\nu}{k_B T_K}\right)$ and defining

$$T_0 = \frac{h\nu}{k_B} \cdot \frac{C_{ul}}{A_{ul}} \tag{4.89}$$

we can translate the above into

$$T_\mathrm{ex} = \frac{T_0 + T_b}{T_0 + T_\mathrm{K}} \cdot T_\mathrm{K} \tag{4.90}$$

- If collisions dominate, T_0 is large and $T_\mathrm{ex} \approx T_\mathrm{K}$ (collisional equilibrium or LTE)
- If radiation dominates, T_0 is small and $T_\mathrm{ex} \approx T_b$ (radiative equilibrium)

The collisional de-excitation probability is

$$C_{ul} = n \cdot \langle \sigma_{ul} \cdot v \rangle \tag{4.91}$$

where n is the number density of the particles responsible for the collisions, v is their velocity and σ their cross section. There exists a critical density at which collisions and radiation are equally important; above this threshold, LTE will hold; so the requirement is

$$n_u \cdot R_{ul} = n_u \cdot C_{ul} \tag{4.92}$$

i.e.

$$C_{ul} = R_{ul} = A_{ul} + B_{ul} \cdot I_\nu = A_{ul}\left(1 + \frac{B_{ul}}{A_{ul}} \cdot I_\nu\right) \tag{4.93}$$

so that

$$n_\mathrm{crit.} = \frac{A_{ul}}{\langle \sigma_{ul} \cdot v \rangle} \cdot \left(1 + I_\nu \cdot \frac{c^2}{2h\nu^3}\right) \tag{4.94}$$

Molecule	Transition	E_u [K]	$n_{\text{crit.}}$ [cm^{-3}]
CO	$(1 \to 0)$	5.5	$3 \cdot 10^3$
	$(2 \to 1)$	16.6	$1 \cdot 10^4$
CS	$(1 \to 0)$	2.4	$1 \cdot 10^5$
	$(2 \to 1)$	7.1	$7 \cdot 10^5$
HCO^+	$(1 \to 0)$	4.3	$1.5 \cdot 10^5$
	$(3 \to 2)$	25.7	$3 \cdot 10^6$
HCN	$(1 \to 0)$	4.3	$4 \cdot 10^6$
	$(3 \to 2)$	25.7	$1 \cdot 10^7$
HNC	$(1 \to 0)$	4.3	$4 \cdot 10^6$
	$(3 \to 2)$	26.1	$1 \cdot 10^7$

4.3 Structure of molecular clouds

Once, a certain density of the gas is reached, it becomes unstable and self-gravitational (there are always slight density fluctuations); criterion for instability can be derived as follows (Jeans 1902); consider spherical ($\sim$ homogeneous) mass

$$M = \frac{4}{3}\pi\rho R^3 \tag{4.95}$$

$$E_{\text{pot}} = \frac{3}{5}G\frac{M^2}{R} \tag{4.96}$$

$$E_{\text{kin}} = \frac{3}{2}N_{\text{tot}}k_BT = \frac{3}{2}\frac{M}{\mu m_u}k_BT \tag{4.97}$$

In viral equilibrium, then

$$\frac{2E_{\text{kin}}}{-E_{\text{pot}}} = 1 = \frac{3k_BT}{\mu m_u}M\left(\frac{3}{5}\frac{GM^2}{R}\right)^{-1} \tag{4.98}$$

Solving for R, we obtain the Jeans radius R_J; a mass with $R < R_J$ collapses:

$$R_J = \frac{1}{5}GM\frac{\mu m_u}{k_BT} \tag{4.99}$$

Then, by the same token, a mass $M > M_J$ will collapse:

$$M_J = 5.46 \cdot \left(\frac{k_BT}{\mu m_u G}\right)^{3/2} \cdot \rho^{-1/2} \qquad \text{Jeans mass} \tag{4.100}$$

$$= 1.20 \cdot 10^{-10} \cdot \left(\frac{T}{\text{T}}\right)^{1.5} \mu^{-1.5} \left(\frac{\rho}{\text{g cm}^{-3}}\right)^{-0.5} \text{M}_\odot \tag{4.101}$$

$$= 20 \cdot \left(\frac{T}{\text{K}}\right)^{1.5} \left(\frac{n}{\text{cm}^{-3}}\right)^{-0.5} \text{M}_\odot \quad \text{for } \mu = 2.7 \text{ (He and heavy elements)} \tag{4.102}$$

During contraction, clouds cool via cooling lines, i.e. spectral line emitted following collisional excitation; efficient if sufficient amount of metals around; if these are locked in dust grains, cooling through molecules becomes important.

4.3.1 Non-LTE solution

So-called LVG approach: large velocity gradient; assumes that line broadening is governd by large scale velocity gradient dv/dr in the observed clouds such that

$$\frac{dv}{dr} \cdot R_{\mathrm{cl}} \gg \Delta v_{\mathrm{th}} \tag{4.103}$$

Then emitted photons at one location in the cloud can only interact with nearby molecules which means that the photons can either leave the cloud unhindered or will be absorbed there, hence the global radiation transport is reduced to local one; equation of local statistical equilibrium can be written as

$$\frac{n_u}{n_l} = \frac{\langle u_\nu(\vec{r})\rangle \cdot B_{lu} + C_{lu}}{A_{ul} + \langle u_\nu(\vec{r})\rangle \cdot B_{ul} + C_{ul}} \tag{4.104}$$

$\langle u_\nu(\vec{r})\rangle$ is the mean radiation field (in units of $\mathrm{erg\,s^{-1}\,Hz^{-1}\,sr^{-1}\,cm^{-3}}$) in the line at current position $\vec{r}$. In LVG approximation no assumption about level population, i.e. no LTE, hence the radiation field enters and must be calculated; kinetic temperature and gas (H_2) density enter into calculations; calculations for, e.g., CO lines then need CO abundance as a parameter [^{12}CO/H_2]

Radiation density and source function $S(\vec{r})$ of the medium linked by convolution

$$\langle u_\nu(\vec{r})\rangle = \int K(\vec{r} - \vec{r}') \cdot S(\vec{r}')\, d\vec{r} \tag{4.105}$$

where the convolution kernel $K(\vec{r})$ "contains the physics" of the radiative transfer, i.e. the radiation field throughout the medium and its propagation.

Source function given by

$$S_\nu = \frac{\varepsilon_\nu}{\varkappa_\nu} = \frac{2h\nu_{ul}^3}{c^2} \cdot \left(\frac{g_u}{g_l}\frac{n_l}{n_u} - 1\right)^{-1} \tag{4.106}$$

This is a complex problem since

$$\langle u_\nu(\vec{r})\rangle = f(S_\nu) \tag{4.107}$$
$$S_\nu = f(n_u, n_l) \tag{4.108}$$
$$n_u = f(\langle u_\nu(\vec{r})\rangle) \tag{4.109}$$
$$n_l = f(\langle u_\nu(\vec{r})\rangle) \tag{4.110}$$

The solution now makes use of LVG assumption. If clouds are assumed to

- be spherical
- be isothermal
- have constant density

then the convolution integral is reduced to (Rolfs & Wilson, Lequex)

$$\langle u_\nu(\vec{r})\rangle = [1 - \beta(\vec{r}) \cdot S_\nu(\vec{r})] \cdot \frac{4\pi}{c} \tag{4.111}$$

where $\beta(\vec{r})$ is the escape probability of a photon at point $\vec{r}$, i.e. probability that photon emitted in transition ul at location $\vec{r}$ escapes from the cloud. Some lengthy algebra (Lequeux, Rolfs & Wilson) yields

$$\beta = \frac{1 - e^{-3\tau_0}}{3\tau_0} \tag{4.112}$$

where τ_0 is the optical depth of the transition at line frequency ν_0. Note that $\lim_{\tau \to 0} \beta = 1$ and $\lim_{\tau \to \infty} \beta = \frac{1}{3\tau}$. Optical depth given by

$$\tau_0 = \frac{c^3}{8\pi \cdot \nu_0^3 \left|\frac{dv}{dr}\right|} \cdot n_l \cdot A_{ul} \cdot \left[1 - \exp\left(-\frac{h\nu_0}{k_B T_{\mathrm{ex}}}\right)\right] \cdot \frac{g_u}{g_l} \tag{4.113}$$

Here, just recall that

$$\varkappa_\nu = \frac{c^2}{8\pi \cdot \nu_0^2} \cdot n_l \cdot \frac{g_u}{g_l} \cdot A_{ul} \cdot \left[1 - \exp\left(-\frac{h\nu_0}{k_B T_{\mathrm{ex}}}\right)\right] \cdot \phi_{ul}(\nu) \tag{4.114}$$

and that

$$\tau_\nu = \int \varkappa_\nu \, dr \tag{4.115}$$

since $\phi_{ul}(\nu) \approx \frac{1}{\Delta\nu}$, where $\Delta\nu$ is the line width, we have

$$\frac{dv}{c} = \frac{d\nu}{\nu_0} \Rightarrow \frac{c}{\nu_0} \cdot \left|\frac{dr}{dv}\right| = \frac{dv}{d\nu} \cdot \left|\frac{dr}{dv}\right| = \frac{dr}{d\nu} \approx \phi_{ul}(\nu)\, dr \tag{4.116}$$

Inserting τ_0 into equation 4.111, and equation 4.111 into equation 4.104, we obtain, assuming that Rayleigh-Jeans approximation holds:

$$T_b = \frac{T_K}{1 + \frac{k_B T_K}{h\nu_0} \cdot \ln\left[1 + \frac{A_{ul}}{3 C_{ul} \tau_0} \cdot (1 - \exp(-3\tau_0))\right]} \tag{4.117}$$

In practice, dv/dr and (e.g.) $[^{12}\mathrm{CO}/\mathrm{H_2}]$ are fixed parameters, while $n_{\mathrm{H_2}}$ and T_{kin} are varied. Procedure then:

- measure several transition of (e.g.) Co and its isotopomeres
- calculate line ratios (better to use ratios, absolute values are influenced by "beam-filling")
- plot lines of constant line ratios in T_{kin} - $n_{\mathrm{H_2}}$ plane
- carry out least-squares fit to find most likely point in T_{kin} - $n_{\mathrm{H_2}}$ plane

4.4 Examples

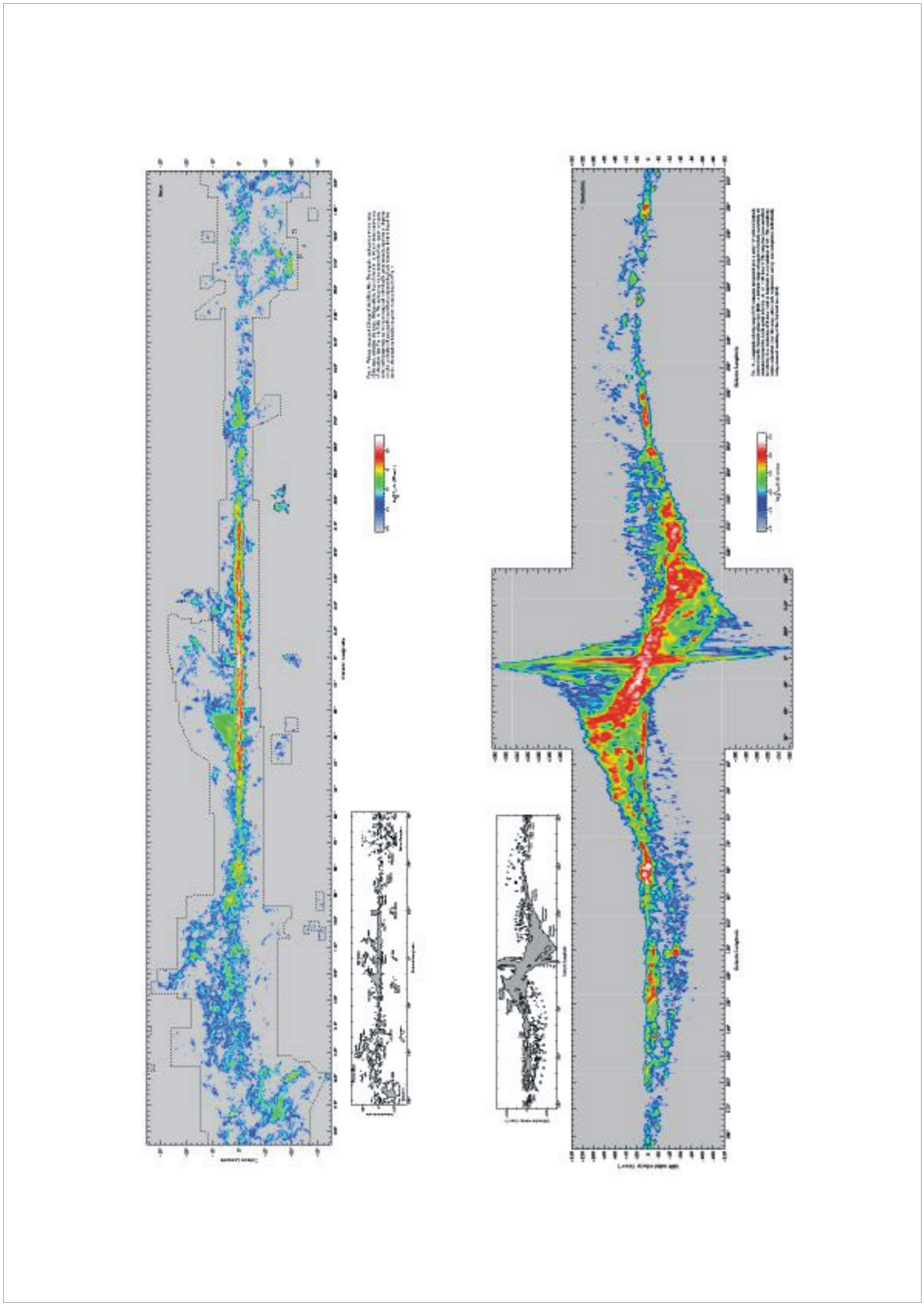

Figure 4.4: The Milky Way in the CO $(1 \rightarrow 0)$ line

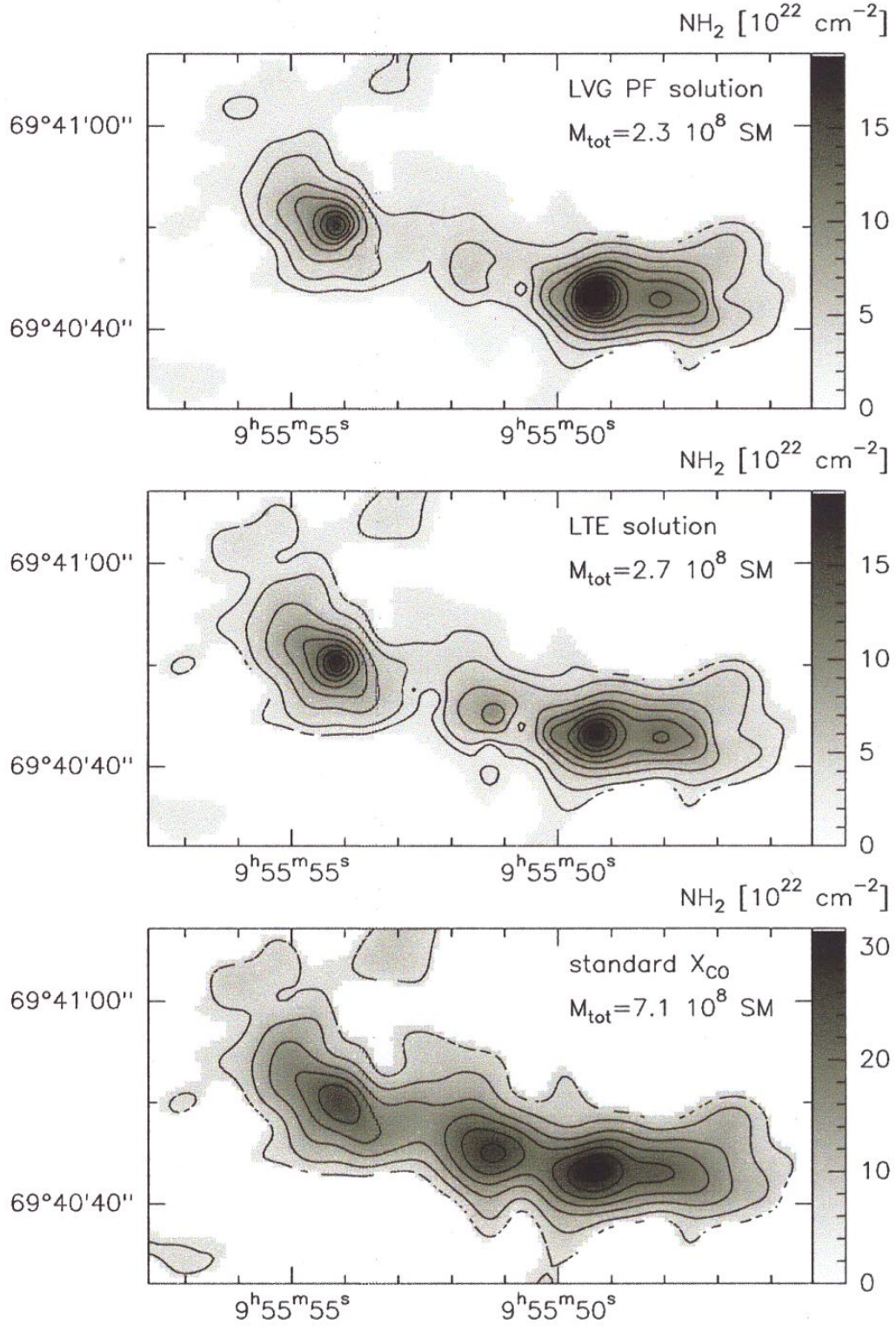

Figure 4.5: Distribution of H_2 in the starburst galaxy M82, derived with different methods

Chapter 5

Hot Gas

5.1 Existence

Hot phase of ISM postulated by Spitzer (1956) in a model to explain the existence of neutral clouds outside (i.e. above / below) the disk of the Milky Way; inferred from obseravtions of CaII absorption lines against early-type stars; velocities of these clouds indicated that they do not participate in galactive rotation, but are directed towards the disk.

It was clear at that time that there is little gas at such distances from the disk; anomalous velocities of the clouds; must have been existent (stable) for some time; why don't they disperse? held together by pressure of a sourrounding hot gas

$$n_1 \cdot k_B \cdot T_1 = n_2 \cdot k_B \cdot T_2 \tag{5.1}$$

More precisely: equate vertical grav. force and all pressure components

$$\frac{dP}{dz} = \overline{\rho} \cdot g_z \tag{5.2}$$

where g_z is the gravitational acceleration

$$\frac{dP}{dz} = \frac{d}{dz}(P_{\mathrm{th}} + P_{\mathrm{h}} + P_{\mathrm{m}} + P_{\mathrm{CR}}) = \overline{\rho} \cdot g_z \tag{5.3}$$

Simple hydrostatic model; $T = 10^6$ K at 10 kpc distance from the plane. Existence of this hot gas meanwhile confirmed by numerous observations

- interstellar absorption lines of highly ionized elements
- X-ray emission: thermal/bremsstrahlung and emission lines

5.2 Heating the gas

What are the heating sources?

Stars hottest MS stars have $T \leq 6 \cdot 10^4$ K

PNe up to $1.5 \cdot 10^5$ K, but small lumiosities; heating of solar corona; $T \approx 1 \cdots 2 \cdot 10^6$ K, probably via shock waves running through the gas and by magnetic reconnection

Shocks here: strong shocks, i.e. $M \gg 1$, where M is the Mach number which is calculated by

$$M = \frac{v}{c_s} \tag{5.4}$$

where v is the shock speed and c_s is the speed of sound of the stationary gas, which can be calculated as follows

$$c_s \approx \sqrt{\frac{P_0}{\rho_0}} = \sqrt{\frac{n \cdot k_B \cdot T_e}{\rho_0}} \tag{5.5}$$

For perfect gas (adiabatic index $\gamma = 5/3$) and strong shocks

$$\frac{\rho_1}{\rho_0} = \frac{\gamma + 1}{\gamma - 1} = 4 \tag{5.6}$$

$$\frac{P_1}{P_0} = \frac{2 \cdot \gamma \cdot M^2}{\gamma + 1 - \frac{\gamma - 1}{\gamma + 1}} \tag{5.7}$$

$$\frac{T_1}{T_0} = \frac{\gamma - 1}{\gamma + 1} \cdot \frac{P_1}{P_0} = 0.35 \cdot M^2 \tag{5.8}$$

It is evident that in case of strong shocks the pressure, temperature and density are substantially uncreased by a shock.

Magnetic reconnection: a complicated process in which particles can be efficiently energized, the connection magnetic loops acting like giant flings. Reconnection occurs within very short time interval; strong acceleration of particles.

Shock waves can be provided by stellar winds and supernovae, e.g. SNII: $E_{\mathrm{SNII}} \approx 10^{51}$ erg. SN rate e.g. 1 every 100 years; $L_{\mathrm{SNII}} = 3 \cdot 10^{41}$ erg s^{-1}. One third is released as radiation and two thirds as mechanical energy.

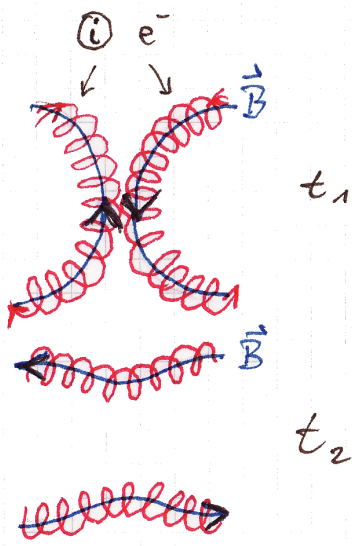

Figure 5.1: Magnetic reconnection

5.3 Observing the hot gas

5.3.1 Absorption lines

Observing hot gas via absorption lines requires elements with sufficiently high ionization potentials that electronic transitions are feasible in the relevant energy range. This implies the UV (150...10 nm) and (soft) X-ray (0.2...2 keV) regime, which must be observed from orbitiong observervatiories (e.g. IUE, ROSAT, FUSE, CHANDRA, XMM). Main absorption lines CIV, NV, OVI; can be used for temperature estimates. For instance OVI has maximum relative abundance at $\log T = 5.5$, with substantially lower probability to exist at temperatures away from this. Similar arguments hold for CIV and NV. Thus, absorption lines of these

ions provide us with very sensitive diagnostics of the temperature of the hot gas (assuming thermodynamic equilibrium).

Because of $n_1 \cdot T_1 = n_2 \cdot T_2$ (pressure balance), hot gas implies tenuous gas; often difficult to carry our absorption measurements.

Ion	λ_{abs} [Å]	Ion. pot. [eV]	a [X/H]	b [K]	c frac.
C^{+3}	1548.195 1550.770	47.9 - 64.5	-3.44	$1.0 \cdot 10^5$	0.35
N^{+4}	1238.821 1242.804	77.5 - 97.9	-3.95	$1.8 \cdot 10^5$	0.25
O^{+5}	1031.926 1037.617	113.9 - 138.1	-3.07	$2.9 \cdot 10^5$	0.25

Table 5.1: Absorption lines for several ions. a: solar abundances; b: temperature of gas in thermodynamical equilibrium at which ion has maximal relative abundance; c: maximal relative abundance

Transitions are iso-electronic, froming doublets each. Intensity is proportional to emission measure $EM = \int n_e^2 \, ds$.

5.3.2 X-ray emission and absorption

Here: thermal X-ray emission (from hot gas). We distinguish

Optically thin radiation from a plasma exhibits rich line spectrum according to all elements contained in it; each photon emitted by an atom or ion escapes the plasma (no self absorption); with increasing temperature, elements are more and more strongly ionized; H- or He-type spectra result; this line radiation dominates below $T \approx 5 \cdot 10^6$ K. Sources are SNRs, hot phase of ISM, galaxy halos, clusters.

terminology: transitions down to $n = 1$ are called the K-series (α, β,...), $n = 2$ are the L-series (α, β,...)

Thermal bremsstrahlung first seen in X-ray tube; results from decelerated electrons as they get braked near a nucleus without going into a bound state; dominates line emission from $T \geq 5 \cdot 10^6$ K, continuum spectrum similar to free-free radiation (see chapter 2), with an exponential tail towards higher energies:

$$I_\nu = 4\pi \int \varepsilon_\nu \cdot dl \tag{5.9}$$

$$\varepsilon_\nu = \frac{8 \cdot Z^2 \cdot e^6 \cdot n_e \cdot n_i}{3 \cdot m_e \cdot c^3} \cdot \sqrt{\frac{2\pi}{3k_B \cdot T_e \cdot m_e}} \cdot e^{-\frac{h\nu}{k_B T_e}} \cdot g_{ff}(T_e, \nu) \tag{5.10}$$

$$g_{ff} = \frac{3}{\sqrt{\pi}} \cdot \ln\left(\frac{9k_B \cdot T_e}{4h \cdot \nu}\right) \tag{5.11}$$

flat spectrum for $h\nu \ll k_B T_e$, exponential decrease beyond that; source emits like optical thin line radiation

Recombination radiation free electrons are captured into bound states by ions; the emissivity of this process is about an order of magnitude lower than in the other two; it is neglible for $T \geq 3 \cdot 10^7$ K.

X-ray absorption in case of the presence of neutral hydrogen between the X-ray source and the observer, H can be ionized by photons with $h\nu > 13.6$ eV. Thus X-ray photons will be absorbed by neutral gas. The photo-absorption cross section of hydrogen is

$$\sigma_{\rm H} = 7.9 \cdot 10^{-18} \cdot g_\nu \cdot \left(\frac{\nu_{\rm ion}}{\nu}\right)^3 \qquad g_\nu = \text{Gaunt factor} \tag{5.12}$$

where $g_\nu \approx 0.9$ for $900 > \lambda > 50$ Åand $g_\nu \approx 0.5$ near $\lambda \approx 10$ Å. Whith line of sight $l \approx 1 \cdots$ a few kpc in the Milky Way, one would expect significant X-ray absorption. Such *X-ray shadows* have actually been found. X-ray absorption is also seen in external galaxies and is an important tool to determine the inclination of galaxies.

X-ray shadows provide an important tool to measure the total hydrogen column, hence mass, in regions that have a hot gas component in their background. Since molecular hydrogen (H_2) is difficult to be measured directly, observations of HI plus X-ray absorption can provide information on the H_2 column density. If CO observations are available for the same region, $X_{\rm CO}$ can be computed in a straigh-forward manner (see chapter).

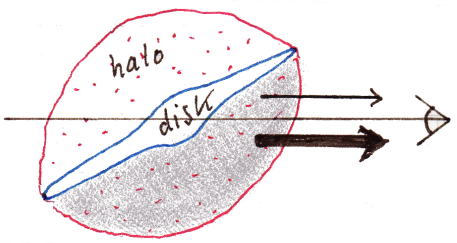

Figure 5.2: Scematic of a X-ray shadow

Observed data commonly fitted with so-called Raymond-Smith spectrum, which for given temperature and metallicity accounts for all radiation processes; while fitting the model spectrum, foreground absorption by neutral hydrogen is also accounted for.

5.4 Cooling of the hot gas

Cooling of the hot gas occurs via line radiation and thermal bremsstrahlung. It is obvious that the higher the element abundances, the more electrons are contained in it. Thus, the interaction probabilities increase, an the (increased) number of photons gives rise to corresponding cooling times. The intricate calculations are beyond the scope of this lecture and we present but qualitative results here. Maximum cooling occurs at $T \approx 10^5$ K. The cooling time is

$$\tau_{\rm cool} = \frac{u}{\Lambda} \tag{5.13}$$

where

$$u = \frac{3}{2} \cdot n \cdot k_B \cdot T_e \tag{5.14}$$

is the energy density and

$$\Lambda(T) = 4\pi \int_0^\infty \varepsilon_\nu \, d\nu \tag{5.15}$$

the cooling function. The emission coefficient ε_ν is given by Eqn. (5.11), and hence $[\Lambda] =$ erg cm^{-3} s^{-1}. The above integral then yields[1] a dependence $\Lambda(T_e) \propto T_e^{1/2}$. The shortest cooling time is found below $T = 10^5$ K, depending on the metallicity of the plasma. Around $T = 10^5$ K the metal dependence of $\tau_{\rm cool}$ is strongest, while above $T \approx 10^7$ K the cooling curves merge. Above this value, line cooling becomes insignificant and cooling by bremsstrahlung dominates. It is given by

$$\tau_{\rm cool} = \frac{u}{\varepsilon_{\rm eff}} \approx 8.5 \cdot 10^{10} \cdot \left(\frac{n_e}{10^{-3}\ {\rm cm}^{-3}}\right)^{-1} \cdot \left(\frac{T_e}{10^8\ {\rm K}}\right)^{\frac{1}{2}} \quad {\rm years} \tag{5.16}$$

The above values, typical for large clusters of galaxies, i.e. the intra-cluster medium, indicate cooling times in excess of a Hubble time!

5.5 Fountains, outflows and winds

Large amounts of mechanical energy released by OB stars and deposited in ISM; stellar winds and supernovae:

$$L_{\rm SN} = \nu_{\rm SN} \cdot E_{\rm SN} \approx 1.6. \cdot 10^{38} \cdot \left(\frac{2 \cdot 10^5\ {\rm yr}}{\Delta\tau}\right) \cdot \left(\frac{E_{\rm SN}}{10^{51}\ {\rm erg}}\right) \quad {\rm erg\ s}^{-1} \tag{5.17}$$

where $\nu_{\rm SN}$ is the supernova rate (e.g. Milky Way $\nu_{\rm SN} = 0.002$ yr^{-1}, M82 $\nu_{\rm SN} = 0.5$ yr^{-1}) and $\Delta\tau$ the duration of the starburst.

That such processes are at work is manifested by yhe numerous holes/bubbles seen in the HI disks of galaxies ($\simeq$ 150 in M31, M33; factor 3 less in dwarf galaxies). If total mechanical energy is sufficiently high breakout of bubbles through the disk; outflow into the halo ("chimney model", Norman & Ikenchi, 1989). We expect hot gas rising into the halo, condensing there and falling back onto the disk: HVCs!

Halo gas is heated to temperatures of $10^6 \cdots 10^7$ K, showing up as large X-ray plumes or halos.

"Bottom-up" scenario of structure formation (CDM): first, low mass galaxies formed, undergoing intense starbursts; strong galactic winds, injecting metals into the IGM. IGM has $Z \approx 0.3 \cdots 0.5\ Z_\odot$; due to early dwarf galaxies? Heating of this gas (cosmological shocks, cluster merging)? Cooling?

5.6 Hot gas in clusters of galaxies

Probably owing to intense starforming at early epochs, groups and clusters of galaxies contain large amounts of hot gas. The cooling time of this, with $n_e \approx 10^{-3} \cdots 10^{-2}$ cm^{-3}, $T_e \approx 10^7 \cdots 10^8$ K, is too large to cool the plasma significantly within a Hubble time. It can be assumed that in a relaxed cluster the gas is in hydrostatic equilibrium. We can then use its observed properties to derive the total mass of the cluster (dark and baryonic). This method, complementary to gravitational lensing, is commonly used with the advent of modern X-ray telescopes.

[1] One makes use of $\int_0^\infty x^{n+1}\ e^{-ax}\ dx = \frac{\Gamma(n+1)}{a^{n+1}} \quad for \quad a > 0, \quad n > -1$

Speed of sound in cluster gas

$$c_s \approx \sqrt{\frac{P}{\rho}} = \sqrt{\frac{nk_BT}{\rho}} \tag{5.18}$$

sound crossing time through cluster

$$\tau_{\text{cross}} = \frac{2R_{\text{cluster}}}{c_s} \approx 7 \cdot 10^8 \text{ yr} \ll \tau_{\text{Hubble}} \quad \text{(age of cluster)} \tag{5.19}$$

hydrostatic equilibrium justified, in the spherically symmetric cas, we then have

$$\frac{1}{\rho}\frac{dP}{dr} = -\frac{d\phi}{dr} = -\frac{G\,M(r)}{r^2} \tag{5.20}$$

where $M(r)$ is the total cluster mass whithin radius r. Equating (m_p proton mass, $\mu = \overline{m}/m_p$)

$$P = \frac{\rho k_B T}{\mu m_p} \tag{5.21}$$

we arrive at

$$M(r) = -\frac{k_B T r^2}{G\mu m_p} \cdot \left(\frac{d\ln\rho}{dr} + \frac{d\ln T}{dr} \right) \tag{5.22}$$

Hence, extracting the radial dependence of density and temperature from (X-ray) observations, we can measure the total (i.e. dark and baryonic) mass and its density as a function of r.

If the gas were pure hydrogen, we would have $\mu = 0.5$ (electron contributes to pressure but not to mass). Since we have $\simeq 25\%$ of the (by mass) plus a little contribution of more heavy elements, the mean molecular mass turns out to be $\mu = 0.63$. Modern X-ray studies come up with

$$M_{\text{Cluster}} = 5 \cdot 10^{14} \cdot 10^{15}\ M_\odot \quad \text{(total mass)} \tag{5.23}$$

of which $60 \cdots 85\%$ is dark matter, $10 \cdots 30\%$ is hot gas and roughly 5% are stars.

Chapter 6

Ionized Gas

In vicinity of young, massive (O,B) stars, gas is ionized by intense UV radiation; these are called HII regions, in line with spectroscopic notation (neutral: I, one electron separated or strongly ionized: II, two electrons separated, or doubly ionized: III and so on)

HII regions are characterized by thermal free-free radiation and recombination lines. A big step towards understanding HII regions was made by Strömgren (1939), who proposed the the size of HII regions is determined by the number of ionizing photons from the stars and by the gas density; assuming balance between ionizations and recombinations, he demonstrated the dominant role of hydrogen in the physics of such nebulae.

6.1 Saha equation

This equation, worked out by Indian physicist Meghand Saha (1920), allows to calculate the relative number of ionized and neutral atoms in a plasma, or of relative number of atoms in different ionization stages; for this we now need two indices characterizing the number density, viz. n_i^m where i denotes the ionization stage (I $\rightarrow i = 0$, II $\rightarrow i = 1$ and so on) and m stands for the excitation stage (E_m). Then

$n^i = \sum_m n_m^i$ total number of atoms of certain element in i-th ionization stage per cm^3

$n = \sum_i n^i$ total number of atoms of certain element per cm^3

population of energy levels follows Boltzmann formula:

$$\frac{n_m^i}{n_1^i} = \frac{g_m^i}{g_1^i} \cdot e^{-\frac{E_m^i}{k_B T}} \tag{6.1}$$

summing over all m one obtains ratio of number density of atoms with i-th ionization stage and excitation energy m to total numern density of atoms with i-th ionization stage:

$$\frac{n_m^i}{n^i} = \frac{g_m^i}{Q_i(T)} \cdot e^{-\frac{E_m^i}{k_B T}} \tag{6.2}$$

where

$$Q_i(T) = \sum_m g_m^i \cdot e^{-\frac{E_m^i}{k_B T}} \tag{6.3}$$

is the partition function. Now the Saha equation describes equilibrium of reaction atom $\rightleftarrows$ ion + electrons.

It can be considered as extension of Boltzmann equation to regime of continuous states of positive energy above $E_\infty = 0$. The energy of such state with respect to the ground state is

$$E = \chi^0 + \frac{1}{2} m_e v^2 \tag{6.4}$$

where χ^0 is the ionization energy of the neutral atom (13.6 eV for hydrogen); because

$\chi^i_m = E_1 - E_m$	excitation energy of i-th atom
$\chi^i = E_1 - E_\infty$	ionization energy of i-th inonization state
χ^0	ionization energy of neutral atom
χ_1	ionization energy of singly ionized atom
	and so forth

quatum theory tells us that continuum of states above $E = 0$ is subdivided into volumes h^3 of phase space; hence, number density of atoms with one seperated electron that finds itself in phase space volume element $x \cdots x + dx, y \cdots y + dy, z \cdots z + dz, P_x \cdots P_x + dP_x, P_y \cdots P_y + dP_y, P_z \cdots P_z + dP_z$, taken per quantum cell (meaning division by h^3) is

$$\frac{dn^1_1}{n^0_1} = 2 \cdot \frac{g^1_1}{g^0_1} \cdot e^{-\frac{1}{k_B T}\left[\chi_0 + \frac{1}{2m_e}(P_x^2 + P_y^2 + P_z^2)\right]} \frac{dx\, dy\, dz\, dP_x\, dP_y\, dP_z}{h^3} \tag{6.5}$$

The factor of 2 accounts for the spin degeneracy of e^- which may take two orientations in external field. We have restricted ourselves here to ions in the ground state ($m = 1$; integration over momentum $(-\infty \cdots + \infty)$ yields a factor $(2\pi m_e k_B T)^{2/3}$:

$$\int_0^\infty e^{-\frac{P^2}{2m_e k_B T}} 4\pi P^2 dP = (2\pi m_e k_B T)^{2/3} \tag{6.6}$$

integration over spatial coordinates has to be restricted to volume in which there is one electron at a time (since there should be only one free e^- per ion), hence this yields a factor n_e^{-1} (the number density of free electrons); then the Saha equation in its final form reads:

$$\frac{n^1_1}{n^0_1} \cdot n_e = 2 \frac{g^1_1}{g^0_1} \cdot \frac{(2\pi m_e k_B T)^{2/3}}{h^3} \cdot e^{-\frac{\chi^0}{k_B T}} \tag{6.7}$$

6.2 Recombination lines

Ionized atoms in HII region recombine, leaving them in some excited state $n = n_u$; when H atom undergoes transition from upper level n_u to lower one, n_l, it radiates at frequency

$$\nu_{ul} = c \cdot R \cdot Z^2 \left(\frac{1}{n_l^2} - \frac{1}{n_u^2}\right) \tag{6.8}$$

where Z is the effective charge of the nucleus (or ion, here $Z = 1$), and R is the Rydberg constant,

$$R = R_\infty \cdot \left(1 - \frac{m_e}{M}\right) \tag{6.9}$$

where M is the mass of the atom. n_l and n_u are the principal quantum numbers. For large M, above equation can be simplyfied by approximation

$$\nu_{ul} \approx 2 \cdot c \cdot R \cdot Z^2 \frac{n_u - n_l}{n_l^3} \tag{6.10}$$

With $R_\infty = 109738.2\text{cm}^{-1}$ and $n_u = 110, n_l = 109$ this gives a frequency in the radio regime $\nu_{ul} = 5.08$ GHz, and for $n_u = 3, n_l = 2$ a wavelength in the optical regime $\lambda_{ul} = 6563$ Å, which is the H_α line. Large values of n are only populated via recombination, hence the name recombination lines, since decay with step $\Delta n = 1$ has larger transition probability than $\Delta n > 1$, $\Delta n = 1$ is referred to as "α" (Lyα, Hα, Pα, Brα, H109α, He137α, ...)

6.3 Absorption coefficient of RRLs[1]

$$\varkappa_L(\nu) = \frac{h\nu}{4\pi} B_{ul} n_l \left(1 - \frac{g_l}{g_u} \cdot \frac{n_u}{n_l}\right) \cdot \phi(\nu) \tag{6.11}$$

$$= \frac{c^2}{8\pi\nu^2} \cdot \frac{g_u}{g_l} \cdot A_{ul} n_l \left(1 - \frac{g_l}{g_u} \cdot \frac{n_u}{n_l}\right) \cdot \phi(\nu) \tag{6.12}$$

notation to discern ionization degree and excitation state:

n	total number density of H atoms
n_0^0	total number density of H atoms, neutral, ground state
n_0^1	total number density of H atoms, ionized, ground state
n_l^0	total number density of H atoms, neutral, excited state E_l
n^0	total number density of H atoms, neutral, all excited states

Consider ratio of neutral atoms with energy E_l relative to ground state, which is given by the Boltzmann distribution, i.e.

$$\frac{n_l^0}{n_0^0} = \frac{g_l}{g_u} \cdot e^{-\frac{E_l}{k_B T}} \tag{6.13}$$

Referring to all neutral H atoms, this reads

$$\frac{n_l^0}{n^0} = \frac{g_l}{Q(T)} \cdot e^{-\frac{E_l}{k_B T}} \tag{6.14}$$

where

$$Q(T) = \sum_l g_l \cdot e^{-\frac{E_l}{k_B T}} \tag{6.15}$$

is the partition function. Now calculate ratio of ionized to neutral H atoms (all excitation states). The Saha equation then reads

$$\frac{n^1}{n^0} \cdot n_e = 2\frac{g_1}{g_0} \cdot \frac{(2\pi m_e k_B T)^{2/3}}{h^3} \cdot e^{\left(-\frac{\chi^1}{k_B T_e}\right.} \tag{6.16}$$

[1] Radio Recombination Lines

Here, χ^1 is the ionization energy of the atom, T_e is the "electron temperature", describing the thermal energy of electrons. Designating $n^1 = n_i$ number density of ions, $g_1 = 1$, $g_l = 2\aleph_l^2$, where $\aleph_l$ is the quantum number of the lower state, and nserting equation 6.14 into the Saha equation 6.16 we obtain

$$n_l^0 = \aleph_l^2 \cdot \frac{h^3}{(2\pi m_e k_B T)^{2/3}} \cdot n_i n_e \cdot e^{-\frac{E_l - \chi^1}{k_B T_e}} \tag{6.17}$$

Now rewrite term in brackets of $\varkappa_L(\nu)$ using Rayleigh-Jeans approximation

$$1 - \frac{g_l}{g_u}\frac{n_u}{n_l} = 1 - e^{-\frac{h\nu}{k_B T_e}} \approx \frac{h\nu}{k_B T_e} \tag{6.18}$$

in the radio regime (e.g. 5 GHz, $T_e = 10^4$ K $\Rightarrow \frac{h\nu}{k_B T_e} \approx 2.4 \cdot 10^{-5}$)

$$\varkappa_L(\nu) = \frac{c^2 h}{8\pi\nu} \cdot \frac{1}{k_B T_e} \cdot \frac{g_u}{g_l} \cdot A_{ul} \cdot n_l^0 \cdot \phi(\nu) \tag{6.19}$$

and with oscillator strength f_{lu}

$$A_{ul} = \frac{g_l}{g_u} \cdot \frac{8\pi^2 e^2}{m_e c^3} \cdot \nu^2 f_{lu} \tag{6.20}$$

we obtain

$$\varkappa_L(\nu) = \frac{\pi e^2}{m_e c} \cdot \frac{h\nu}{k_B T_e} \cdot n_l^0 \cdot \phi(\nu) \cdot f_{lu} \tag{6.21}$$

What about $\phi(\nu)$? Assume Doppler broadening and gaussian line shape, i.e. $\phi(\nu)$ is a one-dimensional Maxwell distribution

$$\phi(v) = \frac{1}{\sqrt{2\pi} \cdot \sigma} \cdot e^{-\frac{v^2}{2\sigma^2}} \tag{6.22}$$

kinetic gas theory:

$$\frac{m}{2}\langle \vec{v}^2 \rangle = \frac{3}{2} k_B T \tag{6.23}$$

$$\frac{m}{2}\langle v_x^2 \rangle = \frac{1}{2} k_B T \qquad \langle v_x^2 \rangle = \sigma(\text{observed}) \tag{6.24}$$

$$\sigma^2 = \frac{k_B T}{m} \tag{6.25}$$

radio astronomy: FWHM. Write FWHM = Δv

$$\phi\left(\frac{\Delta v}{2}\right) = \frac{1}{\sqrt{2\pi}\sigma} \cdot e^{-\frac{(\Delta v/2)^2}{2\sigma^2}} = \frac{1}{2} \cdot \frac{1}{\sqrt{2\pi}\sigma} \tag{6.26}$$

Solve for Δv and find

$$\Delta v = 2\sqrt{2 \ln 2} \cdot \sigma = 2.355 \cdot \sigma \tag{6.27}$$

i.e. $\Delta v^2 = 8 \ln 2 \cdot \frac{k_B T}{m}$ and $T = \frac{m}{8 \ln 2 k_b} \cdot \Delta v^2$. Conversion to frequency: Doppler formula

$$\nu = \nu_0 \cdot \sqrt{\frac{1 - \frac{v}{c}}{1 + \frac{v}{c}}} \approx \nu_0 \cdot \left(1 - \frac{v}{c}\right) \quad \text{approximation in radio astronomy} \tag{6.28}$$

$$v = c \cdot \frac{\nu_0 - \nu}{\nu_0} \tag{6.29}$$

$$d\nu = -\frac{\nu_0}{c} dv \quad \text{and} \quad dv = -\frac{c}{\nu_0} d\nu \tag{6.30}$$

Since

$$\phi(\nu) d\nu = -\phi(v) dv \tag{6.31}$$

we have

$$\phi(\nu) = \phi(v) \cdot \frac{c}{\nu_0} \tag{6.32}$$

so that

$$\phi(\nu) = \frac{1}{\nu_0} \cdot \sqrt{\frac{mc^2}{2\pi k_B T}}\, e^{-\frac{mc^2}{2k_B T} \left(\frac{\nu_0 - \nu}{\nu_0}\right)^2} \tag{6.33}$$

FWHM $\Delta\nu$:

$$\Delta\nu = \Delta v \cdot \frac{\nu_0}{c} = \left(8 \ln 2 \cdot \frac{k_B T}{mc^2}\right)^{1/2} \cdot \nu_0 \tag{6.34}$$

and hence finally

$$\phi(\nu) = \frac{1}{\Delta\nu} \cdot \sqrt{\frac{4 \ln 2}{\pi}} \cdot\, e^{-4 \ln 2 \cdot \left(\frac{\nu_0 - \nu}{\Delta\nu}\right)^2} \tag{6.35}$$

Now, inserting Saha equation for n_l^0 6.17 into expression for $\varkappa_L(\nu)$, we obtain

$$\varkappa_L(\nu) = \frac{\pi e^2 h^4}{m_e c} \cdot \frac{\nu_0}{k_B T_e} \frac{\aleph_l^2}{(2\pi m_e k_B T)^{2/3}} \cdot n_i n_e \cdot\, e^{-\frac{E_l - \chi^1}{k_B T_e}} \cdot f_{lu} \cdot \phi(\nu) \tag{6.36}$$

$l : \aleph, u : \aleph + \Delta\aleph$. For large quantum numbers $\aleph$, i.e. $\Delta\aleph \ll \aleph$, oscillator strength (with g the Gaunt factor, quantum-mechanically correct)

$$f_{mn} = \frac{2^6}{3\pi\sqrt{3}} \cdot \frac{1}{2m^2} \cdot \left(\frac{1}{m^2} - \frac{1}{n^2}\right)^{-3} \cdot \frac{1}{n^3} \cdot \frac{1}{m^3} \cdot g \propto \frac{n}{\Delta n^3} \tag{6.37}$$

can be written as

$$f_{\aleph,\aleph+\Delta\aleph} = \aleph \cdot M(\aleph) \tag{6.38}$$

$\Delta\aleph$	$M(\Delta\aleph)$
1	0.1910
2	0.0263
3	0.0081
4	0.0034

Since $E_l \approx E^i$, the exponential term becomes unity. Furthermore, we use

$$\nu_0 = 6.576 \cdot 10^{15} \frac{\Delta\aleph}{\aleph^3}\,\mathrm{Hz} \quad , \quad \nu = \nu_0 \Rightarrow \phi(\nu_0) = \frac{1}{\Delta\nu}\sqrt{\frac{4\ln 2}{\pi}} \tag{6.39}$$

$$\varkappa_L(\nu) = \frac{\pi e^2 h^4}{m_e c k_B} \cdot \frac{\aleph^3 \cdot M(\Delta\aleph)}{(2\pi m_e k_B T)^{2/3}} \cdot T_e^{-5/2} \cdot n_i n_e \cdot \frac{1}{\Delta\nu}\sqrt{\frac{4\ln 2}{\pi}} \cdot 6.576 \cdot 10^{15} \cdot \frac{\Delta\aleph}{\aleph^3} \tag{6.40}$$

$$= 3.26 \cdot 10^{-12} \cdot M(\Delta\aleph) \left(\frac{T_e}{\mathrm{K}}\right)^{-5/2} \left(\frac{n_i n_e}{\mathrm{cm}^{-6}}\right) \left(\frac{\Delta\nu}{\mathrm{Hz}}\right)^{-1} \cdot \Delta\aleph \tag{6.41}$$

HII regions are electrically neutral which means that $n_i = n_e$ and $n_i \cdot n_e = n_e^2$. Consider $\Delta\aleph$ (α lines)

$$\varkappa_L(\nu) = 6.22 \cdot 10^{-16} \left(\frac{n_e}{\mathrm{cm}^{-6}}\right)^2 \left(\frac{T_e}{\mathrm{K}}\right)^{-5/2} \left(\frac{\Delta\nu}{\mathrm{kHz}}\right)^{-1} \tag{6.42}$$

optical depth

$$\tau_L = \int_0^{s_0} \varkappa_L(\nu)\, ds = 1.92 \cdot 10^3 \left(\frac{T_e}{\mathrm{K}}\right)^{-5/2} \left(\frac{\Delta\nu}{\mathrm{kHz}}\right)^{-1} \cdot EM \tag{6.43}$$

where

$$EM = \int_0^{s_0} n_e^2\, ds = \int_0^{s_0} \left(\frac{n_e}{\mathrm{cm}^{-6}}\right)^2 \left(\frac{ds}{\mathrm{pc}}\right) \quad \mathrm{cm}^{-6}\,\mathrm{pc} \tag{6.44}$$

is the emission measure. This quantitiy and the electron temperature t_e was also an ingredient to the optical depth of the thermal free-free radiation. For small optical depths, $\tau_L \ll 1$, we have $T_L = \tau_L \cdot T_e$. Hence

$$T_L = 1.92 \cdot 10^3 \left(\frac{T_e}{\mathrm{K}}\right)^{-3/2} \left(\frac{\Delta\nu}{\mathrm{kHz}}\right)^{-1} \left(\frac{EM}{\mathrm{cm}^{-6}\,\mathrm{pc}}\right) \quad \mathrm{K} \tag{6.45}$$

For the free-free continuum radiation we found

$$\tau_C = 8.235 \cdot 10^{-2} \cdot \left(\frac{T_e}{\mathrm{K}}\right)^{-1.35} \left(\frac{\nu}{\mathrm{GHz}}\right)^{-2.1} \left(\frac{EM}{\mathrm{cm}^{-6}\,\mathrm{pc}}\right) \tag{6.46}$$

and

$$T_C = 8.235 \cdot 10^{-2} \cdot \left(\frac{T_e}{\mathrm{K}}\right)^{-0.35} \left(\frac{\nu}{\mathrm{GHz}}\right)^{-2.1} \left(\frac{EM}{\mathrm{cm}^{-6}\,\mathrm{pc}}\right) \quad \mathrm{K} \tag{6.47}$$

Dividing the two observed brightness temperatures, viz. T_L and T_C, and assuming them to be produced by the same ionized region, we obtain

$$\frac{T_L}{T_C} \cdot \left(\frac{\Delta\nu}{\mathrm{kHz}}\right) = 2.33 \cdot 10^4 \left(\frac{T_e}{\mathrm{K}}\right)^{-1.15} \left(\frac{\nu}{\mathrm{GHz}}\right)^{2.1} \cdot \frac{1}{1 + n_{\mathrm{He^+}}/n_{\mathrm{H^+}}} \tag{6.48}$$

where the last factor accounts for the presence of ionized helium; in general, $n_{\mathrm{He^+}}/n_{\mathrm{H^+}} \approx 0.1$. Converting the line width from frequency to velocity, we finally arrive at

$$\frac{T_L}{T_C} \cdot \left(\frac{\Delta v}{\mathrm{km\,s^{-1}}}\right) = 6.978 \cdot 10^3 \left(\frac{T_e}{\mathrm{K}}\right)^{-1.15} \left(\frac{\nu}{\mathrm{GHz}}\right)^{1.1} \cdot \frac{1}{1 + n_{\mathrm{He^+}}/n_{\mathrm{H^+}}} \tag{6.49}$$

This equation is of cardinal importance, as it reflects the most straightforward and reliable way to measure the electron temperature in an astrophysical plasma or HII region: if we measure both T_L and T_C we can solve for the electron temperature T_e! This has assumed small optical depth. The effect of optical depth is easily seen by the following consideration. Assume that both, line and continuum are emitted by the same region with electron temperature T_e. At line center, we then have

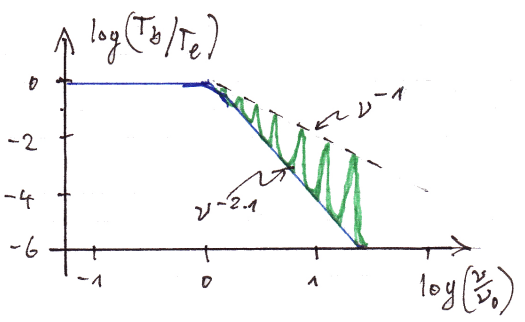

Figure 6.1: Recombination lines

$$T_{L+C} = T_e \cdot \left[1 - e^{-(\tau_L + \tau)}\right] \tag{6.50}$$

away from the line we measure

$$T_C = T_e \cdot \left(1 - e^{-\tau_C}\right) \tag{6.51}$$

hence for the line alone

$$T_L = T_{L+C} - T_C = T_e \cdot e^{-\tau_C} \cdot \left(1 - e^{-\tau_L}\right) \tag{6.52}$$

If $\tau_C \gg 1$, no recombination lines are seen; the are only visible if τ_C is small; but this is nothing but turning the emitting region into a black body as τ_C is increasing; a black body does not emit any spectral lines!

6.4 Non-LTE conditions

Diameter of H atoms strongly dependent on principle quantum number n

$$a_n = \frac{\hbar^2}{Z^2 m e^2} \cdot n^2 \tag{6.53}$$

Collisions have large effect for such atoms. Hence, the assumption of LTE, which implies collision-dominated level population, (may) deviate(s) from LTE with decreasing n; we define a departure coefficient b_n, relating true population level n_n to population under LTE conditions, n_n^*:

$$n_n = b_n \cdot n_n^* \tag{6.54}$$

We have $b_n < 1$ since A coefficient for lower state is larger ($A_n \propto n^{-5}$), atom is smaller which means that collisions are less effective. Hence, $b_n \to 1$ for LTE and

$$\frac{n_u}{n_l} = \frac{b_u}{b_l} \cdot \frac{g_u}{g_l} e^{-\frac{E_{ul}}{k_B T_e}} \tag{6.55}$$

The absorption coefficient then reads

$$\varkappa_L(\nu) = \frac{c^2}{8\pi\nu_{ul}^2} \cdot \frac{g_u}{g_l} \cdot n_l \cdot A_{ul} \cdot \left(1 - \frac{b_u}{b_l} e^{-\frac{h\nu_{ul}}{k_B T_e}}\right) \cdot \phi_{ul}(\nu) \tag{6.56}$$

$$= \varkappa_L^*(\nu) \cdot b_e \cdot \beta_{lu} \tag{6.57}$$

where

$$\beta_{lu} = \frac{1 - \frac{b_u}{b_l}\, e^{-\frac{h\nu_{ul}}{k_B T_e}}}{1 - e^{-\frac{h\nu_{ul}}{k_B T_e}}} \tag{6.58}$$

and $\varkappa_L^*(\nu)$ is the absorption coefficient derived under LTE conditions. Since $h\nu \ll k_B T_e$, this simplifies to

$$\beta_{lu} = \left[1 - \frac{b_u}{b_l}\left(1 - \frac{h\nu_{ul}}{k_B T_e}\right)\right] \frac{k_B T_e}{h\nu_{ul}} \tag{6.59}$$

$$= \frac{b_u}{b_l} \cdot \left[1 - \frac{k_B T_e}{h\nu_{ul}} \cdot \frac{b_u - b_l}{b_u}\right] \tag{6.60}$$

6.5 Strömgren sphere

Massive and hot UV-emitting stars embedded in HI cloud ionize the sourrounding medium; assuming balance between ionization and recombination rates, one can calculate the size of the resulting HII region. This must depend on the total number of emitted Lyman continuum photons; a star emits

$$\dot{N}_{\mathrm{LyC},\Omega} = \int_{\nu_0}^{\infty} \frac{B'(T,\nu)}{h\nu}\, d\nu \quad \text{photons s}^{-1}\text{cm}^{-2}\text{sr}^{-1} \tag{6.61}$$

LyC photons per s and cm^2 into solid angle of 1 steradians, where $\nu_0 = 3.29 \cdot 10^{15}$ Hz (912 Å, 13.6 eV) and

$$B'(T,\nu) = \varkappa(\nu) \cdot B(T) \tag{6.62}$$

$\varkappa(\nu)$ corrections function describing the deviation of the stellar spectrum from a black body. Then the total number of LyC photons emitted by star is

$$\dot{N}_{\mathrm{LyC}} = 4\pi R_\star^2 \cdot \dot{N}_{\mathrm{LyC},\Omega} \tag{6.63}$$

where $R_\star$ is the star's radius. We now assume that the size of the HII region is determined by the fact that all emitted LyC photons ionize the hydrogen (they are all absorbed), and that this ionization is balanced by a corresponding recombination with rate coefficient $\alpha(T)$

$$4\pi R_\star^2 \cdot \dot{N}_{\mathrm{LyC},\Omega} = \frac{4}{3}\pi R_{\mathrm{HII}}^3 \cdot n_e n_p \cdot \alpha(T) \tag{6.64}$$

where R_{HII} is the radius of the HII region, the Strömgren radius, and $\alpha(10^4\ \mathrm{K}) = 3.76 \cdot 10^{-13}$ cm^3 s^{-1}; hence $n_e \cdot n_p \cdot \alpha(T) = \dot{N}_{\mathrm{rec}}$ is the number of recombinations per second and cubic centimeter. Since $n_e = n_p$, we find

$$U := \left[\frac{3 \cdot R_\star^2 \cdot \dot{N}_{\mathrm{LyC},\Omega}}{\alpha(T)}\right]^{1/3} = R_{\mathrm{HII}} \cdot n_e^{2/3} \tag{6.65}$$

where U is the so-called excitation parameter (pc cm^{-3}). E.g. Orion nebula: from free-free absorption $\Rightarrow$ EM $\Rightarrow$ n_e (assuming $\overline{n_e} = \overline{n_e^2}^{1/2}$); observed angular diameter + distance $\Rightarrow$ $R_{\mathrm{HII}} \Rightarrow U \Rightarrow \dot{N}_{\mathrm{LyC}} \Rightarrow$ number of OB stars.

Sp T	$T_{\rm eff}$ / K	$\log \dot{N}_{\rm LyC}$ / s^{-1}	U / pc cm^{-2}
O4	52000	50.01	148
O5	50200	49.76	122
O6	48000	49.37	90
⋮			
B0	32200	47.62	24
B1	22600	45.18	3.5
⋮			
G2	5800	44.26	~ 0

30 Dor in LMC: 470 pc cm^{-2}, M42 Orion Nebula: 150 pc cm^{-2}

$$N_\star = \frac{U_{\rm HII}}{U_\star} \tag{6.66}$$

Chapter 7

Chemistry of the ISM

7.1 Gas-phase chemistry

physical conditions → profound implications for possible chemical reactions

low temperatures: exothermal reactions (but with potential barrier "activation barrier")

higher temperatures: endothermal reactions(e.g. in shocks or photo dissociation regions)

instellar abundances (by number): $\sim$ 90% hydrogen; $\sim$ 10% helium; $\sim$ 0.1% carbon, oxygen, nitrogen; $<$ 0.01% silicon, iron, calcium,...; $\sim 10^{-10}$ dust (silicates, graphites)

140 molecules known in interstellar space to date

Basic processes

- formation processes
  - radiative association: $X + Y \rightarrow XY + h\nu$
  - grain surface formation $X + Y_g \rightarrow XY_g \rightarrow XY$
- destruction processes
  - photodissociation $XY + h\nu \rightarrow X + Y$
  - dissociative recombination $XY^+ + e^- \rightarrow X + Y$
- rearrangement processes
  - ion-molecule reaction $X^+ + YZ \rightarrow XY^+ + Z$
  - charge-transfer reaction $X^+ + YZ \rightarrow X + YZ^+$
  - neutral-neutral reaction $X + YZ \rightarrow XY + Z$

ion-molecule reactions often lack activation barrier; favored in neutral medium; form molecules with increasing complexity

- neutral molecules formed by dissociative recombination with free e^-
- UV photons dissociate molecules into smaller fragments or photoionize them
- collisional dissociation

7.1.1 Ion-molecule reactions

Reactions of type

$$A^+ + B \xrightarrow{K} C^+ + D \tag{7.1}$$

where K is the reaction rate; its definition is such that

$$K \cdot n_{\mathrm{A}^+} \cdot n_{\mathrm{B}} = \dot{n}_r \tag{7.2}$$

is the number of reactions per cm^3 and per second, hence $[K] = \mathrm{cm}^3\mathrm{s}^{-1}$! Ion approaching a neutral molecule induces electric dipole, which is turn exerts attractive force on the ion $\Rightarrow$ can be captured by the molecule. Ion-molecule reactions possible at low temperature, provided they are exothermal and have no activation barrier. If molecule lacks permanent dipole (e.g. H_2), then long range potential is given by

$$V(R) = -\frac{\alpha q^2}{2R^4} \tag{7.3}$$

where α is the polarizability, i.e.

$$\langle \vec{P} \rangle = \alpha \vec{E} \tag{7.4}$$

and $\langle \vec{P} \rangle$ is the average of the induced dipole moment over all possible orientations of the molecule. q is the charge of the ion, R the separation between the ion and the molecule. Assuming that each encounter yields a reaction, one can calculate the reaction rate, called Langevin rate in this case

$$K_L = 2\pi \left(\frac{\alpha q^2}{m_r} \right)^{1/2} \tag{7.5}$$

where

$$m_r = \frac{m_{\mathrm{A}} \cdot m_{\mathrm{B}}}{m_{\mathrm{A}} + m_{\mathrm{B}}} \tag{7.6}$$

is the reduced mass of the collision partners. Langevin rate is independent of temperature. If one of the partners is H_2, with a polarizability of $\alpha = 4.5 \cdot a_0$ and $a_0 = 0.528$ Å the Bohr radius, then $K_L \approx 2 \cdot 10^{-9} \mathrm{cm}^3\ \mathrm{s}^{-1}$. This is about two orders of magnitue faster than neutral-neutral reactions (even disregarding energy barriers generally involved in the latter); small amount of ionization very effective to drive interstellar chemistry; chemistry primarely happens in photo-dominated regions (UV radiation leads to ionization).

In the absence of measurements (lab), it is recommended to use Langervin rates for high temperatures (several 10 K). At low temperatures, rates become sensitive to details of potential surfaces between neutrals and ions which leads to a temperature dependence.; important to measure reaction rates to obtain results useful for low-T interstellar chemistry.

If neutral target molecule has permanent dipole moment, long-distance potential reads

$$V(R, \theta) = -\frac{\alpha q^2}{2R^4} - \frac{q M_D \cdot \cos\theta}{R^2} \tag{7.7}$$

where M_D is the modulus of the permanent dipole moment and $\theta = \sphericalangle(\vec{M}_D, \text{ion-mol. direction})$. Quantum mechanical calculation necessary at low T, because partition function of rotational

reaction			K
$H_2 + H_2$	$\rightarrow$	$H_3^+ + H$	$2.1 \cdot 10^{-9}$
$H_3^+ + O$	$\rightarrow$	$OH^+ + H_2$	$8.0 \cdot 10^{-10}$
$H_3^+ + CO$	$\rightarrow$	$HCO^+ + H_2$	$1.7 \cdot 10^{-9}$
$H_3^+ + H_2O$	$\rightarrow$	$H_3O^+ + H_2$	$1.1 \cdot 10^{-9}$
$OH^+ + H_2$	$\rightarrow$	$H_2O^+ + H$	$6.1 \cdot 10^{-10}$
$H_2O^+ + H_2$	$\rightarrow$	$H_3O^+ + H$	$7.7 \cdot 10^{-10}$
$C^+ + OH$	$\rightarrow$	$CO^+ + H$	$2.7 \cdot 10^{-9}$
$C^+ + H_2O$	$\rightarrow$	$HCO^+ + H$	$2.0 \cdot 10^{-9}$
$He^+ + CO$	$\rightarrow$	$C^+ + O + He$	$1.6 \cdot 10^{-9}$
$He^+ + O_2$	$\rightarrow$	$O^+ + O + He$	$1.0 \cdot 10^{-9}$
$He^+ + H_2O$	$\rightarrow$	$OH^+ + H + He$	$3.7 \cdot 10^{-10}$
$He^+ + H_2O$	$\rightarrow$	$H_2O^+ + He$	$7.0 \cdot 10^{-11}$
$He^+ + OH$	$\rightarrow$	$O^+ + H + He$	$1.1 \cdot 10^{-9}$

Table 7.1: ion-molecule reactions

levels is affected by the interaction. Theory predicts increase of reaction at low T. Useful approximation of rate:

$$K(T) = K_1 \cdot \left[1 - \exp\left(-\frac{K_0}{K_1}\right)\right] \tag{7.8}$$

where

$$K_0 = K_L \cdot \left(1 + \frac{M_D^2}{3\alpha B_0}\right)^{1/2} \tag{7.9}$$

$$K_1 \approx K_L + 0.4 \cdot q \cdot M_D \cdot \left(\frac{8\pi}{m_r \cdot k_B T}\right)^{1/2} \tag{7.10}$$

and B_0 is the rotational constant.

7.1.2 Neutral-neutral reaction

Neutral-neutral reactions of atoms or molecules can play role at low T, but they are fundamental at higher T, such as reached in shocks, PDRs or strong turbulence; bond breaking associated with rearrangement of molecules produces activation barrier; reaction rates take the form:

$$K_f = K_b \, e^{-\frac{E_a}{k_B T}} \tag{7.11}$$

where E_a is the reaction barrier and K_f and K_b are the forward and backward reaction rates, respectively. In neutral-neutral reactions, attractive force is due to can der Waals forces,

$$V(r) = -\frac{\alpha_1 \alpha_2}{R^6} \cdot I \tag{7.12}$$

where α_1 and α_2 are the polarizabilities of species involved and I is the harmonic mean

$$\langle a \rangle_n = \frac{n}{\frac{1}{a_1} + \frac{1}{a_2} + \cdots + \frac{1}{a_n}} \tag{7.13}$$

of the ionization potentials. Rate coefficient then (ignoring for the moment activation barrier):

$$K_f = 13.5 \cdot \pi \cdot \left(\frac{\alpha_1 \alpha_2}{\mu} I \right)^{\frac{1}{3}} \cdot \langle v^{\frac{1}{3}} \rangle \approx 4 \cdot 10^{-11} \text{ cm}^3 \text{ s}^{-1} \tag{7.14}$$

where μ is the reduced mass, and typical values have been assumed ($\alpha = 10^{-24}\text{cm}^3, \mu = 3 \cdot 10^{-24}\text{g}, I = 13.6$ eV$, T = 100$ K. If reaction barrier is involved, reaction rate has to be multiplied by the Boltzmann factor $e^{-\frac{E_a}{k_B T}}$. Even a modest barrier of 1000 K then makes reaction prohibitive at $T = 100$ K for diffuse clouds, let alone at 10 K for dense clouds.

examples: free radicals (molecules in which valence bonds are not saturated and whioch possess one or several single, unpaired electrons):

reaction			α	β
C + OH	$\rightarrow$	CO + H	$1.1 \cdot 10^{-10}$	0.5
C + O_2	$\rightarrow$	CO + O	$3.3 \cdot 10^{-11}$	0.5
O + CH	$\rightarrow$	CO + H	$4.0 \cdot 10^{-11}$	0.5
O + CH	$\rightarrow$	$HCO^+ + e^-$	$2.0 \cdot 10^{-11}$	0.44
O + CH_2	$\rightarrow$	CO + H_2	$2.0 \cdot 10^{-11}$	0.5

where $K = \alpha \cdot \left(\frac{T}{300 \text{ K}}\right)^{\beta}$

Table 7.2: examples for neutral-neutral reactions

7.1.3 Photo-dissociation

FUV photons permeating diffuse ISM are dominant destruction agent for small molecules. Typical bonding energies of molecules are 5 eV to 10 eV, which corresponds to a wavelength $\lambda \lesssim 3000$ Å. Reaction rate

$$K_{\text{pd}} = \int_{\nu_{\text{pd}}}^{\nu_{\text{H}}} 4\pi I_{\text{ISRF}}(\nu) \sigma_{\text{pd}}(\nu) \, d\nu \tag{7.15}$$

where integration runs from photo dissociation frequency ν_{pd} to the hydrogen photo-ionization frequency ν_{H}; $I_{\text{ISRF}}(\nu)$ is the mean photon intensity of the interstellar radiation field and σ_{pd} is the photo dissociation cross section. For homogeneous slabs

$$K_{\text{pd}} = a \cdot e^{-b \cdot A_V} \tag{7.16}$$

where a is the unshielded rate and A_V is the visual extinction due to dust.

Table 7.3: some important photo reactions

			a	b
CH_2	$\rightarrow$	CH + H	$5.0 \cdot 10^{-11}$	1.7
CH	$\rightarrow$	C + H	$2.7 \cdot 10^{-10}$	1.3
O_2	$\rightarrow$	O + O	$3.3 \cdot 10^{-10}$	1.4
OH	$\rightarrow$	O + H	$7.6 \cdot 10^{-10}$	2.0
H_2O	$\rightarrow$	OH + H	$5.1 \cdot 10^{-10}$	1.8

7.1.4 Dissociative recombination

Involves capture of e^- by an ion to from a neutral in excited electronic state that can dissociate. Rate coefficients are typicallay 10^{-7} cm^3 s^{-1}. For large molecules such as PAHs, the electronic excitation energy of the neutral will quickly transfer to the vibrational manifold; radiation at IR wavelenghts.

			α	β
$OH^+ + e^-$	$\rightarrow$	O + H	$3.8 \cdot 10^{-8}$	-0.5
$CO^+ + e^-$	$\rightarrow$	C + O	$2.0 \cdot 10^{-7}$	-0.5
$H_2O^+ + e^-$	$\rightarrow$	O + H + H	$2.0 \cdot 10^{-7}$	-0.5
$H_2O^+ + e^-$	$\rightarrow$	OH + H	$6.3 \cdot 10^{-8}$	-0.5
$HCO^+ + e^-$	$\rightarrow$	CO + H	$1.1 \cdot 10^{-7}$	-1.0
$CH^+ + e^-$	$\rightarrow$	C + H	$1.5 \cdot 10^{-7}$	-0.4

where $K = \alpha \cdot \left(\frac{T}{300\ \mathrm{K}}\right)^{\beta}$

Table 7.4: examples for dissociative recombinations

7.1.5 Grain-surface chemistry

Interstellar grains provide surface on which accreted species can meet and react and to which they can transfer excess energy; grain surface chemistry is therefore governed by the accretion rate.

accretion, diffusion, reaction, ejection

$$K_{\mathrm{ac}} = n_{\mathrm{H}} \cdot \sigma_d \cdot v_{\mathrm{H}} \cdot S(T, T_d) = 10^{-17} \cdot \left(\frac{T}{10\,\mathrm{K}}\right)^{\frac{1}{2}} \cdot n_{\mathrm{H}} \quad \mathrm{s}^{-1} \tag{7.17}$$

where T is the gas temperature and n_{H} the gas density; depletion onto dust grains; $\tau_{\mathrm{depl.}} = 4 \cdot 10^9 \cdot n^{-1}$ years; which means $4 \cdot 10^5$ years in dense cores which is very rapid on astronomical time scales.

chemistry on dust grains extremely important, e.g. H_2: can only form on grains in order to transfer excess energy to grains; also possible:

$$\begin{aligned} \mathrm{H} + \mathrm{e}^- &\rightarrow \mathrm{H}^- + \mathrm{h}\nu \\ \mathrm{H} + \mathrm{H}^- &\rightarrow \mathrm{H}_2 + \mathrm{e}^- \\ \mathrm{H}^+ + \mathrm{H} &\rightarrow \mathrm{H}_2^+ + \mathrm{h}\nu \\ \mathrm{H}_2^+ + \mathrm{H} &\rightarrow \mathrm{H}_2 + \mathrm{H}^+ \end{aligned}$$

but extremely low possibiliy

evidence for other molecules to form on dust grains: e.g. CO_2 detected in inner regions of molecular clouds; ice mantles covering dust grains.

H atom striking dust grain has probability to stick on it (physiosorpition); S depends on temperature T of the gas, temperature T_d of the dust, binding energy D for adsorption and upon nature of the grain; average time for H atom sticking on grain with geometrical cross section

$$\sigma_d = \pi a^2 \tag{7.18}$$

is

$$t_s = \frac{1}{S \cdot n_{\mathrm{H}} \cdot \langle v_{\mathrm{H}} \rangle \cdot \sigma_d} \tag{7.19}$$

where

$$\langle v_{\mathrm{H}} \rangle = \sqrt{\frac{8 k_B T}{\pi m_{\mathrm{H}}}} \tag{7.20}$$

is the mean velocity of the H atoms; adsorbed atom can evaporate within characteristic time scale

$$t_{\mathrm{evap.}} = \nu_0^{-1} \cdot \, e^{\frac{D}{k_B T}} \tag{7.21}$$

where $\nu_0 = 10^{13}$ Hz is characteristic vibration frequency of latticq and T_d grain temperature; then "hopping" follows, which is a quantum mechanical process, depending only weakly on temperature; in favourable temperature range we may assume that each H atom on grain will form H_2 with proper partner

$$K = 0.5 \cdot n_{\mathrm{H}} \cdot \langle n_d(a) \cdot \pi a^2 \rangle \langle v_{\mathrm{H}} \rangle \cdot S \quad \mathrm{cm}^3 \ \mathrm{s}^{-1} \tag{7.22}$$

where n_d is the number density of dust grains of size a. Integrating over grain-size distribution, and assuming gas-to-dust ratio similar to that in solar neighbourhood, we obtain

$$K = 8 \cdot 10^{17} \cdot S \cdot n_{\mathrm{H}} \left(n_{\mathrm{H}} + 2 n_{\mathrm{H}_2} \right) \cdot \left(\frac{T}{100 \ \mathrm{K}} \right)^{\frac{1}{2}} \quad \mathrm{cm}^3 \ \mathrm{s}^{-1} \tag{7.23}$$

other molecules forming on dust grains:

$$
\begin{aligned}
\mathrm{H + C} &\rightarrow \mathrm{CH} \\
\mathrm{H + N} &\rightarrow \mathrm{NH} \\
\mathrm{H + O} &\rightarrow \mathrm{OH} \\
\mathrm{H + CH} &\rightarrow \mathrm{CH_2 \cdots CH_3 \cdots CH_4} \\
\mathrm{H + NH} &\rightarrow \mathrm{NH_2 \cdots NH_3} \\
\mathrm{H + CO} &\rightarrow \mathrm{HCO} \\
\mathrm{H + OH} &\rightarrow \mathrm{H_2O} \\
\mathrm{O + C} &\rightarrow \mathrm{CO} \\
\mathrm{O + CO} &\rightarrow \mathrm{CO_2} \\
\mathrm{OH + OH} &\rightarrow \mathrm{H_2O + H} \\
\mathrm{HCO + OH} &\rightarrow \mathrm{CO + H_2O} \\
\mathrm{HCO + HCO} &\rightarrow \mathrm{H_2 + 2\ CO}
\end{aligned}
$$

7.2 Photodissociation regions

abbreviations PDRs (also: photo-dominated regions); regions in which (F)UV field strong enough to photodissociate molecules;

UV radiation field, definition e.g. Habing (1968)

$$G_0 = 1.3 \cdot 10^{-4}\ \mathrm{erg\ s^{-1}\ cm^{-2}\ sterad^{-1}} \tag{7.24}$$

912 Å$\leq \lambda \leq$2066 Å, 13.6 eV $- E = 6$ eV. $\chi = 1 \Rightarrow G_0$ i.e. χ is the ratio of the local radiation field to G_0.

- encompasses most of the ISM, except for inner parts of molecular clouds (too dense) and HII regions, wich are treated seperatly
- interface between HII regions and molecular clouds, where both, density and UV field are large / strong
- characterized by strong [CII]λ158 μm and [OI]λ63 μm lines, strong rotation and vibration lines of H_2, and by strong aromatic band emission in mid-IR

depth into PDR from HII regions often quantified by visual extinction

$$
\begin{aligned}
&A_V/E(B-V) = 3.1 \\
&N_H/E(B-V) = 5.8 \cdot 10^{21}\mathrm{cm^{-2}\ mag^{-1}} \\
&\qquad A_V = 1 \equiv \qquad\qquad N_H = 1.87 \cdot 10^{21}\ \mathrm{cm^{-2}}
\end{aligned}
$$

schematically, stratified structure

- first, H ionized to H^+ in HII region, recombines to atomic H and finally forms H_2 at $\tau_{\mathrm{UV}} = 0.6$, i.e. $A_V = 0.2$ for density of $\sim 10^3$ cm^{-3} and radiation field $\chi = 100$
- C^{++} in HII region recombines to C^+ in outer parts of PDR
- at $A_V \approx 1$, C^+ recombines to C

- slightly deeper into molecular cloud, CO is formed
- O is present everywhere, outside of HII region atomic; its abundance decreases slightliy towards molecular core where CO is formed
- lines of H_2, CII, OI and CO are very intense in PDRs, since both n and T are high; these lines are coolants.

cooling important: T decreases from $\sim 10^4$ K in HII region to few 10s of K at $A_V \approx 1$. Dust grains also absorb UV radiation and re-emit in IR continuum and aromatic bands.

- most of energy emitted by young stars in SF regions is converted into these forms; emission from PDRs dominates line and thermal dust continuum emission from galaxies
- large fraction of [CII] line emission can also stem from diffuse ISM

7.2.1 Chemistry in PDRs

different from cold (diffuse) ISM and molecular clouds because of high T; many endothermic reactions and reactions with activations barriers can occur, as well as reactions with H_2 in excited states, e.g.

$$\begin{aligned} O + H_2^* &\rightarrow OH + H \\ C^+ + H_2^* &\rightarrow CH^+ + H \end{aligned}$$

in which the formation of OH and CH is enhanced as compared to molecular clouds.

7.2.2 Heating

- photo-electric heating by dust grains; H_2 formation on dust grains; UV radiation; dust; ionization in there; free e^- don't have enough energy to ionize or excite other atoms / molecules / dust particles; interact with free e^- and heat up the gas
- chemical heating: electrons released by dissociative recombination of several ions (H_3^+, HCO^+,...) and by several exothermic reactions with He^+, H_2^+, H_3^+
- collisional de-excitation of excited levels of H_2 after absorption of FUV photons

7.2.3 Cooling

dominated by fine-structure lines and rotational transitions of CO and collisional excitation of H_2; T can be high

- Transitions [OI]λ 63 μm and 146 μm, [CII]λ 158 μm, [OI]λ 6300 Å, [SII]λ 6730 Å, [FeI]λ 1.26 μm and 1.64 μm dominate cooling at $T > 4000$ K
- high-J CO cooling significant in outer layers (large optical depth)
- at high densities, cooling by collisions of atoms and molecules with dust grains
- H_2 quadrupole emission

most recent and most complete modelling of PDRs by Kaufman et al. (1999), considering plane-parallel sheaths of constant density, in the range $n = 10^0 \cdots 10^7$ cm^{-3}, irriated by UV radiation field of $\chi = 10^{-0.5} \cdots 10^{6.5}$

[CII] line at $\lambda = 158$ μm important diagnostic tool (new telescopes); intesity approximately given by

$$I(\mathrm{C\,II}) \propto N(\mathrm{C}^+) \cdot \frac{\exp\left[-92 \cdot \left(\frac{T}{\mathrm{K}}\right)^{-1}\right]}{1 + \frac{n_{\mathrm{cr}}}{n}} \tag{7.25}$$

where $n_{\mathrm{cr}} \approx 3000 cm^{-3}$ is the critical density for collisions with neutrals for this line and $N(\mathrm{C}^+)$ is the column density of ionized carbon. n_{cr} is similar for CO(1-0), [CI], [CII]

Of course, in both cases the intensities per unit volume are proportional to density of emitting particles, hence the cooling rate

$$\Lambda \propto n^2 \text{for} \qquad n < n_{\mathrm{cr}}$$
$$\Lambda \propto n \text{for} \qquad n > n_{\mathrm{cr}}$$

heating rate per unit volume increases faster than n so that temperature is higher at higher densities.

7.2.4 Observations

SOFIA 2.5 meter telescope onboard Boeing 747-SP 41000 ft (12.5 km) altitude; wavelength range 1 μm $\cdots$ 600 μm; operation end 2008 ?

Herschel 3.5 meter telescope, spacecraft; wavelength range 60 μm $\cdots$ 600 μm; L2 Lagrange point of sun-earth system; launch end 2008, 3 years operation

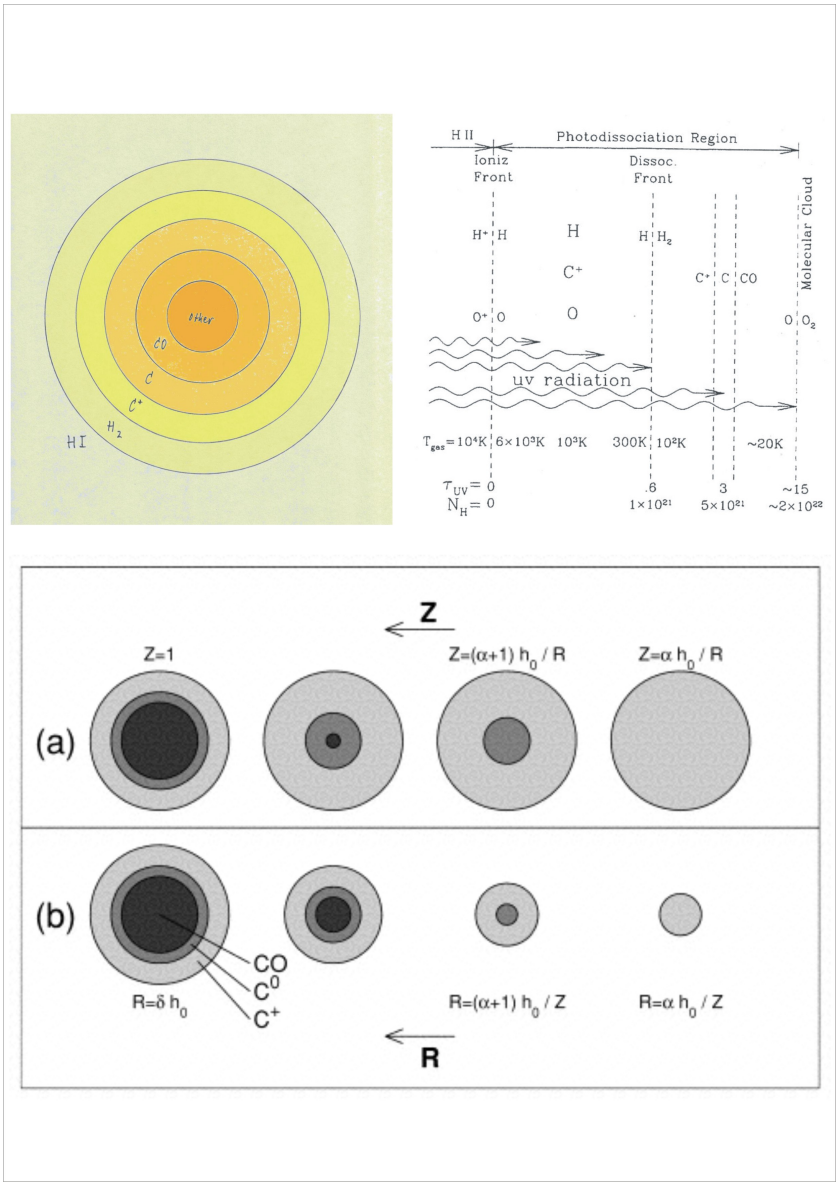

Figure 7.1: Structure of PDRs

Chapter 8

Star formation

8.1 Cloud structure

For perfect gas

$$E_{\text{kin}} = \frac{3}{2} N k_B T = \frac{3}{2} \cdot \frac{M k_B T}{\mu m_{\text{H}}} \tag{8.1}$$

where M is the total mass of the cloud and $\mu \approx 2.7$ is the molecular mass (accounting for H_2, He and heavy elements). A spherical and homogenous cloud has potential energy

$$E_{\text{pot}} = -\frac{3}{5} \frac{GM^2}{R} \tag{8.2}$$

Note: Cloud in equilibrium cannot be isothermal at the same time (and homogeneous), so that our consideration can only be approximate; however, it will lead to a qualitatively useful result, with correct order of magnitude. Application of virial theorem, i.e.

$$E_{\text{kin}} = -\frac{1}{2} \cdot E_{\text{pot}} \tag{8.3}$$

means

$$\frac{3}{2} \frac{M k_B T}{\mu m_{\text{H}}} = \frac{3}{10} \frac{GM^2}{R} \tag{8.4}$$

or

$$R = \sqrt{\frac{15}{4\pi}} \left(\frac{k_B T}{Gn} \right)^{\frac{1}{2}} \frac{1}{\mu m_{\text{H}}} = 3.57 \cdot \left(\frac{T}{\text{K}} \right)^{\frac{1}{2}} \left(\frac{n}{\text{cm}^{-3}} \right)^{-\frac{1}{2}} \text{ pc} \tag{8.5}$$

wich yields

$$R_J = 0.08 \left(\frac{T}{10\,\text{K}} \right)^{\frac{1}{2}} \left(\frac{n}{10^4\,\text{cm}^{-3}} \right)^{-\frac{1}{2}} \text{ pc} \tag{8.6}$$

This is called the Jeans length: a cloud with $R < R_J$ becomes unstable against gravitation and will start collapsing. Likewise, we can compute the Jeans mass M_J above which a cloud becomes "Jeans unstable":

$$M = \frac{5}{2} \sqrt{\frac{15}{4\pi}} \left(\frac{k_B T}{G} \right)^{\frac{3}{2}} \cdot \frac{1}{\mu^2 m_{\text{H}}^2 n} = 4.46 \cdot \left(\frac{T}{\text{K}} \right)^{\frac{3}{2}} \left(\frac{n}{\text{cm}^{-3}} \right)^{-\frac{1}{2}} \text{M}_\odot \tag{8.7}$$

which yields

$$M_J = 2.0 \left(\frac{T}{10\,\mathrm{K}}\right)^{\frac{3}{2}} \left(\frac{n}{10^4\,\mathrm{cm}^{-3}}\right)^{-\frac{1}{2}} \mathrm{M}_\odot \tag{8.8}$$

unstable if $M > M_J$

Another route towards the concept of Jeans instability is by starting out from the hydrodynamic equation describing a uniform, infinitly extended fluid (Jeans, 1902). Let us consider such an isothermal, infinite, magnetized medium lacking any macroscopic motions:

$$\frac{\partial \rho}{\partial t} + \vec{\nabla}\rho \cdot \vec{v} = 0 \qquad \text{continuity equation} \tag{8.9}$$

$$\rho \cdot \left[\frac{\partial \vec{v}}{\partial t} + \left(\vec{v} \cdot \vec{\nabla}\right)\vec{v}\right] = -\vec{\nabla}P - \rho\,\vec{\nabla}\phi \qquad \text{equation of motion} \tag{8.10}$$

$$\vec{\nabla}^2\phi = 4\pi G \cdot \rho \qquad \text{Poisson equation} \tag{8.11}$$

where ϕ is the gravitational potential. Considering perturbations such that (index "1" for perturbed, "0" for equilibrium)

$$v = v_1 \tag{8.12}$$

$$\rho = \rho_0 + \rho_1 \tag{8.13}$$

$$\phi = \phi_0 + \phi_1 \tag{8.14}$$

and assuming a constant speed of sound c_s, such that

$$\frac{P}{\rho} = c_s^2 = \frac{k_B T}{\mu m_\mathrm{H}} \tag{8.15}$$

we obtain, afer linearizing the three above equations,

$$\frac{\partial v_1}{\partial t} = -\vec{\nabla}\phi_1 - \frac{c_s^2}{\rho_0} \cdot \vec{\nabla}\rho_1 \tag{8.16}$$

$$\frac{\partial \rho_1}{\partial t} = -\rho_0 \cdot \left(\vec{\nabla} \cdot \vec{v}_1\right) \tag{8.17}$$

$$\vec{\nabla}^2\phi_1 = 4\pi G\rho_1 \tag{8.18}$$

Taking the divergence of 8.16 to eliminate $\vec{\nabla}\vec{v}_1$ and $\vec{\nabla}^2\phi_1$ with 8.17 and 8.18, we find

$$\frac{\partial^2 \rho_1}{\partial t^2} = \rho_0\vec{\nabla}^2\phi_1 + c_s^2\vec{\nabla}^2\rho_1 = 4\pi G\rho_0 \cdot \rho_1 - c_s^2 \cdot \vec{\nabla}^2\rho_1 \tag{8.19}$$

The ansatz of a periodic perturbation

$$\rho_1 = A \cdot e^{i(kx + \omega t)} \tag{8.20}$$

yields a dispersion relation between the angular frequency ω and the wave number $k = 2\pi/\lambda$:

$$\omega^2 = k^2 c_s^2 - 4\pi G\rho_0 \tag{8.21}$$

unstable modes have $\omega^2 < 0$, i.e. ω imaginary

$$k < k_J = \left(\frac{4\pi G\rho_0}{c_s^2}\right)^{\frac{1}{2}} \tag{8.22}$$

defining the Jeans length

$$\lambda_J = \frac{2\pi}{k_J} \tag{8.23}$$

The Jeans mass is included in a cube of side λ_J

$$M_J = \rho \cdot \left(\frac{2\pi}{k_J}\right)^3 \tag{8.24}$$

Apart from small numerical differences, this result is identical to the more simple approach taken before.

8.2 Density distribution of spherical cloud in equilibrium

Self-gravitating, isothermal cloud in hydrostatic equilibrium cannot have uniform density as force on each particle is a function of radius R; for perfect gas, $\rho(R)$ given by

$$P = \rho\frac{k_B T}{\mu m_{\mathrm{H}}} \qquad \text{equation of state} \tag{8.25}$$

$$-\frac{dP}{dR} = \frac{4\pi G\rho}{R^2}\int_0^R \rho y^2\, dy \qquad \text{equation of hydrostatic equilibrium} \tag{8.26}$$

Differntiating with respect to R we get

$$\frac{1}{R^2}\cdot\frac{d}{dR}\left(\frac{R^2}{\rho}\frac{dP}{dR}\right) = -4\pi G\rho \tag{8.27}$$

or, inserting P from equation of state

$$-\frac{1}{R^2}\frac{d}{dR}\left(\frac{R^2}{\rho}\frac{d\rho}{dr}\right) = -\frac{4\pi G\mu m_{\mathrm{H}}}{k_B T}\cdot\rho \tag{8.28}$$

This can be solved by introducing

$$\rho = \lambda\cdot e^{\xi}, \quad R = \beta^{\frac{1}{2}}\lambda^{-\frac{1}{2}}\cdot\xi \qquad \lambda \text{ being an arbitrary constant} \tag{8.29}$$

$$\beta = \frac{k_B T}{4\pi G\mu m_{\mathrm{H}}} \tag{8.30}$$

Boundary conditions in the centre are

$$\rho = \rho_c \tag{8.31}$$

$$\frac{d\rho}{dR} = 0 \tag{8.32}$$

choosing $\lambda = \rho_c$

$$\rho = 0 \tag{8.33}$$

$$\frac{d\rho}{d\xi} = 0 \tag{8.34}$$

Problem now entirely determined once T, μ and ρ_c are chosen. Solution e.g. in Chandrasekhars "Introduction to the study of stellar structures".

Density is found to be approximately

$$\rho(R) \approx R^{-2} \tag{8.35}$$

except for central regions. Without external pressure, isothermal sphere at equilibrium is expected to extend out to infinity; with external pressure, radius is finite; in reality, interstellar clouds are not isothermal because of heating and cooling processes; more realistic clouds must account for this (e.g. Chiege & Pineau des Forêets (1987))

8.3 Cloud collapse

Dynamical time scale for free fall: how long would it take for a spherical cloud to collapse assuming that the inner pressure is removed all of a sudden. Start out from gravitational acceleration at distance r

$$\frac{d^2r}{dt^2} = -\frac{GM}{r^2} \tag{8.36}$$

integration yields

$$\frac{1}{2}\left(\frac{dr}{dt}\right)^2 = \frac{GM}{r} + C_1 \tag{8.37}$$

with integration constant C_1. Requiring that velocity at objects initial surface, i.e. $r = r_0$ vanishes, we obtain

$$\frac{dr}{dt} = -\left[2GM\left(\frac{1}{r} - \frac{1}{r_0}\right)\right]^{\frac{1}{2}} \tag{8.38}$$

Here we have chosen the negative root because the cloud is collapsing. Substituating

$$\theta = \frac{r}{r_0} \tag{8.39}$$

we have

$$\frac{d\theta}{dt} = -\left[2\frac{GM}{r_0^3}\left(\frac{1}{\theta} - 1\right)\right]^{\frac{1}{2}} \tag{8.40}$$

with the substitution

$$\theta = (\cos\xi)^2 \tag{8.41}$$

this becomes

$$\frac{\xi}{2} + \frac{1}{4}\sin 2\xi = \frac{t}{2} \cdot \left(\frac{2GM}{r_0^3}\right)^{\frac{1}{2}} + C_2 \tag{8.42}$$

The integration constant C_2 vanishes if we require $r = r_0$ for $t = 0$, and $\xi = 0$, respectively. The dynamical time scale is now obtained when the sphere reaches zero radius, i.e. $\theta = 0$, $\xi = \pi/2$. Then

$$t_{\rm ff} = \frac{\pi}{2}\left(\frac{2GM}{r_0^3}\right)^{-\frac{1}{2}} = \left(\frac{\pi^2 r_0^3}{8GM}\right)^{\frac{1}{2}} = \left(\frac{3\pi}{32G\rho_0}\right)^{\frac{1}{2}} \tag{8.43}$$

This does not depend on radius anymore! Inserting $\mu = 2.7$, we finally arrive at

$$t_{\rm ff} = 3.1 \cdot 10^7 \left(\frac{n_0}{\rm cm^{-3}}\right)^{-\frac{1}{2}} \ {\rm yr} \tag{8.44}$$

List of Figures

List of Tables

Index